

Title	DIAS Research Report 2013 - School of Celtic Studies
Creators	DIAS, Council
Date	2013
Citation	DIAS, Council (2013) DIAS Research Report 2013 - School of Celtic Studies.
URL	https://dair.dias.ie/id/eprint/151/

Ρéalτεολογίot 7 Ρéalτρίρíc
Ταίξoe Τυαμάρçáil 2013



Astronomy and Astrophysics
Research Report 2013

Presented to the Governing Board
of the School of Cosmic Physics
on 28 March 2014

Contents

1 Research Work	1
1.1 High-Energy Phenomena	1
1.1.1 Radiation processes	1
1.1.2 High Energy Radiation of Astrophysical sources	2
1.1.3 HESS related activity	5
1.1.4 Electromagnetic Cascades, UHECR, and Neutrinos	5
1.1.5 High energy emission from binary systems.	8
1.2 General Theory	9
1.2.1 The problem of small angular scale structure in the cosmic ray anisotropy data	9
1.2.2 Magnetic field generation in shock precursors	10
1.2.3 Analytic Solution for Self-regulated Collective Escape of Cosmic Rays from Their Acceleration Sites	10
1.3 Star Formation	11
1.3.1 Characterization of Infrared Dark Clouds: NH_3 Observations of an Absorption-contrast Selected IRDC Sample	11
1.3.2 X-Shooter spectroscopy of young stellar objects: Impact of chromospheric emission on accretion rate estimates	11
1.3.3 An Empirical Correction for Activity Effects on the Temperatures, Radii, and Estimated Masses of Low-Mass Stars and Brown Dwarfs	12
1.3.4 Long-Term Monitoring of Accretion and Outflows in Young Stellar Objects: Searching for the Temporal Connection	12
1.3.5 Non-thermal Radio Emission from Young Stellar Object Outflows	13
1.3.6 Very Large Array Observations of DG Tau's Radio Jet: A Highly Collimated Thermal Outflow	13
1.3.7 New brown dwarf discs in Upper Scorpius observed with WISE	13
1.3.8 Protoplanetary Disk Masses from Stars to Brown Dwarfs	14
1.3.9 A systematic survey for eruptive young stellar objects using mid-infrared photometry	14
1.3.10 Water in star-forming regions with Herschel (WISH): A survey of low-J H_2O line profiles	15
1.3.11 High-resolution ammonia mapping of the protostellar core Cha-MMS1	15
1.3.12 Explaining millimetre-sized particles in brown dwarf disks	16
1.3.13 Physical properties of the jet from DG Tauri on sub-arcsecond scales with HST/STIS	16
1.3.14 Near-Infrared spectroscopy of young brown dwarfs	17
1.3.15 Temperaments of young stars: Rapid mass-accretion rate changes in T Tauri and Herbig Ae stars	17
1.3.16 New observations of a "dust trap" around a young star with ALMA	17
1.3.17 The SONYC survey: Towards a complete census of brown dwarfs in star forming regions	18
1.3.18 Investigating Proper Motions in the 2M1207A Jet	18
1.3.19 Sub-arcsecond high-sensitivity measurements of the DG Tau jet with e-MERLIN	18
1.3.20 Constraints on the radial distribution of the dust properties in the CQ Tauri protoplanetary disk	19
1.3.21 The main sequence of three red supergiant clusters	19
1.3.22 Angular momentum and disk evolution in very low mass systems	19
1.3.23 Accurate determination of accretion and photospheric parameters in Young Stellar Objects: the case of two candidate old disks in the Orion Nebula Cluster	20

1.3.24	Discovery of the magnetic field in the pulsating B star β Cephei	20
1.3.25	The evolution of [pseudo]bulges in disk galaxies in the last 8 Gyrs	21
1.4	Invited talks and other conference activities	21
2	Contributions to Third-level Education	22
2.1	Lecture courses delivered	22
2.2	PhD students	22
2.3	Student final year projects	22
2.4	Secondment	22
3	Contributions to research infrastructure and public service	23
3.1	HESS, Fermi, ASTRO-H, KM3NeT, CTA	23
3.2	MIRI, EChO and LBASS	23
3.2.1	MIRI	23
3.2.2	Exoplanet Characterisation Observatory (EChO)	24
3.2.3	L-BASS	24
3.3	DELL HPC summit in Dunsink	24
3.4	ICHEC launch of new super-computer	25
3.5	Training week for National School teachers	25
3.6	Individual Contributions	25
4	Public Outreach	26
4.1	Statutory Public Lecture	26
4.2	Irish Astronomy Trail and proposed European Route des Observatoires	26
4.3	Dunsink	26
4.3.1	General	26
4.3.2	A Mystic Dream of 4	27
4.3.3	Annual Hamilton Walk	27
4.3.4	"Light Echo" exhibition	27
4.3.5	Brecht's "The Life of Galileo"	28
4.3.6	Open nights and other similar events	28
4.4	Other Outreach Contributions	29
5	Detailed Bibliography of Publications	30
5.1	Peer-reviewed Publications in 2013	30
5.2	Publications in 2013 (not subject to peer-review)	33
5.3	Preprints posted in 2013 and not yet published	34

In 2012 the Institute produced a new strategic plan covering the period 2012-2016¹. As part of the development of this overarching Institutional strategy each school also produced its own strategic programme of activities. In the case of the School of Cosmic Physics this identified four broad ‘pillars’ that together support the school. The first and most important of these is the School’s reputation for pioneering and excellent research, the others being its contributions to the third-level educational system, its involvement in shared research infrastructure and general public service and finally its work in public outreach. This report aims as far as possible to follow this structure.

1 Research Work

1.1 High-Energy Phenomena

1.1.1 Radiation processes

Felix Aharonian

The exploration of specifics of high energy radiation processes in different astrophysical environments has been one of the major topics of my research over the last 30+ years. In this regard the period of 2012-2013 was quite productive. Together with my colleagues, I developed an analytical approach for calculations of radiation of relativistic electrons in highly turbulent magnetic fields. We found several interesting features of radiation in both the synchrotron and the so-called “jitter” regimes. These results might have broad implications in astrophysics. We also have studied the character of radiation of relativistic charged particles in regular magnetic fields using, for the first time, the Hamiltonian formalism for determination of trajectories of particles in extremely strong fields. The gamma-radiation components emitted by relativistic electrons in the synchrotron and curvature-radiation regimes have been explored on a quantitative level. The other two

studies currently being under consideration, are nuclear reactions in very hot astrophysical plasmas, and precise analytical parametrizations of the cross-sections of proton-proton interactions from sub-relativistic to ultra high energies. Finally, we have conducted a principally new study of modification of radiation emitted by relativistically moving objects due to the effects of special relativity.

Jitter Radiation S.R. Kelner, E.A. Aharonian, D. Khangulyan

In a small-scale turbulent medium, when the nonrelativistic Larmor radius $R_L = mc^2/eB$ exceeds the correlation length λ of the magnetic field, the magnetic Bremsstrahlung radiation of charged relativistic particles unavoidably proceeds to the so-called jitter radiation regime. The cooling timescale of parent particles is identical to the synchrotron cooling time, thus this radiation regime can be produced with very high efficiency in different astrophysical sources characterized by high turbulence. The jitter radiation has distinct spectral features shifted toward high energies, compared to synchrotron radiation. This effect makes the jitter mechanism an attractive broad-band gamma-ray production channel, which, in highly magnetized and turbulent environments, can compete or even dominate over other high-energy radiation mechanisms. In this paper, we present a novel study of the spectral properties of the jitter radiation performed within the framework of perturbation theory. The derived general expression for the spectral power of radiation is presented in a compact and convenient form for numerical calculations. The work is published in The Astrophysical Journal[22].

Synchrotron-to-curvature transition regime of radiation of charged particles in a dipole magnetic field A. Prosekin, S.R. Kelner, E.A. Aharonian

The details of trajectories of charged particles become increasingly important for proper understanding of processes of formation of radiation in strong and curved magnetic fields. Be-

¹ <http://www.dias.ie/images/stories/admin/Strategystatements/diasstrategic%20plan2012-2016.pdf>

cause of damping of the perpendicular component of motion, the particle's pitch angle could be decreased by many orders of magnitude leading to the change of the radiation regime – from synchrotron to the curvature mode. To explore the character of this transition, we solve numerically the equations of motion of a test particle in a dipole magnetic field, and calculate the energy spectrum of magnetic bremsstrahlung self-consistently, i.e. without a priori assumptions on the radiation regime. In this way we can trace the transitions between the synchrotron and curvature regimes, as well as study the third (intermediate or the so-called synchro-curvature) regime. We briefly discuss three interesting astrophysical scenarios, the radiation of electrons in the pulsar magnetosphere in the polar cap and outer gap models, as well as the radiation of ultrahigh energy protons in the magnetosphere of a massive black hole, and demonstrate that in these models the synchrotron, synchro-curvature and curvature regimes can be realized with quite different relative contributions to the total emission. The work is submitted to *Astrophysical Journal*[78].

Analytical Approximations for Treatment of Inverse Compton Scattering of Relativistic Electrons in the Blackbody Radiation Field
Khangulyan, S.R. Kelner, E.A. Aharonian

The inverse Compton (IC) scattering of relativistic electrons is one of the major gamma-ray production mechanisms in different environments. Often, the target photons for IC scattering are dominated by blackbody (or graybody) radiation. In this case, the precise treatment of the characteristics of IC radiation requires numerical integrations over the Planckian distribution. Formally, analytical integrations are also possible but they result in series of several special functions; this limits the efficiency of usage of these expressions. The aim of this work is the derivation of approximate analytical presentations that would provide adequate accuracy for the calculations of the energy spectra of upscattered radiation, the rate of electron energy losses, and the mean energy of emitted photons. Such formulae have been obtained by merging the analyti-

cal asymptotic limits. The coefficients in these expressions are calculated via the least-squares fitting of the results of numerical integrations. The simple analytical presentations, obtained for both the isotropic and anisotropic target radiation fields, provide adequate (as good as 1%) accuracy for broad astrophysical applications. This work is now published in *The Astrophysical Journal*, Volume 783, Issue 2, article id. 100, 11 pp. (2014).

The beaming pattern of External Compton Emission from relativistic outflows *S.R. Kelner, E. Lefa, F. Rieger, E.A. Aharonian*

The beaming pattern of radiation emitted by a relativistically moving source like jets in microquasars, AGN and GRBs, is a key issue for understanding of acceleration and radiation processes in these objects. In this paper we introduce a formalism based on a solution of the photon transfer equation to study the beaming patterns for emission produced by electrons accelerated in the jet and upscattering photons of low-energy radiation fields of external origin (the so-called External Compton scenario). The formalism allows us to treat non-stationary, non-homogeneous and anisotropic distributions of electrons, but assuming homogeneous/isotropic and non-variable target photon fields. We demonstrate the non-negligible impact of the anisotropy in the electron distribution on angular and spectral characteristics of the EC radiation. The work is submitted to *Astrophysical Journal*[74].

1.1.2 High Energy Radiation of Astrophysical sources

TeV gamma rays from blazars beyond $z = 1$?
E.A. Aharonian, W. Essey, A. Kusenko, A. Prosekin

At TeV energies, the gamma-ray horizon of the Universe is limited to redshifts $z \leq 1$, and, therefore, any observation of TeV radiation from a source located beyond $z = 1$ would call for a revision of the standard paradigm. While robust observational evidence for TeV sources at redshifts

$z \geq 1$ is lacking at present, the growing number of TeV blazars with redshifts as large as $z \approx 0.5$ suggests the possibility that the standard blazar models may have to be reconsidered. We show that TeV gamma rays can be observed even from a source at $z \geq 1$, if the observed gamma rays are secondary photons produced in interactions of high-energy protons originating from the blazar jet and propagating over cosmological distances almost rectilinearly. This mechanism was initially proposed as a possible explanation for the TeV gamma rays observed from blazars with redshifts $z \approx 0.2$, for which some other explanations were possible. For TeV gamma-ray radiation detected from a blazar with $z \geq 1$, this model would provide the only viable interpretation consistent with conventional physics. It would also have far-reaching astronomical and cosmological ramifications. In particular, this interpretation would imply that extragalactic magnetic fields along the line of sight are very weak, in the range $10^{-17} \text{ G} < B < 10^{-14} \text{ G}$, assuming random fields with a correlation length of 1 Mpc, and that acceleration of $E \geq 10^{17} \text{ eV}$ protons in the jets of active galactic nuclei can be very effective. This work is published in Physical Review D[5].

Evidence for a Second Component in the High-energy Core Emission from Centaurus A?

N.V. Sahakyan, R. Yang, F.A. Aharonian, E.M. Rieger

We report on an analysis of Fermi Large Area Telescope data from four years of observations of the nearby radio galaxy Centaurus A (Cen A). The increased photon statistics results in a detection of high-energy ($>100 \text{ MeV}$) gamma-rays up to 50 GeV from the core of Cen A, with a detection significance of about 44σ . The average gamma-ray spectrum of the core reveals evidence for a possible deviation from a simple power law. A likelihood analysis with a broken power-law model shows that the photon index becomes harder above $E_b \approx 4 \text{ GeV}$, changing from $\Gamma_1 = 2.74 \pm 0.03$ below to $\Gamma_2 = 2.09 \pm 0.20$ above. This hardening could be caused by the contribution of an additional high-energy component beyond the common synchrotron self-Compton jet emission. No clear evidence for variability in the high-energy

domain is seen. We compare our results with the spectrum reported by H.E.S.S. in the TeV energy range and discuss possible origins of the hardening observed. The work is published in The Astrophysical Journal Letters[38].

Star-Jet Interactions and Gamma-Ray Outbursts from 3C454.3 *D. V. Khangulyan, M. V. Barkov, V. Ramon-Bosch, F.A. Aharonian, A.V. Dorodnytsin*

We propose a model to explain the ultra-bright GeV gamma-ray flares observed from the blazar 3C454.3. The model is based on the concept of a relativistic jet interacting with compact gas condensations produced when a star (a red giant) crosses the jet close to the central black hole. The study includes an analytical treatment of the evolution of the envelope lost by the star within the jet, and calculations of the related high-energy radiation. The model readily explains the day-long that varies on timescales of hours, GeV gamma-ray flare from 3C454.3, observed during 2010 November on top of a plateau lasting weeks. In the proposed scenario, the plateau state is caused by a strong wind generated by the heating of the stellar atmosphere due to nonthermal particles accelerated at the jet-star interaction region. The flare itself could be produced by a few clouds of matter lost by the red giant after the initial impact of the jet. In the framework of the proposed scenario, the observations constrain the key model parameters of the source, including the mass of the central black hole: $M_{\text{BH}} \approx 10^9 M_{\odot}$, the total jet power: $L_j \approx 10^{48} \text{ ergs}^{-1}$, and the Doppler factor of the gamma-ray emitting clouds: $\delta \approx 20$. Whereas we do not specify the particle acceleration mechanisms, the potential gamma-ray production processes are discussed and compared in the context of the proposed model. We argue that synchrotron radiation of protons has certain advantages compared to other radiation channels of directly accelerated electrons. An injected proton distribution $\nu \propto E^{-1}$ or harder below the relevant energies would be favoured to alleviate the tight energetic constraints and to avoid the violation of the observational low-energy constraints. The work is published in The Astrophysical Jour-

nal[23].

Unraveling the high-energy emission components of gamma-ray binaries.

V. Zabalza, V. Ramon-Bosch, D.V. Khangulyan, E.A. Aharonian

The high and very high energy spectrum of gamma-ray binaries has become a challenge for all theoretical explanations since the detection of powerful, persistent GeV emission from LS 5039 and LS I +61 303 by Fermi/LAT. The spectral cut-off at a few GeV indicates that the GeV component and the fainter, hard TeV emission above 100 GeV are not directly related. We explore the possible origins of these two emission components in the framework of a young, non-accreting pulsar orbiting the massive star, and initiating the non-thermal emission through the interaction of the stellar and pulsar winds. The pulsar/stellar wind interaction in a compact-orbit binary gives rise to two potential locations for particle acceleration: the shocks at the head-on collision of the winds and the termination shock caused by Coriolis forces on scales larger than the binary separation. We explore the suitability of these two locations to host the GeV and TeV emitters, respectively, through the study of their non-thermal emission along the orbit. We focus on the application of this model to LS 5039 given its well-determined stellar wind with respect to other gamma-ray binaries. The application of the proposed model to LS 5039 indicates that these two potential emitter locations provide the necessary conditions for reproduction of the two-component high-energy gamma-ray spectrum of LS 5039. In addition, the ambient postshock conditions required at each of the locations are consistent with recent hydrodynamical simulations. In summary, the scenario based on the interaction of the stellar and pulsar winds is compatible with the GeV and TeV emission observed from gamma-ray binaries with unknown compact objects, such as LS 5039 and LS I +61 303. This work has been published in *Astronomy and Astrophysics*[49].

Nonthermal radiation of young supernova rem-

nants: the case of Cas A *V.N. Zirakashvili, E.A. Aharonian, R. Yang, E. Ose-Wilhelmi, R.J. Tuffs*

The processes responsible for the broad-band radiation of the young supernova remnant Cas A are explored using a new code which is designed for a detailed treatment of the diffusive shock acceleration of particles in nonlinear regime. The model is based on spherically symmetric hydrodynamic equations complemented with transport equations for relativistic particles. Electrons, protons and the oxygen ions accelerated by forward and reverse shocks are included in the numerical calculations. We show that the available multi-wavelength observations in the radio, X-ray and gamma-ray bands can be best explained by invoking particle acceleration by both forward and reversed shocks. Although the TeV gamma-ray observations can be interpreted by interactions of both accelerated electrons and protons/ions, the measurements by Fermi LAT at energies below 1 GeV give a tentative preference to the hadronic origin of gamma-rays. Then, the acceleration efficiency in this source, despite the previous claims, should be very high; 25% of the explosion energy (or approximately $3 \cdot 10^{50}$ erg) should already be converted to cosmic rays, mainly by the forward shock. At the same time, the model calculations do not provide extension of the maximum energy of accelerated protons beyond 100 TeV. In this model, the acceleration of electrons is dominated by the reverse shock; the required 10^{48} erg can be achieved under the assumption that the injection of electrons (positrons) is supported by the radioactive decay of ^{44}Ti . The work is accepted for publication in *Astrophysical Journal*[81].

**The Jet and Arc Molecular Clouds toward West-
erlund 2, RCW 49, and HESS J1023-575; ^{12}CO
and ^{13}CO (J = 2-1 and J = 1-0) observations with
NANTEN2 and Mopra Telescopes** *Furukawa,
N.; Ohama, A.; Fukuda, T.; Torii, K.; Hayakawa,
T.; Sano, H.; Okuda, T.; Yamamoto, H.; Moribe,
N.; Mizuno, A.; Maezawa, H.; Onishi, T.; Kawamura,
A.; Mizuno, N.; Dawson, J. R.; Dame, T. M.;
Yonekura, Y.; Aharonian, E.; de Oña Wilhelmi, E.;
Rowell, G. P.; Matsumoto, R.; Asahina, Y.; Fukui,*

Y.

We have made new CO observations of two molecular clouds, which we call "jet" and "arc" clouds, toward the stellar cluster Westerlund 2 and the TeV γ -ray source HESS J1023–575. The jet cloud shows a linear structure from the position of Westerlund 2 on the east. In addition, we have found a new counter jet cloud on the west. The arc cloud shows a crescent shape in the west of HESS J1023–575. A sign of star formation is found at the edge of the jet cloud and gives a constraint on the age of the jet cloud to be Myr. An analysis with the multi CO transitions gives temperature as high as 20 K in a few places of the jet cloud, suggesting that some additional heating may be operating locally. The new TeV γ -ray images by H.E.S.S. correspond to the jet and arc clouds spatially better than the giant molecular clouds associated with Westerlund 2. We suggest that the jet and arc clouds are not physically linked with Westerlund 2 but are located at a greater distance around 7.5 kpc. A microquasar with long-term activity may be able to offer a possible engine to form the jet and arc clouds and to produce the TeV γ -rays, although none of the known microquasars have a Myr age or steady TeV γ -rays. Alternatively, an anisotropic supernova explosion which occurred Myr ago may be able to form the jet and arc clouds, whereas the TeV γ -ray emission requires a microquasar formed after the explosion. The results are published in *The Astrophysical Journal*, Volume 781, Issue 2, article id. 70, 20 pp. (2014).

1.1.3 HESS related activity

Felix Aharonian

During 2002 to 2007 I was the first convener of the working group of the HESS collaboration on galactic sources. Most of the HESS discoveries reported during the first several years have been conducted in this working group. Recently I was asked to take again the leadership of the same working group, given the accumulated huge amount of data, and a need for quick publications of at least the most exciting result. Currently more than 50% of my research time

goes to the organization of the activity of the working group. In particular, with a help of my two deputy-conveners, we have organized task group with an ambitious aim of preparation and submission of more than 30 papers over the next 8 to 12 months, including three important papers for the high impact journals *Nature* and *Science* on the discovery of (i) VHE gamma-ray sources in the Large Magellanic Cloud, (ii) model-independent derivation of the distribution of electrons up to 300 TeV, and the distribution of the highly turbulent magnetic fields in the pulsar wind nebula Vela -X, (iii) on the evidence of proton acceleration in the vicinity of the massive black hole located in the the centre of our Galaxy.

1.1.4 Electromagnetic Cascades, UHECR, and Neutrinos

Andrew Taylor

Search for Extended γ -ray Emission around AGN with H.E.S.S. and Fermi-LAT *K. Stycz, S. Ohm, A. M. Taylor et al., for the HESS collaboration*

Very-high-energy ($E > 100$ GeV) γ -ray emission from blazars inevitably gives rise to electron-positron pairs through their interaction with the Extragalactic Background Light (EBL). Depending on the magnetic fields in the proximity of the source, the cascade initiated from pair production can result in either an isotropic halo around an initially beamed source or a magnetically broadened cascade flux. Both extended pair halo (PH) and magnetically broadened cascade (MBC) emission from regions surrounding the blazars 1ES 1101-232, 1ES 0229+200 and PKS 2155-304 were searched for, using VHE γ -ray data taken with the High Energy Stereoscopic System (H.E.S.S.), and high energy (HE; $100 \text{ MeV} < E < 100 \text{ GeV}$) γ -ray data with the Fermi Large Area Telescope (LAT). By comparing the angular distributions of the reconstructed γ -ray events to the angular profiles calculated from detailed theoretical models, the presence of PH and MBC was investigated. Upper lim-

its on the extended emission around 1ES 1101-232, 1ES 0229+200 and PKS 2155-304 were found to be at a level of few percent of the Crab nebula flux above 1 TeV, depending on the assumed photon index of the cascade emission. Assuming strong Extra-Galactic Magnetic Field (EGMF) values, $> 10^{-12}$ G, this limits the production of pair halos developing from electromagnetic cascades. For weaker magnetic fields, in which electromagnetic cascades would result in magnetically broadened cascades, EGMF strengths in the range $(0.3 - 3) \times 10^{-15}$ G were excluded for PKS 2155-304 at the 99% confidence level, under the assumption of a 1 Mpc coherence length. This work is to be published in *Astronomy and Astrophysics*.

Measuring the correlation length of intergalactic magnetic fields from observations of gamma-ray induced cascades *A. Neronov, A. M. Taylor, C. Tchernin, Ie. Vovk*

The imaging and timing properties of γ -ray emission from electromagnetic cascades initiated by very-high-energy (VHE) γ -rays in the intergalactic medium depend on the strength B and correlation length λ_B of intergalactic magnetic fields (IGMF). We study the possibility of measuring both B and λ_B via observations of the cascade emission with γ -ray telescopes. For each measurement method, we find two characteristics of the cascade signal, which are sensitive to the IGMF B and λ_B values in different combinations. For the case of IGMF measurement using the observation of extended emission around extragalactic VHE γ -ray sources, the two characteristics are the slope of the surface brightness profile and the overall size of the cascade source. For the case of IGMF measurement from the time delayed emission, these two characteristics are the initial slope of the cascade emission light curve and the overall duration of the cascade signal. We show that measurement of the slope of the cascade induced extended emission and/or light curve can both potentially provide measure of the IGMF correlation length, provided it lies within the range $10 \text{ kpc} < \lambda_B < 1 \text{ Mpc}$. For correlation lengths outside this range, γ -ray observations can provide upper or lower bound on

λ_B . The latter of the two methods holds great promise in the near future for providing a measurement/constraint using measurements from present/next-generation γ -ray-telescopes. Measurement of the IGMF correlation length will provide an important constraint on its origin. In particular, it will enable to distinguish between an IGMF of galactic wind origin from an IGMF of cosmological origin. This work has been published in *Astronomy and Astrophysics*[33].

The Spectra of the Brightest Flaring Objects Observed by Fermi *E. Aharonian, C. Romoli, A. M. Taylor*

We are presently studying the flaring spectra of the brightest objects in the GeV domain observed by Fermi. The shape and evolution of these spectra whose origin, on dimensional grounds, must be from a compact region, hold important clues about the particle acceleration process at play. In particular, the shape of the cutoff at the high energy end of the spectrum, which is thought to be formed through either inverse Compton or synchrotron emission processes, is expected to reflect the underlying cutoff in the parent electron population. For two of the brightest objects we observe, namely the Vela pulsar and the blazar 3C 454.3, the “stretched exponential” shape of the cutoff is well measured, allowing the degree of stretching to be determined with reasonable accuracy. This work is in preparation for publication.

Ensemble Fluctuations of the Flux and Nuclear Composition of Ultra-High Energy Cosmic Ray Nuclei *M. Ahlers, L. A. Anchordoqui, A. M. Taylor*

The flux and nuclear composition of ultra-high energy cosmic rays depend on the cosmic distribution of their sources. Data from cosmic ray observatories are yet inconclusive about their exact location or distribution, but provide a measure for the average local density of these emitters. Due to the discreteness of the emitters the flux and nuclear composition is expected to show ensemble fluctuations on top of the statistical variations, i.e. “cosmic variance”. This ef-

fect is strongest for the most energetic cosmic rays due to the limited propagation distance in the cosmic radiation background and is hence a local phenomenon. For the statistical analysis of cosmic ray emission models it is important to quantify the possible level of this variance. In this work we present a completely analytic method that describes the variation of the flux and nuclear composition with respect to the local source density. We also highlight that proposed future space-based observatories with exposures of $O(10^6 \text{ km}^2 \text{ sr yr})$ will attain sensitivity to observe these spectral fluctuations in the cosmic ray energy spectrum at Earth relative to the overall power-law fit. The work is published in Physical Review D[6].

The need for hard spectra sources of nearby heavy cosmic rays *A. M. Taylor*

Using recent Auger energy spectrum and composition analysis results, an investigation is carried out into the requirements placed on the UHECR sources. The spatial distribution of these sources is investigated along with the energy distribution of UHECR they output. These investigations reveal the need for local UHECR sources which output a hard spectrum of intermediate/heavy UHECR. These results demand that local ($< 80 \text{ Mpc}$) UHECR sources exist, placing exciting and difficult requirements on the local extragalactic candidate sources. None negligible ($> 0.01 \text{ nG}$) extragalactic magnetic fields are noted to further strengthen these results. This work was published as proceedings EDP Sciences[68].

UHECR Composition Models *A. M. Taylor*

In light of the increasingly heavy UHECR composition at the highest energies, as observed by the Pierre Auger Observatory, the implications of these results on the actual source composition and spectra are investigated. Depending on the maximum energy of the particles accelerated, sources producing hard spectra and/or containing a considerably enhanced heavy component appear a necessary requirement. Consideration

is made of two archetypal models compatible with these results. The secondary signatures expected, following the propagation of the nuclear species from source to Earth, are determined for these two example cases. Finally, the effect introduced by the presence of nG extragalactic magnetic fields in collaboration with a large (80 Mpc) distance to the nearest source is discussed. This work is to be published in Astroparticle Physics.

Constraints on the Source of Ultra-High Energy Cosmic Rays using Anisotropy vs Chemical Composition *R. Liu, A. M. Taylor, M. Lemoine, X. Wang, E. Waxman*

The joint analysis of anisotropy signals and chemical composition of ultra-high energy cosmic rays offers strong potential for shedding light on the sources of these particles. Following up on an earlier idea, we investigate the anisotropies produced by protons of energy $> E/Z$, assuming that anisotropies at energy $> E$ have been produced by nuclei of charge Z , which share the same magnetic rigidity. We calculate the number of secondary protons produced through photodisintegration of the primary heavy nuclei. Making the extreme assumption that the source does not inject any proton, we find that the source(s) responsible for anisotropies such as reported by the Pierre Auger Observatory should lie closer than 20-30, 80-100 and 180-200 Mpc if the anisotropy signal is mainly composed of oxygen, silicon and iron nuclei respectively. A violation of this constraint would otherwise result in the secondary protons forming a more significant anisotropy signal at lower energies. Even if the source were located closer than this distance, it would require an extraordinary metallicity $> 120, 1600, 1100$ times solar metallicity in the acceleration zone of the source, for oxygen, silicon and iron respectively, to ensure that the concomitantly injected protons do not produce a more significant low energy anisotropy. This offers interesting prospects for constraining the nature and the source of ultra-high energy cosmic rays with the increase in statistics expected from next generation detectors. This work is published in Astrophysical Journal[25].

Detection Potential of the KM3NeT Detector for High-Energy Neutrinos from the Fermi Bubbles

S. Adrian-Martinez and A. M. Taylor et al., for the Km3NeT collaboration

A recent analysis of the Fermi Large Area Telescope data provided evidence for a high-intensity emission of high-energy gamma rays with a E^{-2} spectrum from two large areas, spanning 50 degrees above and below the Galactic centre (the “Fermi bubbles”). A hadronic mechanism was proposed for this gamma-ray emission making the Fermi bubbles promising source candidates of high-energy neutrino emission. In this work Monte Carlo simulations regarding the detectability of high-energy neutrinos from the Fermi bubbles with the future multi-km³ neutrino telescope KM3NeT in the Mediterranean Sea are presented. Under the hypothesis that the gamma-ray emission is completely due to hadronic processes, the results indicate that neutrinos from the bubbles could be discovered in about one year of operation, for a neutrino spectrum with a cutoff at 100 TeV and a detector with about 6 km³ of instrumented volume. The effect of a possible lower cutoff is also considered. This work was published in *Astroparticle Physics*[24]

1.1.5 High energy emission from binary systems.

Maria Chernyakova - DCU and DIAS

PSR B1259-63 *M. Chernyakova, A. Neronov, D. Malyshev, Yu. Babik, et al.*

In 2013 we have finished data processing from our extensive multi-wavelength observations of the 2010-2011 periastron passage of the gamma-ray loud binary system PSR B1259-63. High resolution interferometric radio observations establish extended radio emission trailing the position of the pulsar. Observations with the Fermi Gamma-ray Space Telescope reveal GeV gamma-ray flaring activity of the system, reaching the spin-down luminosity of the pulsar, around 30 days after periastron. There are no clear signatures of variability at radio, X-ray and TeV en-

ergies at the time of the GeV flare. Variability around periastron in the H α emission line, can be interpreted as the gravitational interaction between the pulsar and the circumstellar disk. The equivalent width of the H α grows from a few days before periastron until a few days later, and decreases again between 18 and 46 days after periastron. In near infrared we observe the similar decrease of the equivalent width of Br γ line between the 40th and 117th day after the periastron. For the idealized disk, the variability of the H α line represents the variability of the mass and size of the disk. We discuss possible physical relations between the state of the disk and GeV emission under assumption that GeV flare is directly related to the decrease of the disk size. The paper about all this findings is accepted by MNRAS.

LS 5039 *A. Neronov, D. Malyshev, M. Chernyakova*

LS 5039 is another high-mass X-ray binary for which the spectral energy distribution is dominated by emission in high-energy gamma-ray band. We investigate orbital modulation of the flux from LS 5039 in the 0.1-100 GeV energy band, with the aim to understand the origin of the high-energy gamma-ray emission. We perform orbital phase resolved spectral analysis based on the data of five year long monitoring of the system with Fermi telescope and supplement the high-energy gamma-ray data with the multi-wavelength data, from radio to very-high-energy gamma-rays. The orbital phase resolved spectra reveal the presence of two spectral components. One component is modulated in time, while the other component, dominating the flux above several GeV is (almost) not variable. The variability pattern of the modulated component dramatically changes below and above 100 MeV energy. This change is readily explained as being due to the orbital-phase dependent shift of the high-energy cut-off in the spectrum of the modulated component. We interpret this modulated component as the synchrotron emission from the interior of the binary system and the shift in high-energy cut-off as being due to the orbital modulation of the magnetic field strength.

We show that the non-variable component of the gamma-ray spectrum could be self-consistently explained as the high-energy IC counterpart of extended radio synchrotron emission originating from a region 10^3 times larger than the binary system size.

Cyg X-1 *Malyshev, Denys; Zdziarski, Andrzej A.; Chernyakova, Maria*

We have also searched for the GeV emission from the classical X-ray binary Cyg X-1. We have obtained measurements and upper limits on the emission of Cyg X-1 in the photon energy range of 0.03-300 GeV based on observations by Fermi. In the hard state, we detect a weak steady emission in the 0.1-10 GeV range with a power-law photon index of $\Gamma = 2.6 \pm 0.2$ at a 4σ statistical significance. This measurement, even if considered to be an upper limit, strongly constrains Compton emission of the steady radio jet, present in that state. The number of relativistic electrons in the jet has to be low enough for the spectral components due to Compton upscattering of the stellar blackbody and synchrotron radiation to be within the observed fluxes. If optically thin synchrotron emission of the jet is to account for the MeV tail, as implied by the recently claimed strong polarization in that energy range, the magnetic field in the jet has to be much above equipartition. The GeV-range measurements also strongly constrain models of hot accretion flows, most likely present in the hard state, in which γ -rays are produced from decay of neutral pions produced in collisions of energetic ions in an inner part of the flow. In the soft state, the obtained upper limits constrain electron acceleration in a non-thermal corona, most likely present around a blackbody accretion disc. The coronal emission above 30 MeV has to be rather weak, which is most readily explained by absorption of γ -rays in pair-producing photon-photon collisions. Then, the size of the bulk of the corona is less than a few tens of the gravitational radii. This work is published in MNRAS[29]

1.2 General Theory

1.2.1 The problem of small angular scale structure in the cosmic ray anisotropy data

L. O'C. Drury

A puzzling feature of the cosmic ray arrival direction distribution on the sky at TeV energies (which is now rather well determined as the background in a number of gamma-ray and neutrino experiments) is that there is clear evidence of structure on quite small angular scales (a few to twenty degrees on the sky). While it is easy to produce low order dipole, quadrupole etc anisotropies in most transport theories, the small scale structure (first seen by the Milagro experiment in its report of two "hot spots" in the arrival distribution) is much harder to explain in terms of transport processes. The amplitude of the signal is quite low at about 10^{-4} but it is statistically significant and the observations by several independent groups agree and must be taken seriously.

While there has been some speculation linking the small scale structure to heliospheric processes, this has generally been dismissed on the basis that the energy scales are wrong and that heliospheric effects (such as solar modulation) are negligible above about a GeV. However the amplitude of the signal is only at the level of 10^{-4} and thus if all particles coming from a given direction have their energy shifted slightly by a retarding or accelerating electric field of order 100MV (which is easily generated in the heliosphere by simple electromagnetic induction) it is possible to create a signal at the level of 10^{-4} in the flux of TeV particles.

This process requires incoming particles that travel in an essentially rectilinear way through the heliosphere while probing the local electric fields which naturally explains why the effect is seen at TeV energies. It also naturally explains the low observed amplitude without any fine-tuning. A further implication of the model is that negative as well as positive signals should occur (i.e. there should be cold spots and not just hot spots)

as appears to be observed.

This idea was presented at the 2013 International Cosmic Ray Conference[77].

1.2.2 Magnetic field generation in shock precursors

Turlough Downes and Luke Drury

Following on from work in 2012, the toy model developed by Drury & Downes (2012) has been further explored from the point of view of the dimensionality of the system, the angle of the initial magnetic field to the shock normal, and through incorporating a simplified radiative cooling treatment in the simulations. The dimensionality of the system considered, while clearly influencing the nature of the turbulence generated in the precursor of the blastwave, does not significantly influence the magnetic field amplification achieved. The angle of the initial magnetic field to the shock normal is found to be an important factor in determining the field amplification with a parallel shock leading to amplification roughly a factor of three less than that for a perpendicular shock. The incorporation of radiative cooling might, at first glance, appear to be likely to make a significant difference to the field amplification since it gives rise to more severe compressions in the gas in the precursor and therefore more differential acceleration. However, in spite of a detailed parameter space survey radiative cooling was found to have little impact.

The nature of the turbulence in the 2D and 3D simulations of this model was further investigated with Aoife Curran, a final year TCD project student. She calculated a series of time-averaged power spectra for different regions of the precursor, and for each of the sets of simulations described above. The 3D simulations lead, as expected, to a cascade of energy from large to small lengthscales while 2D simulations lead to the reverse. The cascading to small lengthscales leads to kinetic energies at these lengthscales which are less than that in the local magnetic field, resulting in lower amplification in 3D.

1.2.3 Analytic Solution for Self-regulated Collective Escape of Cosmic Rays from Their Acceleration Sites

M. A. Malkov, P. H. Diamond, R. Z. Sagdeev, E.A. Aharonian, Moskalenko I.A.

Supernova remnants (SNRs), as the major contributors to the galactic cosmic rays (CRs), are believed to maintain an average CR spectrum by diffusive shock acceleration regardless of the way they release CRs into the interstellar medium (ISM). However, the interaction of the CRs with nearby gas clouds crucially depends on the release mechanism. We call into question two aspects of a popular paradigm of the CR injection into the ISM, according to which they passively and isotropically diffuse in the prescribed magnetic fluctuations as test particles. First, we treat the escaping CR and the Alfvén waves excited by them on an equal footing. Second, we adopt field-aligned CR escape outside the source, where the waves become weak. An exact analytic self-similar solution for a CR "cloud" released by a dimmed accelerator strongly deviates from the test-particle result. The normalized CR partial pressure may be approximated as

$$P(p, z, t) = 2[|z|^{5/3} + z_{dif}^{5/3}(p, t)]^{-3/5} \exp[-z^2/4D_{ISM}(p)t],$$

where p is the momentum of CR particle, and z is directed along the field. The core of the cloud expands as $z_{dif} \propto \sqrt{D_{NL}(p)t}$ and decays in time as $P \propto 2z_{dif}^{-1}(t)$. The diffusion coefficient D_{NL} is strongly suppressed compared to its background ISM value D_{ISM} : $D_{NL} \approx D_{ISM} \exp(-\Pi) \ll D_{ISM}$ for sufficiently high field-line-integrated CR partial pressure Π . When $\Pi \gg 1$, the CRs drive Alfvén waves efficiently enough to build a transport barrier ($P \approx 2/|z|$ —"pedestal") that strongly reduces the leakage. The solution has a spectral break at $p = p_{br}$, where p_{br} satisfies the equation $D_{NL}(p_{br}) \simeq z^2/t$. This work is published in the *Astrophysical Journal*[28].

1.3 Star Formation

1.3.1 Characterization of Infrared Dark Clouds: NH_3 Observations of an Absorption-contrast Selected IRDC Sample

R.-A. Chira (Heidelberg), H. Beuther (Heidelberg), H. Linz (Heidelberg), F. Schuller (ESO), C. M. Walmsley, K. M. Menten (Bonn), and L. Bronfman (Santiago)

Despite increasing research in massive star formation, little is known about its earliest stages. Infrared Dark Clouds (IRDCs) are cold, dense and massive enough to harbour the sites of future high-mass star formation. But up to now, mainly small samples have been observed and analysed. To understand the physical conditions during the early stages of high-mass star formation, it is necessary to learn more about the physical conditions and stability in relatively unevolved IRDCs. Thus, for characterising IRDCs studies of large samples are needed. Walmsley et al. have investigated a complete sample of 218 northern hemisphere high-contrast IRDCs using the ammonia (1,1)- and (2,2)-inversion transitions. They detected ammonia (1,1)-inversion transition lines in 109 of their IRDC candidates. Using the data they were able to study the physical conditions within the star-forming regions statistically. They compared them with the conditions in more evolved regions that have been observed in the same fashion as their sample sources. Their results show that IRDCs have, on average, rotation temperatures of 15 K, are turbulent (with line width FWHMs around 2 km s^{-1}), have ammonia column densities on the order of 10^{14} cm^{-2} and molecular hydrogen column densities on the order of 10^{22} cm^{-2} . Their virial masses are between 100 and a few 1000 solar masses. The comparison of bulk kinetic and potential energies indicate that the sources are close to virial equilibrium. IRDCs are on average cooler and less turbulent than a comparison sample of high-mass protostellar objects, and have lower ammonia column densities. Virial parameters indicate that the majority of IRDCs are currently stable, but are expected to collapse in the future. This work

was published in *Astronomy and Astrophysics* [8].

1.3.2 X-Shooter spectroscopy of young stellar objects: Impact of chromospheric emission on accretion rate estimates

C.F. Manara (ESO), L. Testi (ESO), E. Rigliaco (Arizona), J.M. Alcalá (Naples), A. Natta, B. Stelzer (Palermo), K. Biazzo (Naples), E. Covino (Naples), S. Covino (Merate), G. Cupani (Trieste), V. D'Elia (Rome), S. Randich (Arcetri)

The lack of knowledge of photospheric parameters and the level of chromospheric activity in young low-mass pre-main sequence stars introduces uncertainties when measuring mass accretion rates in accreting (Class II) young stellar objects. A detailed investigation of the effect of chromospheric emission on the estimates of mass accretion rates in young low-mass stars is still missing. This can be undertaken using samples of young diskless (Class III) K and M-type stars. With these ideas in mind, Natta and her collaborators have measured the chromospheric activity of Class III pre-main sequence stars to determine its effect on the estimates of the accretion luminosity (L_{acc}) and mass accretion rate (\dot{M}_{acc}) in young stellar objects with disks. Using VLT/X-shooter spectra, they have analyzed a sample of 24 non-accreting young stellar objects of spectral type between K5 and M9.5. They identified the main emission lines normally used as tracers of accretion in Class II objects, and they determined their fluxes in order to estimate the contribution of the chromospheric activity to the line luminosity. They have used the relationships between line luminosity and accretion luminosity derived in the literature for Class II to evaluate the impact of chromospheric activity on the accretion rate measurements. They find that typical chromospheric activity would bias the derived accretion luminosity by $L_{\text{acc,noise}} < 10^{-3} L_{\text{sun}}$, with a strong dependence on the T_{eff} of the objects. The noise on \dot{M}_{acc} depends on stellar mass and age, and the typical values of $\log \dot{M}_{\text{acc,noise}}$ range between -9.2 to $-11.6 M_{\text{sun}}/\text{yr}$. In summary, values of $L_{\text{acc}} \leq 10^{-3} L_{\text{sun}}$ obtained in accreting low-mass pre main sequence stars

through line luminosity should be treated with caution because the line emission may be dominated by the contribution of chromospheric activity. These results have been published in *Astronomy and Astrophysics* [31].

1.3.3 An Empirical Correction for Activity Effects on the Temperatures, Radii, and Estimated Masses of Low-Mass Stars and Brown Dwarfs

K. Stassun (Vanderbilt University), K.M. Kratter (Harvard), A. Scholz, T.J. Dupuy (Harvard)

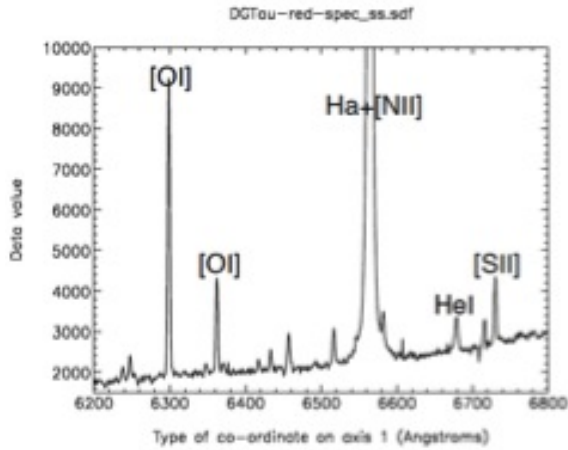
Scholz and his collaborators have presented empirical relations for determining the amount by which the effective temperatures and radii—and therefore the estimated masses—of low-mass stars and brown dwarfs are altered due to chromospheric activity. They base their relations on a large set of low-mass stars in the field with $H\alpha$ activity measurements, and on a set of low-mass eclipsing binaries with X-ray activity measurements from which they indirectly infer the $H\alpha$ activity. Both samples yield consistent relations linking the amount by which an active object's temperature is suppressed, and its radius inflated, to the strength of its $H\alpha$ emission. These relations are found to approximately preserve bolometric luminosity. They have applied these relations to the peculiar brown-dwarf eclipsing binary 2M0535-05, in which the active, higher-mass brown dwarf has a cooler temperature than its inactive, lower-mass companion. The relations correctly reproduce the observed temperatures and radii of 2M0535-05 after accounting for the $H\alpha$ emission; 2M0535-05 would be in precise agreement with theoretical isochrones were it inactive. The relations that they present are applicable to brown dwarfs and low-mass stars with masses below $0.8 M_{\text{sun}}$ and for which the activity, as measured by the fractional $H\alpha$ luminosity, is in the range $-4.6 < \log L_{H\alpha}/L_{\text{bol}} < -3.3$. They expect these relations to be most useful for correcting radius and mass estimates of low-mass stars and brown dwarfs over their active lifetimes (few Gyr) and when the ages or distances (and therefore luminosities) are unknown. Accurate estimates of stellar masses and radii are especially impor-

tant in the context of searches for transiting exoplanets, which rely upon the assumed stellar radius/density to infer the planet radius/density. They have also considered the implications of this work for improved determinations of young cluster initial mass functions. These results were presented at the January American Astronomical Society (AAS) Meeting at Long Beach, California.

1.3.4 Long-Term Monitoring of Accretion and Outflows in Young Stellar Objects: Searching for the Temporal Connection

A. Scholz, T.P. Ray, C. Davis (Liverpool), D. Froebrich (Kent), M.D. Smith (Kent)

The combined accretion and outflow process for young stars is a violent and episodic affair: Young Stellar Objects (YSOs) usually exhibit photometric variability, while the Herbig-Haro (HH) jets they drive often comprise chains of knots that probably result from variable mass loss rates and jets speeds. Scholz, Ray et al. have begun a long-term (several year) program on the robotic Liverpool Telescope (LT) on La Palma in the Canary Islands to monitor variability in young stars and, specifically, to probe the temporal link between infall and outflow using (primarily) $H\alpha$ and forbidden [OI] emission lines as proxies. Their intention is to establish how rapidly a change in accretion translates into a variation in the outflow mass loss rate and in what manner as this can reveal details of the outflow mechanism. Test observations carried out early in 2013 clearly demonstrate that the LT is very well suited to this long-term monitoring campaign.



Liverpool Telescope FRODOSpec spectrum of a outflow source.

1.3.5 Non-thermal Radio Emission from Young Stellar Object Outflows

R. Ainsworth, T.P. Ray, A. Taylor, A. Scaife (Southampton) and D. Green (Cambridge)

Most protostellar outflows have been found to produce thermal radio emission consistent with bremsstrahlung radiation from 10^4 K gas (i.e. the gas that also produces the optical/near-infrared emission by which these jets are seen). Hints however of non-thermal emission has been found in a few cases and so it was decided to image a small number of young stars at much lower radio frequencies (around 300 and 600 MHz) than normally used. These observations were carried out by R. Ainsworth (DIAS PhD student) at the Giant Metre Wave Telescope (GMRT) near Pune, India. In all cases long wavelength emission was detected, and its radio spectrum appears inverted as expected from non-thermal radiation. The origin of this emission is currently unclear but could come from diffusive shock acceleration of electrons in the outflow. Surprisingly all targets are low mass stars, suggesting low mass young stars may be a source of low energy cosmic rays.

1.3.6 Very Large Array Observations of DG Tau's Radio Jet: A Highly Collimated Thermal Outflow

C. Lynch (Iowa), R. Mutel (Iowa), M. Güdel (Vienna), T. P. Ray, S.L. Skinner (Colorado), P.C. Schneider (Hamburg), and K.G. Gayley (Iowa)

The active young protostar DG Tau has an extended jet that has been well studied at radio, optical, and X-ray wavelengths. This group have reported sensitive new Very Large Array (VLA) full-polarization observations of the core and jet between 5 GHz and 8 GHz. Their high angular resolution observation at 8 GHz clearly shows an unpolarized inner jet with a size of 42 au ($0.''35$) extending along a position angle similar to the optical-X ray outer jet. Using their nearly coeval 2012 VLA observations, we find a spectral index $\alpha = +0.46 \pm 0.05$, which combined with the lack of polarization, is consistent with bremsstrahlung (free-free) emission, with no evidence for a non-thermal coronal component. By identifying the end of the radio jet as the optical depth unity surface, and calculating the resulting emission measure, they find that their radio results are in agreement with previous optical line studies of electron density and consequent mass-loss rate. They also detect a weak radio knot at 5 GHz located $7''$ from the base of the jet, coincident with the inner radio knot detected by Rodríguez et al. in 2009 but at lower surface brightness. They interpret this as due to expansion of post-shock ionized gas in the three years between observations. These results have been published in the *Astrophysical Journal* [26].

1.3.7 New brown dwarf discs in Upper Scorpius observed with WISE

P. Dawson, A. Scholz, T.P. Ray, K.A. Marsh (Cardiff), K. Wood (St. Andrews), A. Natta, D. Padgett (NASA Goddard), and M.E. Ressler (JPL)

This group have presented a census of the disc population for UKIDSS selected brown dwarfs in the 5-10 Myr old Upper Scorpius OB asso-

ciation. For 116 objects originally identified in UKIDSS (United Kingdom Infrared Digital Sky Survey), the majority of them not studied in previous publications, they obtain photometry from the Wide-Field Infrared Survey Explorer (WISE) data base. The resulting colour-magnitude and colour-colour plots clearly show two separate populations of objects, interpreted as brown dwarfs with discs (class II) and without discs (class III). They have identified 27 class II brown dwarfs, 14 of them not previously known. This disc fraction (27 out of 116, or 23%) among brown dwarfs was found to be similar to results for K/M stars in Upper Scorpius, suggesting that the lifetimes of discs are independent of the mass of the central object for low-mass stars and brown dwarfs. 5 out of 27 discs (19%) lack excess at 3.4 and 4.6 μm and are potential transition discs (i.e. are in transition from class II to class III). The transition disc fraction is comparable to low-mass stars. They estimate that the time-scale for a typical transition from class II to class III is less than 0.4 Myr for brown dwarfs. These results suggest that the evolution of brown dwarf discs mirrors the behaviour of discs around low-mass stars, with disc lifetimes of the order of 5-10 Myr and a disc clearing time-scale significantly shorter than 1 Myr. This work has been published in Monthly Notices of the Royal Astronomical Society [26].

1.3.8 Protoplanetary Disk Masses from Stars to Brown Dwarfs

S. Mohanty (Imperial), J. Greaves (St. Andrews), D. Mortlock (Imperial), I. Pascucci (Arizona), A. Scholz, M. Thompson (Hertfordshire), D. Apai (Arizona), G. Lodato (Milan), and D. Loper (Hawaii)

This group have presented SCUBA-2 850 μm observations for 7 very low mass stars (VLMS) and brown dwarfs (BDs): 3 in Taurus, 4 in the TW Hydra Association (TWA), and all classical T Tauri (cTT) analogs. They detect 2 of the 3 Taurus disks, but none of the TWA ones. Their 3 sigma limits correspond to a dust mass of 1.2 Earth masses in Taurus and a mere 0.2 Earth masses in the TWA (3–10 times deeper than previous work).

They have combined their data with other sub-mm/mm surveys of Taurus, rho Oph and the TWA to investigate trends in disk mass and grain growth during the cTT phase. They find: (1) The minimum disk outer radius required to explain the upper envelope of sub-mm/mm fluxes is 100 au for intermediate-mass stars, solar-types and VLMS, and 20 au for BDs. (2) While the upper envelope of disk masses increases with central object mass from BDs to VLMS to solar-types, no increase is seen from solar-type to intermediate-mass stars. They propose this is due to enhanced photoevaporation around intermediate masses. (3) Many disks around Taurus and rho Oph intermediate-mass and solar-type stars evince an opacity index β of 0–1, indicating large grains. Of the only four VLMS/BDs in these regions with multi-wavelength data, three are consistent with large grains, though optically thick disks are not ruled out. (4) For the TWA VLMS (TWA 30A,B), combining their fluxes with accretion rates and ages suggests substantial grain growth by 10 Myr. The degree of grain growth in the TWA BDs (2M1207A, SSPM1102) remains largely unknown. (5) A Bayesian analysis shows that mean $(\log[M_{\text{disk}}/M_{\text{star}}]) = -2.4$, roughly constant all the way from intermediate-mass stars to VLMS/BDs, and (6) the disk mass in close solar-type Taurus binaries is significantly lower than in singles (by a factor of 10), while that in wide solar-type Taurus binaries is closer to that in singles (lower by a factor of 3). (7) They discuss the implications for planet formation, and for the dependence of accretion rate on mass of the central object. This work has been published in Astrophysical Journal [32].

1.3.9 A systematic survey for eruptive young stellar objects using mid-infrared photometry

A. Scholz, D. Froebrich (Kent) and K. Wood (St. Andrews)

Accretion in young stellar objects (YSOs) is at least partially episodic, i.e. periods with high accretion rates, i.e. bursts, are interspersed by quiescent phases. These bursts manifest themselves as eruptive variability. Scholz et al. have

presented a systematic survey for eruptive YSOs aiming to constrain the frequency of accretion bursts. They have compared mid-infrared photometry from Spitzer and WISE separated by about 5 years for two samples of YSOs, in nearby star-forming regions and in the Galactic plane, each comprising about 4000 young sources. All objects for which the brightness at 3.6 and 4.5 μm is increased by at least 1 mag between the two epochs may be eruptive variables and burst candidates. For these objects, they have carried out follow-up observations in the near-infrared. They have discovered two new eruptive variables in the Galactic Plane that could be FU Ori-type objects, with K-band amplitudes of more than 1.5 mag. One object known to undergo an accretion burst, V2492 Cyg, is recovered by their search as well. In addition, the young star ISO-Oph-50, previously suspected to be an eruptive object, is found to be better explained by a disc with varying circumstellar obscuration. In total, the number of burst events in a sample of 4000 YSOs is 1-4. Assuming that all YSOs undergo episodic accretion, this constraint can be used to show that phases of strong accretion ($>10^{-6} M_{\text{sun}} \text{ yr}^{-1}$) occur in intervals of about 10^4 years, most likely between 5000 and 50,000 years. This is consistent with the dynamical time-scales for outflows, but not with the separations of emission knots in outflows, indicating that episodic accretion could either trigger or stop collimated large-scale outflow. These results have been published in Monthly Notices of the Royal Astronomical Society [41].

1.3.10 Water in star-forming regions with Herschel (WISH): A survey of low-J H_2O line profiles

F. van der Tak (SRON), L. Chavarria (Bordeaux), F. Herpin (Bordeaux), F. Wyrowski (Bonn), M. Walmsley, E. van Dishoeck (Leiden), and the WISH Coordinating Team

To understand the origin of water line emission and absorption during high-mass star formation, this group have decomposed high-resolution Herschel-HIFI line spectra toward 19 high-mass star-forming regions into three distinct physical

components. Protostellar envelopes are usually seen as narrow absorptions or emissions in the H_2O 1113 and 1669 GHz ground-state lines, the H_2O 987 GHz excited-state line, and the H_2^{18}O 1102 GHz ground-state line. Broader features due to outflows are usually seen in absorption in the H_2O 1113 and 1669 GHz lines, in 987 GHz emission, and not seen in H_2^{18}O , indicating a low column density and a high excitation temperature. The H_2O 1113 and 1669 GHz spectra show narrow absorptions by foreground clouds along the line of sight, which have a low column density and a low excitation temperature, although their H_2O ortho/para ratios are close to 3. The intensities of the H_2O 1113 and 1669 GHz lines do not show significant trends with luminosity, mass, or age. In contrast, the 987 GHz line flux increases with luminosity and the H_2^{18}O line flux decreases with mass. Furthermore, appearance of the envelope in absorption in the 987 GHz and H_2^{18}O lines seems to be a sign of an early evolutionary stage. They conclude that the ground state transitions of H_2O trace the outer parts of the envelopes, so that the effects of star formation are mostly noticeable in the outflow wings. These lines are heavily affected by absorption, so that line ratios of H_2O involving the ground states must be treated with caution. The average H_2O abundance in high-mass protostellar envelopes does not change much with time. The 987 GHz line appears to be a good tracer of the mean weighted dust temperature of the source, which may explain why it is readily seen in distant galaxies. This work has been published by Astronomy and Astrophysics [47].

1.3.11 High-resolution ammonia mapping of the protostellar core Cha-MMS1

M. Väisälä (Helsinki), J. Harju (Turku), M. Mantere (Helsinki), O. Miettinen (Helsinki), and M. Walmsley

This group have mapped the nearby protostellar core Cha-MMS1 in the NH_3 (1, 1) line and the 1.2 cm continuum using the Australia Telescope Compact Array, ATCA. In addition, observations from the Spitzer Space Telescope and Herschel Space Observatory were used to help the inter-

pretation. An elongated condensation with a maximum length of 9000 au is seen in ammonia. The condensation has a clear velocity gradient directed perpendicularly to the axis of elongation. The gradient can be interpreted as rotation around this axis. They suggest that the observed ammonia structure delineates a rotating envelope and dense gas entrained by a very young protostellar outflow. This work has been published in IAU Symposium 292, Molecular Gas, Dust and Star Formation in Galaxies.

1.3.12 Explaining millimetre-sized particles in brown dwarf disks

P. Pinilla (Heidelberg), T. Birnstiel (Harvard), M. Benisty (Grenoble), L. Ricci (Caltech), A. Natta, C.P. Dullemond (Heidelberg), C. Dominik (Amsterdam), and L. Testi (ESO)

Planets have been detected around a variety of stars, including low-mass objects, such as brown dwarfs. However, such extreme cases are challenging for planet formation models. Recent sub-millimetre observations of disks around brown dwarf measured low spectral indices of the continuum emission that suggest that dust grains grow to mm-sizes even in these very low mass environments. To understand the first steps of planet formation in scaled-down versions of T-Tauri disks, this group have investigated the physical conditions that can theoretically explain the growth from interstellar dust to millimetre-sized grains in disks around brown dwarf. They have modelled the evolution of dust particles under conditions of low-mass disks around brown dwarfs. They used coagulation, fragmentation and disk-structure models to simulate the evolution of dust, with zero and non-zero radial drift. For the non-zero radial drift, they considered strong inhomogeneities in the gas surface density profile that mimic long-lived pressure bumps in the disk. They studied different scenarios that could lead to an agreement between theoretical models and the spectral slope found by millimetre observations. They find that fragmentation is less likely and rapid inward drift is more significant for particles in brown dwarf disks than in T-Tauri disks. They present different scenarios that

can nevertheless explain millimetre-sized grains. This work has been published in Astronomy and Astrophysics [36].

1.3.13 Physical properties of the jet from DG Tauri on sub-arcsecond scales with HST/STIS

L. Maurri (Arcetri), F. Bacciotti (Arcetri), L. Podio (Grenoble), J. Eislöffel (Tautenburg), T. P. Ray, R. Mundt (Heidelberg), U. Locatelli (Rome), and D. Coffey (UCD, Dublin)

Stellar jets are believed to play a key role in star formation, but the question of how they originate is still under debate. This group derived the physical properties at the base of the jet from DG Tau along and across the flow, and as a function of velocity. They analyze seven optical spectra of the DG Tau jet, taken with the Hubble Space Telescope Imaging Spectrograph. The spectra were obtained by placing a long-slit parallel to the jet axis, and stepping it across the jet width. The resulting position-velocity diagrams, in optical forbidden emission lines, allowed access to plasma conditions via calculation of emission line ratios. In this way, they produced a 3-D map (2-D in space and 1-D in velocity) of the jet's physical parameters i.e. electron density n_e , hydrogen ionization fraction x_e , and total hydrogen density n_H . They find at the base of the jet a high electron density, $n_e \sim 10^5$, and a very low ionization, $x_e \sim 0.02 - 0.05$, which combine to give a total density up to $n_H \sim 3 \times 10^6$. Furthermore, a spatial coincidence is revealed between sharp gradients in the excitation parameters and supersonic velocity jumps. This strongly suggests that the emission is caused by shock excitation. The derived global properties of the DG Tau jet are demonstrated to be consistent with magneto-centrifugal theory. However, non-stationary modeling is required in order to explain all of the features revealed at high resolution. This work has been accepted by Astronomy and Astrophysics.

1.3.14 Near-Infrared spectroscopy of young brown dwarfs

P. Dawson, A. Scholz, T.P. Ray, D.E. Peterson (CfA, Harvard), and D. Rodgers-Lee

Spectroscopic follow-up is a pre-requisite for studies on the formation and early evolution of brown dwarfs. This group have obtained NASA IRTF/SpeX near-infrared spectroscopy of 30 candidate members of the young Upper Scorpius Association (UpSco), selected from their previous survey work. All 24 high confidence members are confirmed as young very low mass objects with spectral types from M5 to L1, 15-20 of them are likely brown dwarfs with masses between 0.01 to 0.08 solar masses. This high yield confirms that brown dwarfs in UpSco can be identified from photometry and proper motions alone, with negligible contamination from field objects. They demonstrate that some very low mass Class II objects exhibit radically different spectra, with strong excess emission increasing towards longer wavelengths and partially filled in features in the Z and Y band. Thus, they caution against the uncritical use of near infrared spectral types for objects with discs. Furthermore, they show that hints of the same characteristics can be seen in most Class II and even a significant fraction of Class III objects (approximately 30%), indicating that some 'disc-less' objects are still surrounded by traces of circum-(sub)-stellar dust. This work has been submitted to Monthly Notices of the Royal Astronomical Society.

1.3.15 Temperaments of young stars: Rapid mass-accretion rate changes in T Tauri and Herbig Ae stars

G. Costigan, J. Vink (Armagh), A. Scholz, T.P. Ray, L. Testi (ESO)

Variability in emission lines is a characteristic feature in young stars and can be used as a tool to study the physics of the accretion process. This group conducted a study of H α variability in 15 T Tauri and Herbig Ae stars (B2 -K7) over a wide range of time windows, from minutes, to hours, to days, and years. They have assessed the vari-

ability using line-width measurements and the time series of line profiles. All objects show gradual, slow profile changes on timescales of days. In addition, in three cases there is evidence for rapid variations in H α with typical timescales of 10 min, which occurs in 10% of the total covered observing time. The mean accretion-rate changes, inferred from the line fluxes, are 0.01-0.09 dex for timescales of < 1 h, 0.1-0.4 dex for timescales of days, and 0.15-0.46 dex for timescales of years. This strongly suggests that accretion rate variability in young stars is dominated by timescales of days, in line with the upper limit found in Costigan et al. (2012). A plausible explanation for these gradual variations over days is an asymmetric accretion flow resulting in a rotational modulation of the accretion-related emission, although other interpretations are possible as well. In conjunction with their previous work, they find that the timescales and the extent of the variability is similar for objects ranging in mass from 0.1 to several solar masses. This indicates that a single mode of accretion is at work from T Tauri to Herbig Ae stars – across a wide range of stellar masses.

1.3.16 New observations of a “dust trap” around a young star with ALMA

Nienke van der Marel (Leiden), Ewine F. van Dishoeck (Leiden, Garching), Simon Bruderer (Garching), Til Birnstiel (CfA), Paola Pinilla (Heidelberg), Cornelis P. Dullemond (Heidelberg), Tim A. van Kempen (Leiden), Markus Schmalzl (Leiden), Joanna M. Brown (CfA), Gregory J. Herczeg (Beijing), Geoffrey S. Mathews (Leiden) and Vincent Geers

This group have reported the detection of a dust trap in the disk around the young star Oph-IRS 48 using observations from the new Atacama Large Millimeter/submillimeter Array (ALMA). The 0.44 mm wavelength continuum map shows high-contrast crescent-shaped emission on one side of the star originating from millimetre-sized grains, whereas both the mid-infrared image (micrometer-sized dust) and the gas traced by CO J=6-5 indicate ring-like emission centered on the star. The difference in distribution of big grains

versus small grains/gas suggests the action of a vortex-shaped dust trap triggered by a companion. Recent disk and dust evolution models have predicted the formation of dust traps, as an answer to the long-standing “meter-sized barrier” to dust growth and eventual planet formation. These models were applied here to predict the evolution of dust size inside the trap. For the conditions in this system, the dust trap is predicted to grow particles from millimeter to comet size. This work appeared in *Science* [46].

1.3.17 The SONYC survey: Towards a complete census of brown dwarfs in star forming regions

C. K. Mužić (ESO), A. Scholz, V.C. Geers, R. Jayawardhana (Toronto), M. Tamura (Tokyo), P. Dawson and T. Ray

SONYC, short for “Substellar Objects in Nearby Young Clusters”, is a survey program to provide a census of the substellar population in nearby star forming regions. The group have conducted deep optical and near-infrared photometry in five young regions (NGC1333, rho Ophiuchi, Chamaeleon-I, Upper Sco, and Lupus-3), combined with proper motions, and followed by extensive spectroscopic campaigns with Subaru and VLT, in which they have obtained more than 700 spectra of candidate low-mass objects. They have identified and characterized more than 60 new sub-stellar objects, among them a handful of objects with masses close to, or below the Deuterium burning limit. Through SONYC and surveys by other groups, the sub-stellar IMF is now well characterized down to 5 - 10 Jupiter masses, and they find that the ratio of the number of stars with respect to brown dwarfs lies between 2 and 6. A comprehensive survey of NGC 1333 reveals that, down to 5 Jupiter masses, free-floating objects with planetary masses are 20-50 times less numerous than stars, i.e. their total contribution to the mass budget of the clusters can be neglected [63].

1.3.18 Investigating Proper Motions in the 2M1207A Jet

E. Whelan (Tübingen/DIAS), T. Ray, F. Cameron (ESO), F. Bacciotti (Arcetri), P. Kavanagh (Tübingen)

The 24 Jupiter Mass brown dwarf (BD), 2MASSJ12073347-3932540 (2M1207A), was first discovered to be driving an outflow through the spectro-astrometric analysis of its [OI]6300 emission region. It is now known to drive a bipolar outflow with a position angle (PA) of 65 degrees. [SII] narrowband images obtained by the group revealed a series of knots along the PA of the outflow. The furthest knot from the BD was bow-shock shaped and these results confirmed for the first time that BD outflows could be well collimated i.e. are jets, and episodic. In order to conduct a proper motion study of the knots they obtained follow-up images in [SII] and H α using FORS-2/VLT, in early 2013. The proper motion of the source is an important consideration as it is approximately along the same direction as the jet and likely has a similar magnitude. While no significant proper motion is detected in the [SII] knots there are morphological changes. It is possible that the velocity of the knots has slowed significantly with distance. From the comparison of the [SII] and H α images, H α seems to trace the shock fronts whereas [SII] the cooling zone behind the shock front. Future work includes simulating the jet to try to understand how the proper motion of the source affects the morphology of the jet and an analysis of the spectra of the knots.

1.3.19 Sub-arcsecond high-sensitivity measurements of the DG Tau jet with e-MERLIN

R. Ainsworth, T. Ray, A. Scaife (Southampton), J. Greaves (St. Andrews), and R. Beswick (Manchester)

The group have presented very high spatial resolution deep radio continuum observations at 5 GHz (6 cm) made with the new extended Multi-Element Radio Linked Interferometer Net-

work (e-MERLIN) of the young stars DG Tau A and B. Assuming it is launched very close (≈ 1 au) from the star, their results suggest that the DG Tau A outflow initially starts as a poorly focused wind and undergoes significant collimation farther along the jet (≈ 50 au). They derive jet parameters for DG Tau A and find an initial jet opening angle of 86° within 2 au of the source, a mass-loss rate of 1.5×10^{-8} solar masses per year for the ionized component of the jet, and the total ejection-to-accretion ratio to range from 0.06 to 0.3. These results are in line with predictions from magneto-hydrodynamic jet-launching theories and have been published in Monthly Notices of the Royal Astronomical Society [7].

1.3.20 Constraints on the radial distribution of the dust properties in the CQ Tauri protoplanetary disk

F. Trotta (Bologna), L. Testi (ESO), A. Natta, A. Isella (CalTech), and L. Ricci (CalTech)

Grain growth in protoplanetary disks is the first step towards the formation of the rocky cores of planets. Models predict that grains grow, migrate, and fragment in the disk and predict varying dust properties as a function of radius, age, and physical properties. High-angular resolution observations at more than one (sub-)mm wavelength are the essential tool for constraining grain growth and migration on the disk mid-plane. The group have developed a procedure to analyse self-consistently multi-wavelength (sub-)mm continuum interferometric observations of protoplanetary disks to constrain the radial distribution of dust properties. They have applied this technique to existing multi-frequency continuum mm observations of the disk around CQ Tau, an A8 pre-main sequence star with a well-studied disk. In CQ Tau, the best-fitting model has a radial dependence of the maximum grain size, which decreases from a few cm in the inner disk (≤ 40 au) to a few mm at 80 au. Nevertheless, the currently available dataset does not allow them to exclude the possibility of a uniform grain size distribution at a 3σ level. A paper on this topic has been published in Astronomy and Astrophysics [45].

1.3.21 The main sequence of three red supergiant clusters

D. Frobrich (Kent) and A. Scholz (DIAS/St. Andrews)

Massive clusters in our Galaxy are an ideal test-beds to investigate the properties and evolution of high-mass stars. They provide statistically significant samples of massive stars of uniform ages. To accurately determine the intrinsic physical properties of these stars, we need to establish the distances, ages and reddening of the clusters. One avenue to achieve this is the identification and characterization of the main-sequence (MS) members of red supergiant (RSG) rich clusters. The group have utilized publicly available data from the UKIDSS Galactic Plane Survey. They show that point spread function photometry in conjunction with standard photometric decontamination techniques allows them to identify the most likely MS members in the 10-20 Myr old clusters RSGC 1-3. They confirm the previous detection of the MS in RSGC 2 and provide the first MS detection in RSGC 1 and RSGC 3. There are in excess of 100 stars with more than 8 solar masses identified in each cluster. These MS members are concentrated towards the spectroscopically confirmed RSG stars. The group have utilized the J - K colours of the bright MS stars to determine the K-band extinction towards the clusters. The differential reddening is three times as large in the youngest cluster RSGC 1 as compared to the two older clusters RSGC 2 and RSGC 3. Spectroscopic follow-up of the cluster MS stars should lead to more precise distance and age estimates for these clusters as well as the determination of the stellar mass function in these high-mass environments. A paper has been published in Monthly Notices of the Royal Astronomical Society [10].

1.3.22 Angular momentum and disk evolution in very low mass systems

A. Scholz (DIAS/St. Andrews)

A. Scholz has recently reviewed observational results regarding the evolution of angular momentum and disks in brown dwarfs. The observations

clearly show that brown dwarfs beyond ages of 10 Myr are exclusively fast rotators and do not spin down with age. This suggests that rotational braking by magnetic winds becomes very inefficient or ceases to work in the sub-stellar regime. There is, however, some evidence for braking by disks during the first few Myrs in evolution, similar to stars. Brown dwarf disks turn out to be scaled down versions of circumstellar disks, with dust settling, grain growth, and in some cases cleared out inner regions. The global disk properties roughly scale with central object mass. The evolutionary timescales in sub-stellar disks are entirely consistent with what is found for stars, which may be challenging to understand. Given these findings, it is likely that brown dwarfs are able to form miniature planetary systems [66].

1.3.23 Accurate determination of accretion and photospheric parameters in Young Stellar Objects: the case of two candidate old disks in the Orion Nebula Cluster

C. F. Manara (ESO), G. Beccari (ESO), N. Da Rio (ESA), G. De Marchi (ESA), A. Natta, L. Ricci (CalTech), M. Robberto (STScI), L. Testi (ESO)

Current planet formation models are largely based on the observational constraint that protoplanetary disks have lifetimes around 3 Myr. Recent studies, however, report the existence of PMS stars with signatures of accretion (strictly connected with the presence of circumstellar disks) and photometrically determined ages of 30 Myr, or more. This group have presented a spectroscopic study of two major age outliers in the Orion Nebula Cluster (ONC). They use broad band, intermediate resolution VLT/X-Shooter spectra combined with an accurate method to determine the stellar parameters and the related age of the targets to confirm their peculiar age estimates and the presence of ongoing accretion. The analysis is based on a multi-component fitting technique, which derives simultaneously spectral type, extinction, and accretion properties of the objects. With this method they confirm and quantify the ongoing accretion. From

the photospheric parameters of the stars they derive their position on the HR Diagram, and the age given by evolutionary models. Together with other age indicators like the lithium equivalent width they estimate with high accuracy the age of the objects. Their study shows that the two objects analyzed are not older than the typical population of the ONC. Their results show that, while photometric determination of the photospheric parameters are an accurate method to estimate the parameters of the bulk of young stellar populations, those of individual objects with high accretion rates and extinction may be affected by large uncertainties. Broad band spectroscopic determinations should thus be used to confirm the nature of individual objects. Their analysis shows that this method allows one to obtain an accurate determination of the photospheric parameters of accreting YSOs in any nearby star-forming region. They suggest that our detailed, broad-band spectroscopy method should be used to derive accurate properties of candidate old and accreting YSOs. This work has been published in *Astronomy and Astrophysics* [30].

1.3.24 Discovery of the magnetic field in the pulsating B star β Cephei

H. Henrichs (Amsterdam), J. de Jong (Amsterdam), E. Verdugo (ESA), R. Schnerr (Amsterdam), C. Neiner (Meudon), J. Donati (Toulouse), C. Catala (Meudon), S. Shorlin (Ontario), G. Wade (Ontario), P. Veen (Amsterdam), S. Nichols (Harvard), E. Damen (Amsterdam), A. Talavera (ESA), G. Hill (Keck Observatory), L. Kaper (Amsterdam), A. Tjani (Amsterdam), V. Geers, K. Wiersema (Amsterdam), B. Plaggenborg (Amsterdam), K. Rygl (Amsterdam)

This group published the results from a long running survey (1998-2005) of circular polarisation spectroscopy of the pulsating B star β Cephei, which was suspected to host a strong magnetic field, based on the periodicity and variability in its UV wind lines, even though not helium-enriched. Results showed that β Cep hosts a sinusoidally varying magnetic field, with an amplitude of 97 ± 4 G and an average value of -

6 ± 3 G. This represents the first confirmed detection of a dipolar magnetic field in an upper main-sequence pulsating star. This work was published in *Astronomy and Astrophysics* [11].

1.3.25 The evolution of [pseudo]bulges in disk galaxies in the last 8 Gyrs

R. Azzollini, I. Trujillo (IAC, Tenerife), C. Conselice (Nottingham)

The surface brightnesses and colours of the [pseudo-]bulges of two samples of galaxies at $z \sim 0$ (742) and $0.1 < z < 1.1$ (170) were compared using deep, archive, imaging from SDSS and HST-ACS/WFC3. This group found a significant evolution of these properties in the surveyed cosmic time (~ 8 Gyr): these central structures decreasing in surface brightness by $\mu_0(g)$ of 2.5 mag/arcsec^2 , and their rest-frame g-r color reddening by 0.3 mags. These variations are almost parallel to the evolution of the stellar disks, but a slight, relative over-reddening of the centres seems to agree with an inside-out progressive dearth of star formation. Further observations however are still required to confirm this.

1.4 Invited talks and other conference activities

Felix Aharonian IAP Colloquium, Paris, Jan 11, 2013, *Astrophysics and Cosmology with next generation gamma-ray detectors*; 2nd Bego Rencontres School, 13-31 May 2013, Nice, France, *Gamma Ray Sources and Source Populations*; Chair of SOC for the 4th Workshop on High Energy Phenomena in Relativistic Outflows (HEPRO IV) 23-26 July, 2013 Heidelberg.

Luke Drury Co-chair of the SOC for meeting *Cosmic Ray Origins - beyond the Standard Model(s)* to be held in San Vito, Italy, 16-22 March 2014.

Tom Ray Plasma Astrophysics Workshop, Turin, 12-14 March; EChO Meeting, Rutherford Appleton Laboratory, 9-11 April; ESO OPC, Munich, 21-24 April; MIRI Consortium,

Chalmers, Sweden, 28-31 April; Protostars and Planets, Heidelberg, 15-19 July; SFI Summit, Athlone, 4-5 November; ESO OPC, Munich, 18-21 November.

Vincent Geers ETH Zurich Institute of Astronomy, March; MIRI Consortium, Chalmers, Sweden, 28-31 April; Protostars and Planets, Heidelberg, 15-19 July; Space Telescope Science Institute, September.

Ruymán Azzollini MIRI Consortium, Chalmers, Sweden, 28-31 April; EChO Consortium Meeting, Imperial College London, 10-13 September; Deconstructing Galaxies: Structure and Morphology in the Era of Large Surveys, ESO, Santiago, Chile, 18-22 November.

Rachael Ainsworth The Lowest Frequency Observations of Young Stars with the GMRT, The Metrewavelength Sky, Pune, India, 9-13 December.

2 Contributions to Third-level Education

2.1 Lecture courses delivered

Tom Ray gave a course of 9 lectures on introductory Astronomy and Astrophysics to Junior Freshman students and 14 lectures on Galactic Dynamics to Junior Sophister students in TCD. He also gave a seminar on the James Webb Space Telescope as part of the course for a Masters in Space Science and Technology at UCD, Dublin

Luke Drury gave a guest lecture on shock physics to the TCD taught MSc in plasma physics.

2.2 PhD students

Rachael Ainsworth Registered in TCD and supervised by Tom Ray and Anna Scaife worked on radio observations of young stellar objects, see section 1.3.5.

Iurii Babik co-funded with DCU and supervised by Masha Chernyakova worked on gamma-ray observations of binary systems, see section 1.1.5.

Grainne Costigan the Lindsay Scholar (jointly funded with Armagh Observatory), registered in QUB and supervised by Tom Ray and Aleks Scholz successfully defended her PhD thesis on "Accretion Variability in Young Stellar Objects" in October 2013.

Paul Dawson Registered in TCD and supervised by Tom Ray and Aleks Scholz worked on brown dwarf surveys, see section 1.3.7

Nakisa Nooraee Registered in UCC and supervised by Paul Callanan and Luke Drury submitted her thesis on "X-ray and optical studies of soft X-ray transients in M31". The oral examination was held in Munich on July 18th and the thesis was accepted subject to significant corrections.

Donna Rodgers-Lee Registered in TCD and supervised by Tom Ray, Antonella Natta and

Aleks Scholz worked on multi-wavelength studies of circumstellar discs, see section 1.3.14

Carlo Romoli registered in DCU and supervised by Felix Aharonian, Andrew Taylor and Masha Chernyakova began work on Fermi observations of transient sources, see section 1.1.4.

2.3 Student final year projects

Luke Drury Is supervising two theoretical physics students in TCD, Andrew Thornbury and Nikki Truss, working on analytic and computational estimates of the power requirement for re-acceleration models of cosmic ray propagation in the Galaxy.

Tom Ray supervised two Final Year Astrophysics student projects (those of Victoria McCormac and Brian Doherty) in TCD for 3 months.

2.4 Secondment

Senior technical officer Mike Smyth was seconded to UCD to assist with the development of their taught MSc programme in space technology.

3 Contributions to research infrastructure and public service

3.1 HESS, Fermi, ASTRO-H, KM3NeT, CTA

The high-energy and astroparticle physics group in DIAS remains an active member of the HESS collaboration and participates in the production of high-impact papers of HESS. We also are involved in the data analysis, interpretation and publication of results based on the publicly available data banks of the the Fermi Large Array Telescope (LAT). We actively participate in the process of writing papers on the potential of the future gamma-ray (CTA) and neutrino (KM3NeT) telescopes. Finally, we play an important role in the preparation of scientific program of the future X-ray mission ASTRO-H.

3.2 MIRI, EChO and LBASS

3.2.1 MIRI

The Mid-Infrared Instrument (MIRI) for the James Webb Space Telescope (JWST) was placed inside the Integrated Science Instrument Module (ISIM) in May in the clean room facilities at NASA Goddard (see figure). Integration was carried out using the appropriately named Horizontal Integration Tool (HIT!). Metrology tests have shown that the positioning of MIRI appears perfect and it underwent its first cryo-test in August (see below).



DIAS-related MIRI Activities:

R. Azzollini now chairs the Medium Resolution Spectroscopy (MRS) Pipeline Working Group. This involves liaising with the Software Science Branch at the Space Telescope Science Institute (STScI) as regards the JWST pipeline, coordinate actions with the other software groups regarding common issues, etc.

V. Geers worked with the Software Science Branch at STScI and Steven Beard at the UK Astronomical Technology Center (UKATC) Edinburgh to create and expand MIRI definitions and data models, and to ensure continuing compatibility between these and the JWST software created by STScI.

R. Azzollini and V. Geers worked on producing and collecting MIRI calibration data products (CDPs) from the European Consortium team. They also updated these CDPs to be compatible with the JWST MIRI data models and pipeline reduction software. The results were part of the official deliveries of CDPs from ESA to NASA, the first delivery was made in March and the second in November of 2013.

R. Azzollini has been working on the definition and implementation of an algorithm for the optimal extraction of spectra from the MRS directly from the detector. This approach has several benefits over doing it from “spectral cubes”. He is also developing a polynomial parametrisation of the spectral and spectral distortion of MRS spectra on the detector.

V. Geers worked on implementing code to insert World Coordinate System (WCS) from housekeeping logs, to prepare “dithered” data sets for testing the data reduction pipeline.

R. Azzollini and V. Geers attended several team meetings such as:

MRS working group in Leiden (April), on Optimal Extraction

MIRI test team meeting in Sweden on ISIM Cryo-Vac test campaigns, pipeline working

group activities, CDPs, etc.

R. Azzollini and V. Geers also played a major role (requiring several working weeks on site) in the JWST ISIM Cryo-Vac 1 testing campaign at NASA Goddard which MIRI was part of. Prior to this V. Geers also participated in the warm MIRI System Functional Testing at Goddard, in part as training to work on the ISIM Cryo-Vac test campaigns.

Finally R. Azzollini and V. Geers participated in testing and reviewing Build 2 of the STScI JWST Pipeline in December.

The MIRI team has reached an agreement with PASP (Publications of the Astronomical Society of the Pacific) to produce a monograph about MIRI to be published in 2014. These papers will stand as a reference for astronomers applying for time to JWST/MIRI in the future.

3.2.2 Exoplanet Characterisation Observatory (EChO)

EChO is a proposed ESA medium sized mission to determine atmospheric conditions in planets orbiting nearby stars using planetary transits. The University College London (UCL) lead consortium (G. Tinetti as Principal Investigator), which includes DIAS as a partner (T. Ray as a Co-Principal Investigator) was successful in its proposal to ESA to be considered for the next Cosmic Vision medium mission (M3) launch in 2024. It is proposed that DIAS provide the EChO filters and beam-splitters and assist with the detector software development.

3.2.3 L-BASS

L-BASS is a proposed L-Band All Sky Survey (Jodrell Bank/TCD/DIAS) with the goal of making a low-resolution (~ 13 degree), absolutely calibrated radio map of the sky at 1.4 GHz with unprecedented accuracy ($<0.1K$). It is proposed to site the instrument at Birr, Co. Offaly. The project is now at a sufficiently advanced stage that a request has been submitted to the Paul Instrument Fund (administered by the Royal Society)

to finance the building of LBASS. The novel features are: a twin tipping beam architecture using two large symmetric waveguide horns with exceptionally low sidelobes and with high polarisation purity; the use of the celestial pole as an intermediate temperature reference and use of an active cryostat to cool a matched load to produce the absolute temperature reference. The results will settle a current astrophysical controversy concerning the reality of an excess of low frequency radio emission (ARCADE 2); enhance the interpretation of the latest maps of the cosmic microwave background (CMB) radiation by enabling superior foreground subtraction; and place constraints on distortions of the CMB spectrum arising from energy inputs in the early universe.

3.3 DELL HPC summit in Dunsink

DELL held its 2nd annual HPC summit in Dunsink Observatory on 28 Nov 2013.

Following the format of last year's meeting, it featured a comprehensive programme of interactive discussions, debates and activities including an examination of the challenges facing the HPC community in both the academic and industrial space. The agenda was developed by and for the HPC community, with expert speakers and panelists from across the community, the Dell HPC team and carefully selected specialists in the field.

09:30 - 10:00	Registration & Coffee
10:00 - 10:15	Welcome and Introduction
10:15 - 11:00	Acceleration and scaling of molecular dynamics on specialist and massively-parallel hardware platforms
11:00 - 11:45	Using space-filling curves for efficient scaling in HPC
11:45 - 12:30	Power and Cooling for modern HPC
12:30 - 13:30	Lunch
13:30 - 14:15	PRACE Use Forum
14:15 - 14:45	Green MPI and Code optimization
14:45 - 15:15	Coffee Break
15:15 - 15:45	Industrial Compute Cluster for Oil and Gas
15:45 - 16:15	Many-Core Computing
16:15 - 16:45	Big Data Analytics
16:45 - 17:00	Q&A and Close

3.4 ICHEC launch of new super-computer

The Irish Centre for High-End Computing, co-founded by the section, continues to have a close association with DIAS and participates in a number of Institute events such as culture night. To announce the name and formal launch of their new super-computer (funded largely through an SFI infrastructure grant submitted by DIAS on behalf of ICHEC) an event was held in Dunsink on 13 November attended by a number of coder-dojo groups, ICHEC staff, the President of DCU and the Minister of State for Research and Innovation, Sean Sherlock TD. The Minister officially named the new machine Fionn after the legendary Irish giant.



3.5 Training week for National School teachers

In association with the Department of Education and Skills a training week for National School science teachers was held in Dunsink from 1 to 5 July.

3.6 Individual Contributions

Felix Aharonian continued as vice president of the division of the International Astronomical Union (IAU) 'High Energy Phenomena and Fundamental Physics'; as an ESA representative in the ASTRO-H project; served as an editor of the International Journal of Modern Physics; chaired the International Advisory Council of the Institute of Sciences of the Cosmos at the University of Barcelona; and was a Member of the Scientific Advisory Committee of Astroparticle Physics European Consortium (APPEC).

Luke Drury served as President of the Royal Irish Academy.

Tom Ray served as a Panel Chair (Interstellar Medium, Star Formation and Solar System) for the Observing Programme Committee (OPC) of the European Southern Observatory; on the Marie Curie Fellowship Physics Panel; on the Council of the Royal Irish Academy; as Postgraduate Studies Adviser to the School (until June 2013), on the Science and Technology Facilities Council (STFC) e-MERLIN Steering Committee; on the RIA Astronomy and Space Science Committee; on ESA's MIRI Steering Committee, as a member of the Irish Fulbright Panel, on the Management Committee of the Armagh Observatory and Planetarium and on the Management Committee of ORIGINS (a European Commission COST project).

Malcolm Walmsley continued to serve as an editor of Astronomy and Astrophysics.

4 Public Outreach

4.1 Statutory Public Lecture

University College Dublin and the Dublin Institute for Advanced Studies

4 December 2013 at 18:00
The Moore Auditorium
O'Brien Centre for Science
University College Dublin

Professor Lars Bergström
Oscar Klein Centre for Cosmoparticle Physics
University of Stockholm

2013 Statutory Public Lecture, DIAS School of Cosmic Physics

Solving the Puzzle of Dark Matter ?

Galaxy Cluster MACS J0025.4-1222:
Hubble Space Telescope ACS/WFC
Chandra X-ray Observatory

1.5 million light-years
460 kiloparsecs

The inferred distribution of dark matter (blue) and normal matter (red) in a system of two interacting galaxy clusters.
Credit: NASA, ESA, CXO, M. Bradač (UC Santa Barbara) and S. Allen (U. Stanford). The dark matter constitutes about 30% of the mass in the universe but its nature remains one of the great mysteries of contemporary physics.

The statutory public lecture of the School for 2013 was given by Professor Lars Bergström of the Oscar Klein Centre for Cosmoparticle physics in the University of Stockholm. His title was "Solving the Puzzle of Dark Matter?" and the lecture was hosted by University College Dublin in the Moore auditorium of the new O'Brien Centre for Science. A recording of the lecture is available on <https://www.youtube.com/watch?v=sQ8EA7U2GWI>.

4.2 Irish Astronomy Trail and proposed European Route des Observatoires

Within the framework of the project "Route of astronomical observatories" and of the programme "World Astronomical Heritage" of UNESCO, a preparatory mission was organized in Ireland

by the French Embassy from 26th to 30th of September 2013. The main event was a meeting held in the Crawford Observatory, Cork, on the 27th September and attended by Luke Drury and Hilary O'Donnell, Dunsink Observatory; Prof. Paul Callanan, University College Cork; Dr. Niall Smith, Blackrock Castle Observatory; Prof. Nandivada Rathnasree, Nehru Planetarium Director (India); Dr. Roger Ferlet, Institut d'Astrophysique de Paris (IAP, France); Dr. Jean-Marc Bonnet-Bidaud, Commissariat à l'Energie Atomique (France); and Dr. Claude Detrez, Embassy of France in Ireland. The Irish Astronomy Trail was presented at the meeting and it was agreed that this was a useful and simple starting point which should be replicated in France. Dr Ferlet and Prof Bonnet-Bidaud subsequently visited Dunsink Observatory on their way back to France.

4.3 Dunsink

4.3.1 General

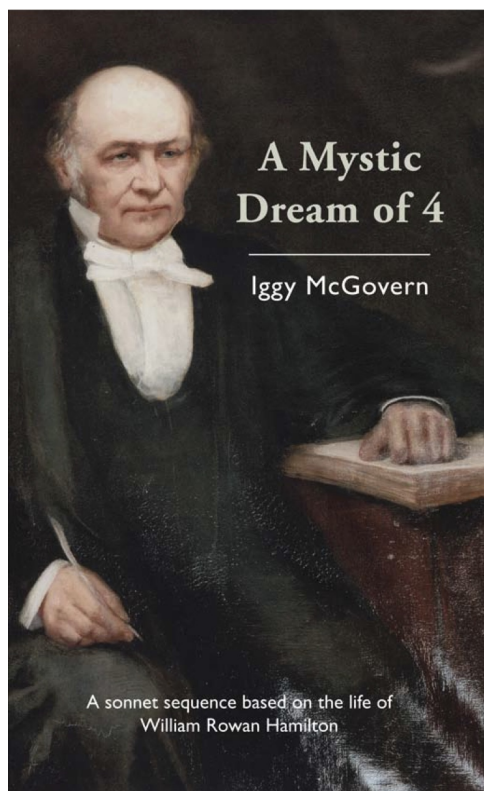
With the assistance of R. Jones, T.P. Ray carried out an audit of historical items held by the Observatory using the 1992 inventory produced by the late Patrick Wayman (Senior Professor in the School of Cosmic Physics). Of approximately 90 listed artefacts, almost all were recovered with the exception of 2 items that are currently being sought. In advance of these items being moved to make way for redecoration of the basement of Observatory House, it is intended to both re-tag and photograph all artefacts. In the course of this work, and as a result of an investigation using the archives of the Royal Irish Academy, Royal Society London and the Royal Astronomical Society, a very important historical item was recovered, a Grubb 4-inch lens (of 19 foot focal length) that is not listed in the inventory. This lens was used at Sobral, Brazil to test Einstein's Theory of General Relativity. The lens was sent to University College London, following a recommendation from the Conservation Department of the Royal Greenwich Observatory, to be dismantled and cleaned.

Albert McClure from Belfast, a professional en-

gineer who restores and maintains telescopes, has carried out routine maintenance work on the Grubb 12-inch Refractor including an overhaul of its polar axis clock, slow motion controls, finder and dome. Following discovery of rot in the dome windows, the Office of Public Works (OPW) has agreed not only to refurbish the windows but also carry out essential maintenance and preservation work on the rest of the building. It was discovered, using a historical image from the time of its construction, that the dome woodwork (including benching) is original. The OPW agreed to preserve as much of the original structure as possible.

4.3.2 A Mystic Dream of 4

Physicist and poet Iggy McGovern launched his latest volume of poetry, "A Mystic Dream of 4", a sequence of sonnets based around the life of Sir William Rowan Hamilton in Dunsink Observatory on 15 October.



4.3.3 Annual Hamilton Walk



The annual Hamilton walk, organised by NUIM in association with DIAS, took place as usual on the 16th October and attracted about a hundred participants, including some who had travelled from as far away as Finland. Sir Roger Penrose gave a short address before the walkers set off.

4.3.4 "Light Echo" exhibition

Artist Bernadette Dignam exhibited a series of textile works entitled "Light Echo" and inspired by astronomical images in Dunsink Observatory from 5-23 November. The exhibition vernisage was held on 9th Nov with a short address by Christy Dignam and a performance of two specially composed pieces for the dulcimer by musician Ute Schmidt.



**light
echo**
at dunsink observatory.

An exhibition of work
by Bernie Dignam

Opening reception
Saturday 9th November 2013 at 1.30pm
Opened by Christy Dignam

Bernie requests the pleasure of your company at the
launch where musician *Ute Schenke* will perform a
recital of *Light Echo Tune* and *Light Echo Fantasy*
especially composed by Ute for this exhibition

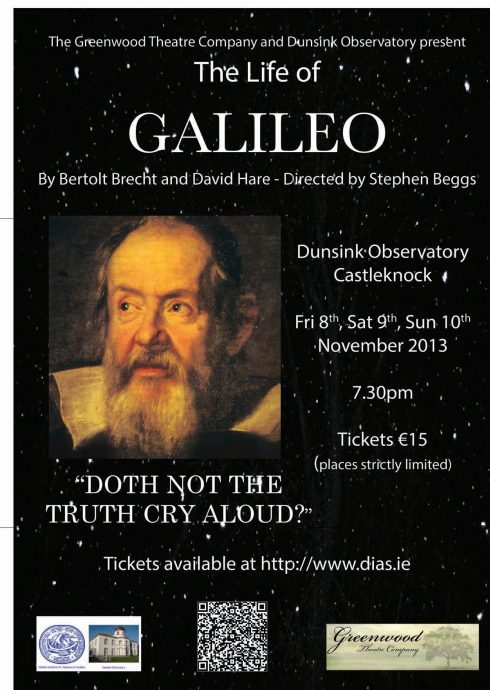
Dunsink Observatory Castleknock, Dublin 15
Exhibition open from 5th - 13th November 2013

Image: *Light Echo II* Mixed-media

www.berniedignam.com

4.3.5 Brecht's "The Life of Galileo"

As part of the lead up to Science Week, and on the initiative of Tom Ray, the Greenwood Theatre Company's acclaimed production of Brecht's "The Life of Galileo" was staged in Dunsink Observatory in a specially adapted version by David Hare from 8-10 November.



The players did four performances in total including one for Transition Year students. There was also a school's workshop held on the morning of Friday November 8 involving St Kilian's German School, Clonskeagh, and Malahide Community School.

4.3.6 Open nights and other similar events

Hilary O'Donnell et al

Continuing a long tradition the observatory runs 'public open night' (PON) events, normally on the first and third Wednesday of each month, during the winter months. In addition a large number of special events were organised for interested parties, schools, graduate associations, scout groups etc. The typical programme involves a short presentation on the solar system while people assemble followed by a short introduction to the history of the observatory and a presentation by one of our researchers or associates before, weather permitting, people are allowed to look through the Grubb refractor. This programme is run in partnership with the Irish Astronomical Association whose assistance is gratefully acknowledged.

January 2013 Wednesday 9th/16th/30th PON;
Thursday 31st Dean Mc Carthy and his 1st
and 2nd year students from Physics NUIM

February 2013 Friday 1st Family Evening Event; Monday 4th Mature Student Group UCD; Tuesday 5th PON; Wednesday 6th Family Evening event; Thursday 7th Family Evening Event Tuesday 19th Youth Study Groups from secondary schools in D15; Wednesday 20th PON; Thursday 21st Transition Students UCD

March 2013 Tuesday 5th PON; Wednesday 6th TCD Graduates association evening group; Thursday 7th Pop Up Group Evening; Friday 8th Scout Group Evening Astronomy Badge D13; Tuesday 12th PON; Wednesday 13th PON; Thursday 14th Family Evening Event; Tuesday 26th PON; Wednesday 27th Family Evening Event; Thursday 28th Pop Up Group Evening

April 2013 Wednesday 10th Association Evening Event from Co Meath; Thursday 11th French School Group from Normandy; Friday 12th Group from an International English School in Dublin; Thursday 18th Pop Up Evening Group; Friday 19th St Finian's College Mullingar

May 2013 9th/10th May Scout/Guides Groups Evening Astronomy Badge D8/15; 28th May Training Day for the Science Summer Workshop for National School Teachers scheduled for July 2013

June 2013 18th/19th International English School evening visit; Saturday 29th Solarfest all day event

July 2013 1st/5th July 2013 Training Week for National Schools science Teachers; 8th/9th International English School Visit evening visits; Saturday 13th July 2013 Round Wood History Society Visit afternoon/evening; 25th July IAA evening visit (Irish Architectural Archive Group)

September 2013 17th National School visit from West Dublin; 18th National School Visit from Ashbourne; Friday 20th Culture Evening; Friday 27th Two groups of Cubs came together, Astronomy Badge, Lucan Area

October 2013 Wednesday 2nd/17th/23rd PON; 15th Book Launch TCD Poetry; 16th Hamilton Walk afternoon; 16th Secondary School Visit, Claremorris Co Mayo; 19th Antiquarian Visit; 29th/30th Family Evening Events

November 2013 6th Arrival of players and crew for the Life of Galileo; 7th Rehearsal day for the play itself; 8th Workshop plus play for the two school groups (afternoon); 8th/9th/10th Life of Galileo performance nights; 9th Launch of Light Echo, art work stayed in situ through to the New Year; Science Week 11th/12th/14th/15th Two School visits each day; 13th November ICHEC Launch event with Minister Sean Sherlock; 13th November Social group event later that evening from Birr; 20th PON; 27th Fine Arts Group from the National College of Art; 28th Dell HPC day

December 2013 03rd Transition Students from all over Ireland through TCD afternoon and evening event; 05th/18th PON

4.4 Other Outreach Contributions

Tom Ray The James Webb Space Telescope, Astrofest, Galway, February 2; Astronomy and the Tides, Royal Irish Yacht Club, February 7, 2013 and Malahide Yacht Club, February 27; From Pebbles to Planets: Our Changing Ideas of How Planets Form, Irish Astronomical Association, Belfast, March 6; The Life and Times of Thomas and Howard Grubb, Maynooth Astronomical Society, April 6; Making Billiard Tables, Money and Telescopes: The Life and Times of the Grubbs, Malahide Historical Society, November 13; From the Solstice to Pulsars: Measuring Time in Astronomy, Solstice Public Lecture, Slane, December 20.

5 Detailed Bibliography of Publications

Note that where possible hyperlinks have been provided to the journal article and preprint version.

5.1 Peer-reviewed Publications in 2013

- [1] A. Abramowski et al. “Constraints on axionlike particles with H.E.S.S. from the irregularity of the PKS 2155-304 energy spectrum”. In: *Phys. Rev. D* 88.10, 102003 (Nov. 2013), p. 102003. DOI: [10.1103/PhysRevD.88.102003](#). arXiv: [1311.3148 \[astro-ph.HE\]](#).
- [2] A. Abramowski et al. “Search for Photon-Linelike Signatures from Dark Matter Annihilations with H.E.S.S.” In: *Physical Review Letters* 110.4, 041301 (Jan. 2013), p. 041301. DOI: [10.1103/PhysRevLett.110.041301](#). arXiv: [1301.1173 \[astro-ph.HE\]](#).
- [3] B. S. Acharya et al. “Introducing the CTA concept”. In: *Astroparticle Physics* 43 (Mar. 2013), pp. 3–18. DOI: [10.1016/j.astropartphys.2013.01.007](#).
- [4] F. A. Aharonian. “Gamma rays from supernova remnants”. In: *Astroparticle Physics* 43 (Mar. 2013), pp. 71–80. DOI: [10.1016/j.astropartphys.2012.08.007](#).
- [5] F. Aharonian et al. “TeV gamma rays from blazars beyond $z=1$?” In: *Phys. Rev. D* 87.6, 063002 (Mar. 2013), p. 063002. DOI: [10.1103/PhysRevD.87.063002](#). arXiv: [1206.6715 \[astro-ph.HE\]](#) (cit. on p. 3).
- [6] M. Ahlers, L. A. Anchordoqui, and A. M. Taylor. “Ensemble fluctuations of the flux and nuclear composition of ultrahigh energy cosmic ray nuclei”. In: *Phys. Rev. D* 87.2, 023004 (Jan. 2013), p. 023004. DOI: [10.1103/PhysRevD.87.023004](#). arXiv: [1209.5427 \[astro-ph.HE\]](#) (cit. on p. 7).
- [7] R. E. Ainsworth et al. “Subarcsecond high-sensitivity measurements of the DG Tau jet with e-MERLIN”. In: *MNRAS* 436 (Nov. 2013), pp. L64–L68. DOI: [10.1093/mnrasl/slt114](#). arXiv: [1308.2522 \[astro-ph.SR\]](#) (cit. on p. 19).
- [8] R.-A. Chira et al. “Characterization of infrared dark clouds. NH_3 observations of an absorption-contrast selected IRDC sample”. In: *A&A* 552, A40 (Apr. 2013), A40. DOI: [10.1051/0004-6361/201219567](#). arXiv: [1302.6774 \[astro-ph.SR\]](#) (cit. on p. 11).
- [9] P. Dawson et al. “New brown dwarf discs in Upper Scorpius observed with WISE”. In: *MNRAS* 429 (Feb. 2013), pp. 903–914. DOI: [10.1093/mnras/sts386](#).
- [10] D. Froebrich and A. Scholz. “The main sequence of three red supergiant clusters”. In: *MNRAS* 436 (Dec. 2013), pp. 1116–1122. DOI: [10.1093/mnras/stt1633](#). arXiv: [1308.6436 \[astro-ph.GA\]](#) (cit. on p. 19).
- [11] H. F. Henrichs et al. “Discovery of the magnetic field in the pulsating B star β Cephei”. In: *A&A* 555, A46 (July 2013), A46. DOI: [10.1051/0004-6361/201321584](#). arXiv: [1305.2601 \[astro-ph.SR\]](#) (cit. on p. 21).
- [12] H.E.S.S. Collaboration et al. “Discovery of high and very high-energy emission from the BL Lacertae object SHBL J001355.9-185406”. In: *A&A* 554, A72 (June 2013), A72. DOI: [10.1051/0004-6361/201220996](#). arXiv: [1304.4023 \[astro-ph.HE\]](#).
- [13] H.E.S.S. Collaboration et al. “Discovery of TeV γ -ray emission from PKS 0447-439 and derivation of an upper limit on its redshift”. In: *A&A* 552, A118 (Apr. 2013), A118. DOI: [10.1051/0004-6361/201321108](#). arXiv: [1303.1628 \[astro-ph.HE\]](#).
- [14] H.E.S.S. Collaboration et al. “Discovery of very high energy γ -ray emission from the BL Lacertae object PKS 0301-243 with H.E.S.S.” In: *A&A* 559, A136 (Nov. 2013), A136. DOI: [10.1051/0004-6361/201321639](#). arXiv: [1309.6174 \[astro-ph.HE\]](#).

- [15] HESS Collaboration et al. “HESS and Fermi-LAT discovery of γ -rays from the blazar 1ES 1312-423”. In: MNRAS 434 (Sept. 2013), pp. 1889–1901. DOI: [10.1093/mnras/stt1081](#). arXiv: [1306.3186 \[astro-ph.HE\]](#).
- [16] H.E.S.S. Collaboration et al. “H.E.S.S. discovery of VHE γ -rays from the quasar PKS 1510-089”. In: A&A 554, A107 (June 2013), A107. DOI: [10.1051/0004-6361/201321135](#). arXiv: [1304.8071 \[astro-ph.HE\]](#).
- [17] H.E.S.S. Collaboration et al. “H.E.S.S. observations of the binary system PSR B1259-63/LS 2883 around the 2010/2011 periastron passage”. In: A&A 551, A94 (Mar. 2013), A94. DOI: [10.1051/0004-6361/201220612](#). arXiv: [1301.3930 \[astro-ph.HE\]](#).
- [18] H.E.S.S. Collaboration et al. “Measurement of the extragalactic background light imprint on the spectra of the brightest blazars observed with H.E.S.S.” In: A&A 550, A4 (Feb. 2013), A4. DOI: [10.1051/0004-6361/201220355](#). arXiv: [1212.3409 \[astro-ph.HE\]](#).
- [19] H.E.S.S. Collaboration et al. “Search for very-high-energy γ -ray emission from Galactic globular clusters with H.E.S.S.” In: A&A 551, A26 (Mar. 2013), A26. DOI: [10.1051/0004-6361/201220719](#). arXiv: [1301.1678 \[astro-ph.HE\]](#).
- [20] L. Ji et al. “X-ray bursts as a probe of the corona: the case of XRB 4U 1636-536”. In: MNRAS 432 (July 2013), pp. 2773–2778. DOI: [10.1093/mnras/stt625](#). arXiv: [1304.5371 \[astro-ph.HE\]](#).
- [21] V. Joergens et al. “Disks, accretion and outflows of brown dwarfs”. In: *Astronomische Nachrichten* 334 (Feb. 2013), p. 159. DOI: [10.1002/asna.201211745](#). arXiv: [1208.0596 \[astro-ph.SR\]](#).
- [22] S. R. Kelner, F. A. Aharonian, and D. Khangulyan. “On the Jitter Radiation”. In: ApJ 774, 61 (Sept. 2013), p. 61. DOI: [10.1088/0004-637X/774/1/61](#). arXiv: [1304.0493 \[astro-ph.HE\]](#) (cit. on p. 1).
- [23] D. V. Khangulyan et al. “Star-Jet Interactions and Gamma-Ray Outbursts from 3C454.3”. In: ApJ 774, 113 (Sept. 2013), p. 113. DOI: [10.1088/0004-637X/774/2/113](#). arXiv: [1305.5117 \[astro-ph.HE\]](#) (cit. on p. 4).
- [24] KM3NeT Collaboration et al. “Detection potential of the KM3NeT detector for high-energy neutrinos from the Fermi bubbles”. In: *Astroparticle Physics* 42 (Feb. 2013), pp. 7–14. DOI: [10.1016/j.astropartphys.2012.11.010](#). arXiv: [1208.1226 \[astro-ph.HE\]](#) (cit. on p. 8).
- [25] R.-Y. Liu et al. “Constraints on the Source of Ultra-high-energy Cosmic Rays Using Anisotropy versus Chemical Composition”. In: ApJ 776, 88 (Oct. 2013), p. 88. DOI: [10.1088/0004-637X/776/2/88](#). arXiv: [1308.5699 \[astro-ph.HE\]](#) (cit. on p. 7).
- [26] C. Lynch et al. “Very Large Array Observations of DG Tau’s Radio Jet: A Highly Collimated Thermal Outflow”. In: ApJ 766, 53 (Mar. 2013), p. 53. DOI: [10.1088/0004-637X/766/1/53](#). arXiv: [1302.0751 \[astro-ph.SR\]](#) (cit. on pp. 13, 14).
- [27] J. Mackey and A. J. Lim. “Effects of strong magnetic fields on photoionised clouds”. In: *High Energy Density Physics* 9 (Mar. 2013), pp. 1–7. DOI: [10.1016/j.hedp.2012.09.007](#). arXiv: [1210.5385 \[astro-ph.GA\]](#).
- [28] M. A. Malkov et al. “Analytic Solution for Self-regulated Collective Escape of Cosmic Rays from Their Acceleration Sites”. In: ApJ 768, 73 (May 2013), p. 73. DOI: [10.1088/0004-637X/768/1/73](#). arXiv: [1207.4728 \[astro-ph.HE\]](#) (cit. on p. 10).
- [29] D. Malyshev, A. A. Zdziarski, and M. Chernyakova. “High-energy gamma-ray emission from Cyg X-1 measured by Fermi and its theoretical implications”. In: MNRAS 434 (Sept. 2013), pp. 2380–2389. DOI: [10.1093/mnras/stt1184](#). arXiv: [1305.5920 \[astro-ph.HE\]](#) (cit. on p. 9).
- [30] C. F. Manara et al. “Accurate determination of accretion and photospheric parameters in young stellar objects: The case of two candidate old disks in the Orion Nebula Cluster”. In: A&A 558, A114 (Oct. 2013), A114. DOI: [10.1051/0004-6361/201321866](#). arXiv: [1307.8118 \[astro-ph.SR\]](#) (cit. on p. 20).

- [31] C. F. Manara et al. “X-shooter spectroscopy of young stellar objects. II. Impact of chromospheric emission on accretion rate estimates”. In: A&A 551, A107 (Mar. 2013), A107. DOI: [10.1051/0004-6361/201220921](#). arXiv: [1301.3058 \[astro-ph.GA\]](#) (cit. on p. 12).
- [32] S. Mohanty et al. “Protoplanetary Disk Masses from Stars to Brown Dwarfs”. In: ApJ 773, 168 (Aug. 2013), p. 168. DOI: [10.1088/0004-637X/773/2/168](#). arXiv: [1305.6896 \[astro-ph.SR\]](#) (cit. on p. 14).
- [33] A. Neronov et al. “Measuring the correlation length of intergalactic magnetic fields from observations of gamma-ray induced cascades”. In: A&A 554, A31 (June 2013), A31. DOI: [10.1051/0004-6361/201321294](#). arXiv: [1307.2753 \[astro-ph.HE\]](#) (cit. on p. 6).
- [34] N. Nooraee. “Light curves of six bright soft X-ray transients in M31”. In: MNRAS 428 (Jan. 2013), pp. 205–211. DOI: [10.1093/mnras/sts024](#).
- [35] J. M. Paredes et al. “Binaries with the eyes of CTA”. In: *Astroparticle Physics* 43 (Mar. 2013), pp. 301–316. DOI: [10.1016/j.astropartphys.2012.09.004](#). arXiv: [1210.3215 \[astro-ph.HE\]](#).
- [36] P. Pinilla et al. “Explaining millimeter-sized particles in brown dwarf disks”. In: A&A 554, A95 (June 2013), A95. DOI: [10.1051/0004-6361/201220875](#). arXiv: [1304.6638 \[astro-ph.EP\]](#) (cit. on p. 16).
- [37] F. M. Rieger, E. de Oña-Wilhelmi, and F. A. Aharonian. “TeV astronomy”. In: *Frontiers of Physics* 8 (Dec. 2013), pp. 714–747. DOI: [10.1007/s11467-013-0344-6](#). arXiv: [1302.5603 \[astro-ph.HE\]](#).
- [38] N. Sahakyan et al. “Evidence for a Second Component in the High-energy Core Emission from Centaurus A?” In: ApJ 770, L6 (June 2013), p. L6. DOI: [10.1088/2041-8205/770/1/L6](#). arXiv: [1302.7173 \[astro-ph.HE\]](#) (cit. on p. 3).
- [39] Á. Sánchez-Monge et al. “A candidate circumbinary Keplerian disk in G35.20-0.74 N: A study with ALMA”. In: A&A 552, L10 (Apr. 2013), p. L10. DOI: [10.1051/0004-6361/201321134](#). arXiv: [1303.4242 \[astro-ph.GA\]](#).
- [40] Á. Sánchez-Monge et al. “Evolution and excitation conditions of outflows in high-mass star-forming regions”. In: A&A 557, A94 (Sept. 2013), A94. DOI: [10.1051/0004-6361/201321589](#). arXiv: [1305.3471 \[astro-ph.GA\]](#).
- [41] A. Scholz, D. Froebrich, and K. Wood. “A systematic survey for eruptive young stellar objects using mid-infrared photometry”. In: MNRAS 430 (Apr. 2013), pp. 2910–2922. DOI: [10.1093/mnras/stt091](#). arXiv: [1301.3152 \[astro-ph.SR\]](#) (cit. on p. 15).
- [42] A. Scholz et al. “Substellar Objects in Nearby Young Clusters. VII. The Substellar Mass Function Revisited”. In: ApJ 775, 138 (Oct. 2013), p. 138. DOI: [10.1088/0004-637X/775/2/138](#). arXiv: [1309.0823 \[astro-ph.SR\]](#).
- [43] H. Sol et al. “Active Galactic Nuclei under the scrutiny of CTA”. In: *Astroparticle Physics* 43 (Mar. 2013), pp. 215–240. DOI: [10.1016/j.astropartphys.2012.12.005](#). arXiv: [1304.3024 \[astro-ph.HE\]](#).
- [44] B. Stelzer et al. “X-shooter spectroscopy of FU Tauri A”. In: A&A 551, A106 (Mar. 2013), A106. DOI: [10.1051/0004-6361/201220736](#). arXiv: [1301.0410 \[astro-ph.SR\]](#).
- [45] F. Trotta et al. “Constraints on the radial distribution of the dust properties in the CQ Tauri protoplanetary disk”. In: A&A 558, A64 (Oct. 2013), A64. DOI: [10.1051/0004-6361/201321896](#). arXiv: [1308.5070 \[astro-ph.SR\]](#) (cit. on p. 19).
- [46] N. van der Marel et al. “A Major Asymmetric Dust Trap in a Transition Disk”. In: *Science* 340 (June 2013), pp. 1199–1202. DOI: [10.1126/science.1236770](#). arXiv: [1306.1768 \[astro-ph.EP\]](#) (cit. on p. 18).
- [47] F. F. S. van der Tak et al. “Water in star-forming regions with Herschel (WISH). IV. A survey of low-J H₂O line profiles toward high-mass protostars”. In: A&A 554, A83 (June 2013), A83. DOI: [10.1051/0004-6361/201220976](#). arXiv: [1304.2949 \[astro-ph.GA\]](#) (cit. on p. 15).

- [48] A. A. Vidotto et al. “M-dwarf stellar winds: the effects of realistic magnetic geometry on rotational evolution and planets”. In: MNRAS 438 (Feb. 2014), pp. 1162–1175. DOI: [10.1093/mnras/stt2265](#). arXiv: [1311.5063 \[astro-ph.SR\]](#).
- [49] V. Zabalza et al. “Unraveling the high-energy emission components of gamma-ray binaries”. In: A&A 551, A17 (Mar. 2013), A17. DOI: [10.1051/0004-6361/201220589](#). arXiv: [1212.3222 \[astro-ph.HE\]](#) (cit. on p. 4).

5.2 Publications in 2013 (not subject to peer-review)

- [50] F. Aharonian. “Gamma Rays at Very High Energies”. In: *Astrophysics at Very High Energies, Saas-Fee Advanced Course, Volume 40*. ISBN 978-3-642-36133-3. Springer-Verlag Berlin Heidelberg, 2013, p. 1. Ed. by F. Aharonian, L. Bergström, and C. Dermer. 2013, p. 1. DOI: [10.1007/978-3-642-36134-0_1](#).
- [51] F. A. Aharonian. “Gamma-Ray Emission of Supernova Remnants and the Origin of Galactic Cosmic Rays”. In: *Planets, Stars and Stellar Systems. Volume 5: Galactic Structure and Stellar Populations*. Ed. by T. D. Oswalt and G. Gilmore. 2013, p. 789. DOI: [10.1007/978-94-007-5612-0_15](#).
- [52] F. Aharonian, L. Bergström, and C. Dermer. *Astrophysics at Very High Energies*. 2013. DOI: [10.1007/978-3-642-36134-0](#).
- [53] R. Ainsworth et al. “The Lowest Frequency Observations of YSOs with the GMRT”. In: *Protostars and Planets VI, Heidelberg, July 15-20, 2013. Poster #1H019*. July 2013, p. 19.
- [54] S. Antonucci et al. “Accretion in Young Stellar Objects: the POISSON Spectral Survey”. In: *Protostars and Planets VI, Heidelberg, July 15-20, 2013. Poster #1B089*. July 2013, p. 89.
- [55] F. Bacciotti et al. “Physical properties of the DG Tau jet on sub-arcsecond scales with HST/STIS”. In: *Protostars and Planets VI, Heidelberg, July 15-20, 2013. Poster #1K023*. July 2013, p. 23.
- [56] G. Costigan et al. “The Importance of Rotational Time-scales in Accretion Variability”. In: *Protostars and Planets VI, Heidelberg, July 15-20, 2013. Poster #1H033*. July 2013, p. 33.
- [57] V. Geers et al. “SONYC: Sub-stellar Objects in Nearby Young Clusters”. In: *Protostars and Planets VI, Heidelberg, July 15-20, 2013. Poster #1K069*. July 2013, p. 69.
- [58] P. Hartigan et al. “Time-Series Position-Velocity Diagrams of the Jet and Low-Velocity Components in HH444”. In: *Protostars and Planets VI, Heidelberg, July 15-20, 2013. Poster #1K058*. July 2013, p. 58.
- [59] E. Lefa, F. M. Rieger, and F. A. Aharonian. “Hard Gamma-Ray Source Spectra in TeV Blazars”. In: *International Journal of Modern Physics Conference Series* 8 (2012), pp. 31–36. DOI: [10.1142/S2010194512004382](#).
- [60] C. F. Manara et al. “A VLT/X-Shooter study of accretion and photoevaporation in Transitional Disks”. In: *Protostars and Planets VI, Heidelberg, July 15-20, 2013. Poster #2S036*. July 2013, p. 36.
- [61] A. Miotello et al. “Grain growth in the envelopes of Class I protostars”. In: *Protostars and Planets VI, Heidelberg, July 15-20, 2013. Poster #1H036*. July 2013, p. 36.
- [62] G. C. Murphy, M. E. Dieckmann, and L. O’C Drury. “Field Amplification, Vortex Formation, and Electron Acceleration in a Plasma Protoshock: Effect of Asymmetric Density Profile”. In: *International Journal of Modern Physics Conference Series* 8 (2012), pp. 376–379. DOI: [10.1142/S201019451200493X](#). arXiv: [1112.5285 \[astro-ph.HE\]](#).
- [63] K. Mužić et al. “The SONYC survey: Towards a complete census of brown dwarfs in star forming regions”. In: *Mem. Soc. Astron. Italiana* 84 (2013), p. 931. arXiv: [1306.6890 \[astro-ph.GA\]](#) (cit. on p. 18).
- [64] T. Paul et al. “Sensitivity of JEM-EUSO to Ensemble Fluctuations in the Ultra-High Energy Cosmic Ray Flux”. In: *APS April Meeting Abstracts*. Apr. 2013, p. 8001.

- [65] L. Ricci et al. “ALMA and CARMA observations of brown dwarfs disks: testing the models of dust evolution .” In: *Mem. Soc. Astron. Italiana* 84 (2013), p. 885. arXiv: [1307.0463 \[astro-ph.EP\]](#).
- [66] A. Scholz. “Angular momentum and disk evolution in very low mass systems ”. In: *Mem. Soc. Astron. Italiana* 84 (2013), p. 890. arXiv: [1306.5703 \[astro-ph.SR\]](#) (cit. on p. 20).
- [67] H. Sol et al. “Prospect on intergalactic magnetic field measurements with gamma-ray instruments”. In: *IAU Symposium*. Ed. by A. G. Kosovichev, E. de Gouveia Dal Pino, and Y. Yan. Vol. 294. IAU Symposium. July 2013, pp. 459–470. DOI: [10.1017/S1743921313002925](#).
- [68] A. M. Taylor. “The need for hard spectra sources of nearby heavy cosmic rays”. In: *European Physical Journal Web of Conferences*. Vol. 53. European Physical Journal Web of Conferences. June 2013, p. 6007. DOI: [10.1051/epjconf/20135306007](#) (cit. on p. 7).
- [69] N. van der Marel et al. “Planet formation in action: Resolved gas and dust images of a transitional disk and its cavity”. In: *Protostars and Planets VI, Heidelberg, July 15-20, 2013. Poster #2H001*. July 2013, p. 1.
- [70] E. Whelan et al. “Investigating Proper Motions in the 2M1207A Jet”. In: *Protostars and Planets VI, Heidelberg, July 15-20, 2013. Poster #1K033*. July 2013, p. 33.

5.3 Preprints posted in 2013 and not yet published

- [71] F. Aharonian et al. “Pathway to the Square Kilometre Array - The German White Paper -”. In: *ArXiv e-prints* (Jan. 2013). arXiv: [1301.4124 \[astro-ph.IM\]](#).
- [72] M. Ahlers et al. “Sensitivity of JEM-EUSO to Ensemble Fluctuations in the Ultra-High Energy Cosmic Ray Flux”. In: *ArXiv e-prints* (June 2013). arXiv: [1306.0910 \[astro-ph.CO\]](#).
- [73] T. CTA Consortium et al. “CTA contributions to the 33rd International Cosmic Ray Conference (ICRC2013)”. In: *ArXiv e-prints* (July 2013). arXiv: [1307.2232 \[astro-ph.HE\]](#).
- [74] S. R. Kelner et al. “The beaming pattern of External Compton Emission from relativistic outflows”. In: *ArXiv e-prints* (Aug. 2013). arXiv: [1308.5157 \[astro-ph.HE\]](#) (cit. on p. 2).
- [75] R.-Y. Liu et al. “Diffuse PeV neutrinos from hypernova remnants in star-forming galaxies”. In: *ArXiv e-prints* (Oct. 2013). arXiv: [1310.1263 \[astro-ph.HE\]](#).
- [76] M. V. McSwain et al. “Multiwavelength Observations of Gamma-ray Binary Candidates”. In: *ArXiv e-prints* (Mar. 2013). arXiv: [1303.2018 \[astro-ph.HE\]](#).
- [77] L. O’C. Drury. “The problem of small angular scale structure in the cosmic ray anisotropy data”. In: *ArXiv e-prints* (May 2013). arXiv: [1305.6752 \[astro-ph.HE\]](#) (cit. on p. 10).
- [78] A. Y. Prosekin, S. R. Kelner, and F. A. Aharonian. “Synchrotron-to-curvature transition regime of radiation of charged particles in a dipole magnetic field”. In: *ArXiv e-prints* (May 2013). arXiv: [1305.0783 \[astro-ph.HE\]](#) (cit. on p. 2).
- [79] VERITAS Collaboration et al. “Long-term TeV and X-ray Observations of the Gamma-ray Binary HESS J0632+057”. In: *ArXiv e-prints* (Nov. 2013). arXiv: [1311.6083 \[astro-ph.HE\]](#).
- [80] R.-z. Yang, E. de Oña Wilhelmi, and F. Aharonian. “Probing Cosmic Rays in Nearby Giant Molecular Clouds with the Fermi Large Area Telescope”. In: *ArXiv e-prints* (Mar. 2013). arXiv: [1303.7323 \[astro-ph.HE\]](#).
- [81] V. N. Zirakashvili et al. “Nonthermal radiation of young supernova remnants: the case of Cas A”. In: *ArXiv e-prints* (Aug. 2013). arXiv: [1308.3742 \[astro-ph.HE\]](#) (cit. on p. 4).

2013 Research Report
School of Cosmic Physics: Geophysics Section
Draft v0.2 19 March 2013

Contents

2013 Research Report.....	1
Contents	1
1 General.....	4
1.1 Research highlights	4
1.1.1 Global Seismic Tomography	4
1.1.2 Short-listing for the Staff Member of the Year Award.....	5
1.1.3 Poster award.....	5
1.2 New external funding received in 2013	5
1.2.1 CTBTO Young Scientist Award.....	5
1.2.2 Petroleum Infrastructure Award	5
2 Electromagnetic research activities	5
2.1 IRE THERM	5
2.1.1 Research Focus 1: Geophysical assessment of the potential for Hot Dry Rock (HDR) geothermal energy provision in Ireland.....	6
2.1.2 Research Focus 2: Geophysical assessment of the potential for Hot Sedimentary Aquifer (HSA) geothermal energy provision in Ireland.....	8
2.1.3 Research Focus 3: Warm springs in Ireland	14
2.1.4 Research Focus 4: Heat production and heat distribution in Ireland’s crust	15
2.1.5 Tool development	15
2.1.6 IRE THERM publications and presentations.....	15
2.2 SAMTEX: Southern African Magnetotelluric Experiment	17
2.3 IRC SSEM.....	17
2.4 WAXI: West African Exploration Initiative	17
2.5 INDEPTH.....	19
2.5.1 1D, 2D and 3D deep-probing electromagnetic studies and petro-physical modelling of the Tibetan Plateau.....	20
2.5.2 Tibetan Plateau’s northern boundary	22
2.6 TopoMed: Plate re-organization in the western Mediterranean: Lithospheric causes and topographic consequences	23
2.7 Multi-parameter modelling/inversion	27

2.8	SIMER: Simulation of Electromagnetic response of real Rocks	27
2.9	Magnetotelluric theory and tool development	28
2.9.1	Electrical anisotropy	28
2.9.2	Distortion effects.....	28
2.9.3	Inter-station transfer functions.....	28
2.9.4	Porosity-permeability relations.....	29
2.10	Three-dimensional modelling and inversion.....	29
2.11	Other electromagnetic research.....	29
2.11.1	New Zealand geothermal activity	29
2.11.2	MaSca (Magnetotellurics in Scandes)	30
2.11.3	Electrical Moho.....	30
2.11.4	Canada.....	30
2.11.5	Other contributions	30
2.12	Main international collaborations.....	31
3	Petrological-geophysical modelling	31
3.1	Correlation of electromagnetic data with other geoscientific data.....	31
3.2	Water in olivine.....	31
3.3	Modelling Ireland's lithosphere	31
3.3.1	In two-dimensions (2D)	31
3.4	Probabilistic Inversion.....	32
3.5	Meyer-Neldel Rule	32
3.6	Other petrological-geophysical modelling activities.....	32
4	Geodynamic research activities	32
4.1	Mass-density Green's functions for the GOCE gravitational gradient tensor	32
4.2	Antarctic ice-mass balance 2003 to 2012.....	34
4.3	Interpretation of GOCE data over Congo basin	34
4.4	A benchmark study for geoid model computation codes.....	35
4.5	The adjoint sensitivity method of global electromagnetic induction for downward continuation of secular magnetic variations.....	36
4.6	The deformational response of a coupled thermomechanical ice sheet model and a viscoelastic solid Earth model.....	37
4.7	A benchmark study for global 3-D electromagnetic computation codes.....	37
5	Seismology and geodynamics	38
5.1	Ireland Array	38
5.2	Global seismic tomography.....	40

5.3	Seismic anisotropy of the Earth's mantle.....	42
5.4	Lithospheric structure of North America	43
5.5	Structure and evolution of the Arctic region.....	44
5.6	Surface-wave imaging of Asia	46
5.7	Regional seismic tomography of China	47
5.8	Seismic structure and evolution of Mongolia	48
5.9	Structure and deformation of southern Africa's lithosphere	49
5.10	Seismic study of the structure and dynamics of Tibet	51
5.11	Geodynamic modelling of continental deformation.....	53
5.12	Mapping the Moho with seismic surface waves	54
5.13	Crustal anisotropy, patterns of mechanical weakness, and destructive earthquakes in Canterbury, New Zealand.	55
5.14	Main collaborations.....	56
6	Seismological and potential field activities	56
6.1	PIMS (Porcupine Irish Margin Seismics)	56
6.2	TRIM (Tobi Rockall Irish Margins).....	57
6.3	ISUME (Irish Seismological Upper Mantle Experiment).....	58
6.4	NAPSA (North Atlantic Petroleum Systems Assessment group).....	58
6.5	Collaborations	59
7	Seismic imaging of the Irish crust for geothermal energy.....	60
7.1	Project overview.....	60
7.2	Fieldwork updates	60
7.3	Results update	60
7.4	Publications and meeting abstracts	61
8	Irish Geoscience Graduate Programme (IGGP)	62
9	The Irish National Seismic Network (INSN)	64
9.1	Local Seismic Events:	65
9.2	Teleseismic Events:.....	66
9.2.1	Earthquake in Pakistan 24-9-2013	66
9.3	North East Atlantic Mediterranean Tsunami Warning Group (NEAMTWG).....	68
10	Irish National Magnetotelluric Observatory (INMTO)	68
11	CTBTO - Comprehensive Nuclear-Test-Ban Treaty Organisation, National Data Centre (NDC).....	69
11.1	CTBTO Operations in Ireland.....	70
11.2	Involvement in CTBTO Internationally	72

11.3	CTBTO studentship.....	73
12	Collaboration with wider research community	73
12.1	Collaborations	73
12.2	Visitors	74
13	Public outreach.....	74
13.1	Seismology in Schools (Seismeolaíocht sa Scoil) Project	74
13.2	BT Young Scientist Exhibition Jan 2013	76
13.3	Other Media.....	76
14	Training, Short Courses, Workshops and Seminars	76
14.1	Training	76
14.1.1	Summer of Applied Geophysical Experience.....	76
14.1.2	International German Summer School on Hydrology	76
14.2	Short Courses	76
14.3	Seminars	76
15	Invitations and Conference Sessions organized.....	77
15.1	Invitations.....	77
15.2	Sessions organized	78
16	Miscellanea	78
	<i>A.G. Jones</i>	78
	<i>S. Lebedev</i>	78
	<i>Z. Martinec</i>	79
17	Productivity.....	79
17.1	Publications in International Literature.....	79
17.2	Theses.....	82
17.3	Invited presentations	82

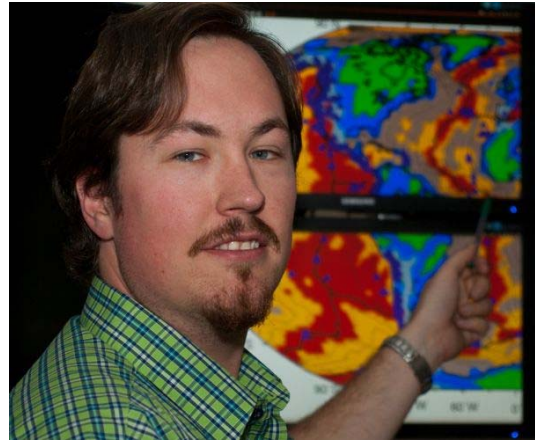
1 General

1.1 Research highlights

1.1.1 Global Seismic Tomography

Andrew Schaeffer's paper "Global shear-speed structure of the upper mantle and transition zone", with Sergei Lebedev, won one of the two 2013 Student Author Awards of the Geophysical Journal International. The awards have been established to recognise the best papers submitted to the journal by young scientists in the field. They are voted for by the journal's Editorial Board and each come with a cash prize and a framed certificate. The awards are being announced on the journal website, at the American Geophysical Union Fall Meeting in December 2013 and the European Geophysical Union General Assembly in 2014.

Andrew's paper presents global tomography of the Earth's upper mantle with an unprecedentedly large waveform dataset. His tomographic model reveals the global structure of the Earth's tectonic plates and underlying mantle in finer detail than was possible previously. Andrew's winning paper has been granted Free Access on the journal website.



1.1.2 Short-listing for the Staff Member of the Year Award

Andrew Schaeffer was short-listed for the Staff Member of the Year Award in the Irish Laboratory Awards competition, sponsored by SFI, IRC and other Irish research organisations.

1.1.3 Poster award

Sarah Blake was awarded 2nd Place in the Research & Academic Poster category competition at the Geothermal Association of Ireland Annual Conference held in Killkenny.

1.2 New external funding received in 2013

1.2.1 CTBTO Young Scientist Award

Emily Neenan was successful in her application for a CTBTO Young Scientist Award Grant, which she submitted with S. Lebedev and T. Blake of DIAS Geophysics. Her project funded by CTBTO is on high-resolution tomography of Asia using novel, automated surface-wave analysis techniques. A TCD geology graduate, Emily previously worked at DIAS as a seismology intern in 2011 and as a seismology and Seismology-in-Schools intern in late 2012-early 2013. Emily's funding, awarded to her directly, has started on March 1, 2013, after a delay of a few months due to CTBTO administration issues. Emily is now working on her MSc in the seismology group at 5 Merrion Sq. The grant covers one year of her stipend and the student fees at TCD, where she is registered.

1.2.2 Petroleum Infrastructure Award

Name: Brian O'Reilly

Funding Body: Department of Communications Energy and Natural Resources, Irish Petroleum Infrastructure Program (PIPco).

Title: An integrated geophysical and geological study of the Porcupine Basin

Amount Awarded: €352,627

2 Electromagnetic research activities

Group Leader: Senior Professor Alan G. Jones

2.1 IRE THERM

A.G. Jones, Dr. Jan Vozar (PDF), Dr. Joan Campanyà (PDS), Sarah Blake, Robert Delhaye, Thomas Farrell, plus many collaborators in Irish academia, government and industry.

IRE THERM continued on its quest until mid-2015 to develop a strategic and holistic understanding of Ireland's deep geothermal energy potential.

IRETHERM saw a significant setback in early 2013 with the sudden departure of Dr. Mark Muller in March. Muller had been the Technical Leader of the IRETHERM project, and had supervised and led the DIAS group of Dr. Jan Vozar (Post-Doctoral Fellow) and Ph.D. students Sarah Blake, Robert Delhaye and Thomas Farrell. As an immediate response, Dr. Joan Campanyà was hired on a one-year Post-Doctoral Scholarship. The advertisement for a Schrödinger Fellow was placed in the media in mid-June, and the top candidate, Dr. Volker Rath, was hired in November with a start date of April, 2014. Dr. Rath comes with considerable experience in geothermal energy issues and also a very broad modelling and numerical background.

Despite the setback of Muller leaving, the year 2013 saw yet again tremendous progress made in acquiring the geophysical and geochemical data that are needed (i) to understand the origin and distribution of heat in Ireland's upper-crust and (ii) to define the subsurface characteristics of a range of different geological settings that offer potential for geothermal energy provision in different parts of Ireland.

2.1.1 Research Focus 1: Geophysical assessment of the potential for Hot Dry Rock (HDR) geothermal energy provision in Ireland

Farrell, Jones, Dr. Martin Feely (NUIG), Professor Andrew Brock (NUIG retired)

In January to March 2013, MT and AMT data were acquired at 32 locations across the Tullow pluton of the Leinster granite and at 22 locations across the buried Kentstown granite in county Meath. This winter fieldwork season was undertaken to take advantage of the reduced electric cow-fence noise as most livestock were indoors during the cold weather.

MT and AMT data were acquired in August 2013 at 46 locations across the Galway granite and the surrounding rocks. This is in addition to data acquired at 29 locations during 2012. The data have been processed and preliminary 3d inversions have been run as an initial assessment of the data.

A connection has been made with Professor Andrew Brock, formerly with the Applied Geophysics Unit of UCG (now NUIG). Professor Brock has previously conducted research in geothermal energy in Ireland and has particular experience in borehole temperature measurements, thermal conductivity and heat-flow.

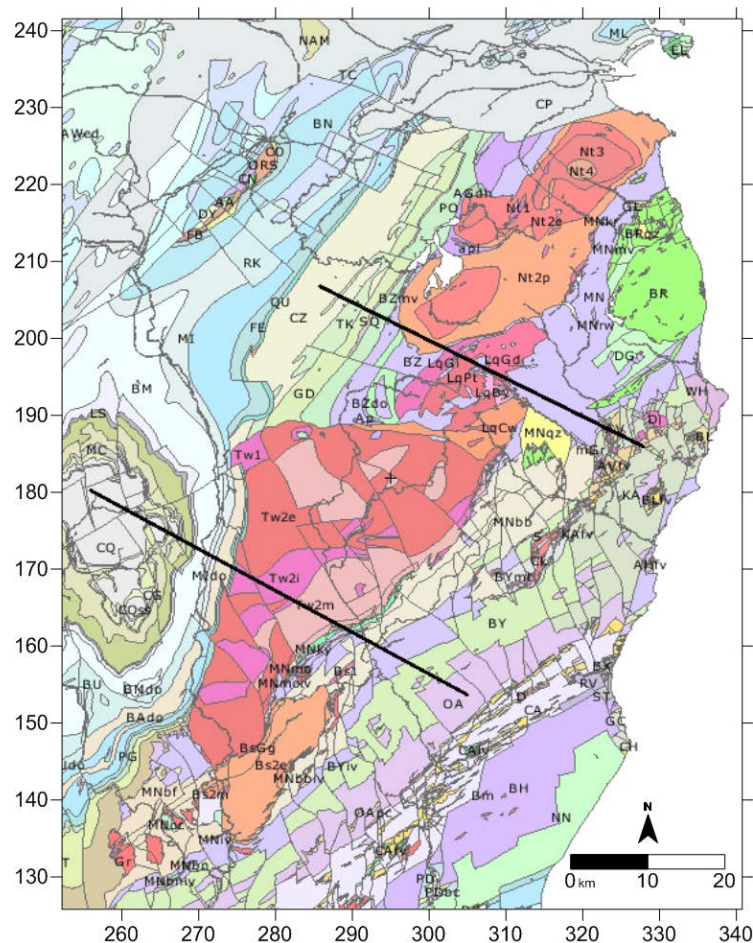


Figure 2.1.1.1 Location of the MT survey line across the Tullow pluton of the Leinster granite (southern black line)

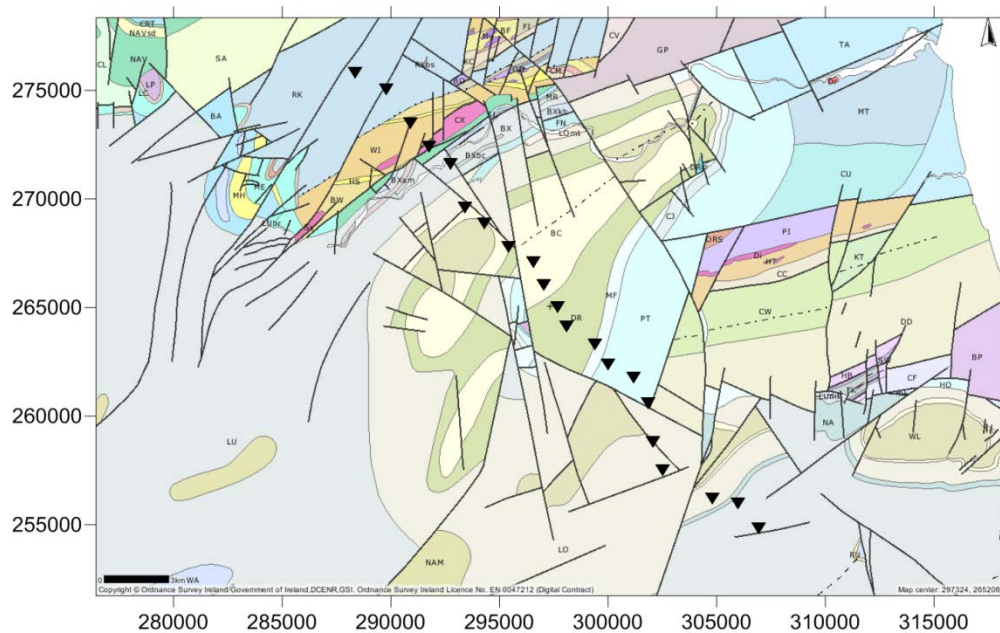


Figure 2.1.1.2 Site locations of the MT survey line across the buried Kentstown granite

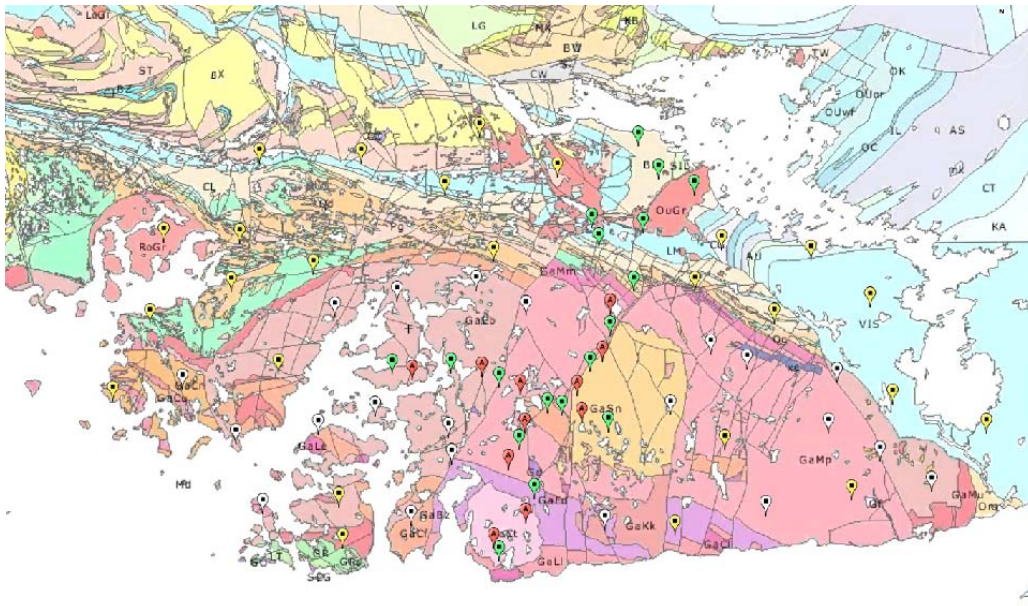


Figure 2.1.1.3: A map of the Galway MT sites. Yellow and white locations represent work done in 2013; red and green are from 2012.

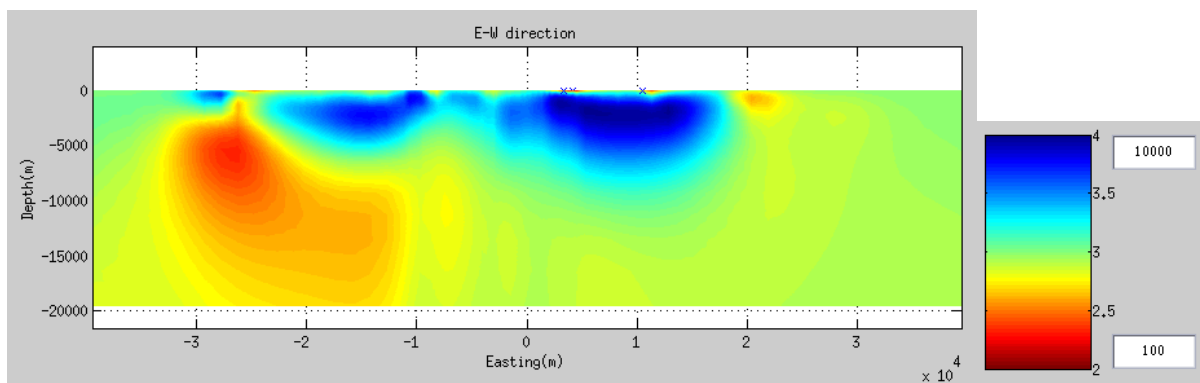


Figure 2.1.1.4: East-west 2-d slice through preliminary 3-d model of Galway granite

2.1.2 Research Focus 2: Geophysical assessment of the potential for Hot Sedimentary Aquifer (HSA) geothermal energy provision in Ireland

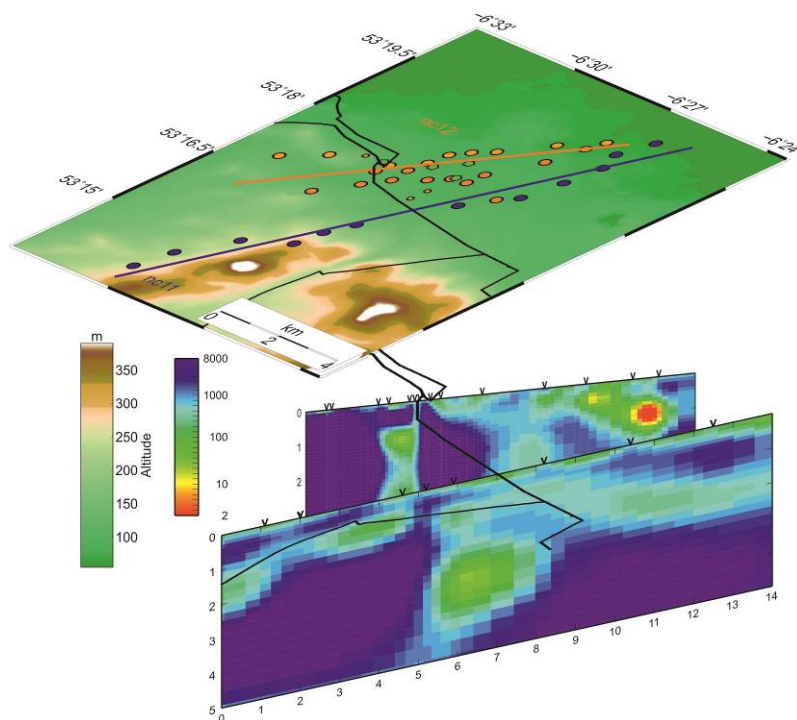
2.1.2.1 Dublin Basin

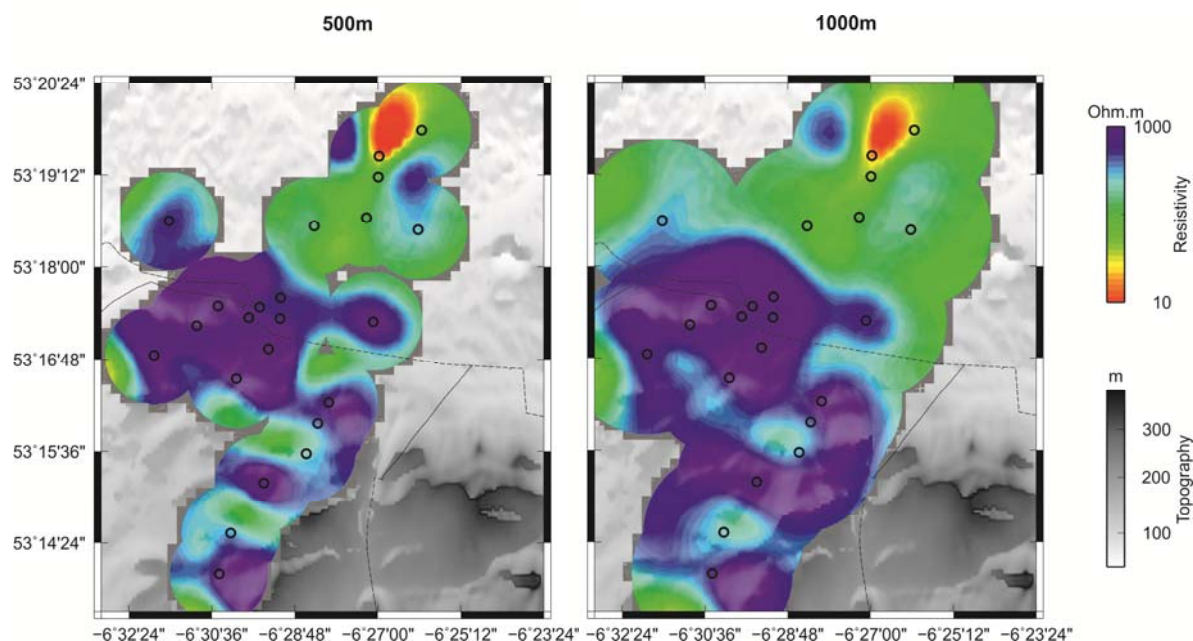
Vozar, Jones, Ric Pasquali (GT Energy)

The processing and interpretation of the Newcastle magnetotelluric (MT) data was prepared with GT energy as an industry IRETherm collaborator. The MT soundings were carried out in the highly urbanized Dublin suburb in 2011 and 2012. The MT data were heavily noise-contaminated and distorted due to electromagnetic noise from nearby industry and DC tram/railway system; processing using several robust codes to be able to obtain reliable and interpretable MT impedance and geomagnetic transfer functions. The most “quiet” 4-hour subsets of data during the night time were used in multi-site and multi-variate processing, with the most reliable sounding curves spanning the frequency range 10 kHz to 0.001 Hz. A

new novelty technique using inter-station transfer functions has been implemented as a processing tool to get broader primary data for final multi-dimensional modelling. In order to reduce galvanic distortion in the MT data, the regional 2-D strike direction must be determined. Tensor decomposition was applied at each site to determine if the data are suitable for 2D modelling and to determine the appropriate geoelectric strike direction to adopt. The final 2-D models underwent examination using a new stability technique, and the final two 2-D profiles with reliability estimations, expressed through conductance and resistivity, were prepared. As a concluding of the modelling, 3-D models of all MT data in the Newcastle area have been prepared and further on-going 3D modelling along with inter-station magnetic transfer functions have been prepared.

The modelling reveals that the Blackrock to Newcastle Fault (BNF) is imaged as a conductive area to depths of 4 km and is highly fractured. Generally, the southern area is more resistive and compact with a horizontal conductive layer at an approximately 1 km depth, and with a very thin sedimentary layer on top. The structures north of the BNF are more heterogeneous, with deeper conductive layers (2-3 km) and thicker (several hundred metres) sedimentary layers above. The deeper conductive layers are interpreted as water bearing.





2.1.2.2 Rathlin Basin

Delhaye, Jones, Annamarie Smyth (Providence Resources)

Onshore MT soundings of the Rathlin Basin were carried out in 2012, with additional MT soundings gathered on the offshore Rathlin Island in 2013 with Providence Resources' joining of IRE THERM as an industry collaborator. Data quality of each survey was generally good, with a handful of sites suffering from cultural electromagnetic noise. Impedance data from the frequency range of 10 kHz to 0.01 Hz have been used to generate 2-D models for both the offshore and onshore sounding profiles, with a preliminary 3-D model also generated for the onshore sounding array. Further analysis of the distortion and dimensionality of the data is desired to ensure clear imaging of the sediments within the basin, as the two major Mesozoic sediment groups have a subtle resistivity contrast.

Locations of MT stations over Rathlin Basin

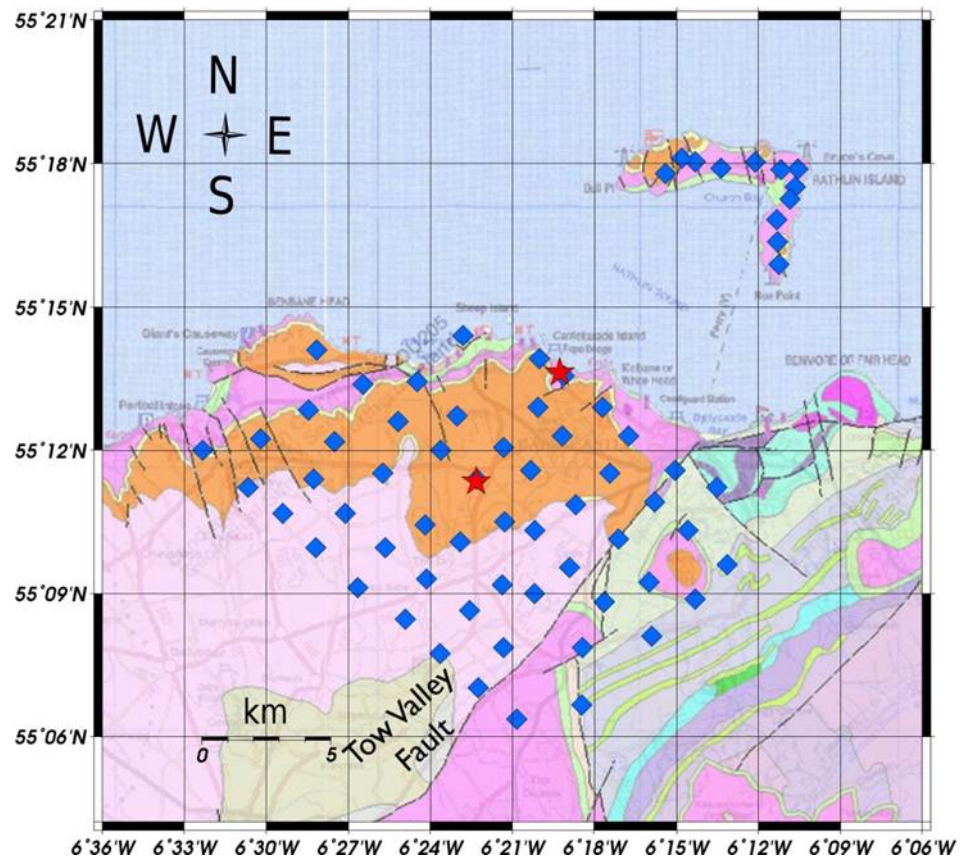


Figure 2.1.2.2.1. Map of magnetotelluric soundings over Rathlin Basin & Island (blue diamonds). Borehole locations denoted by red stars.

Depth Slices of Preliminary 3D Resistivity Model of Onshore Rathlin Basin

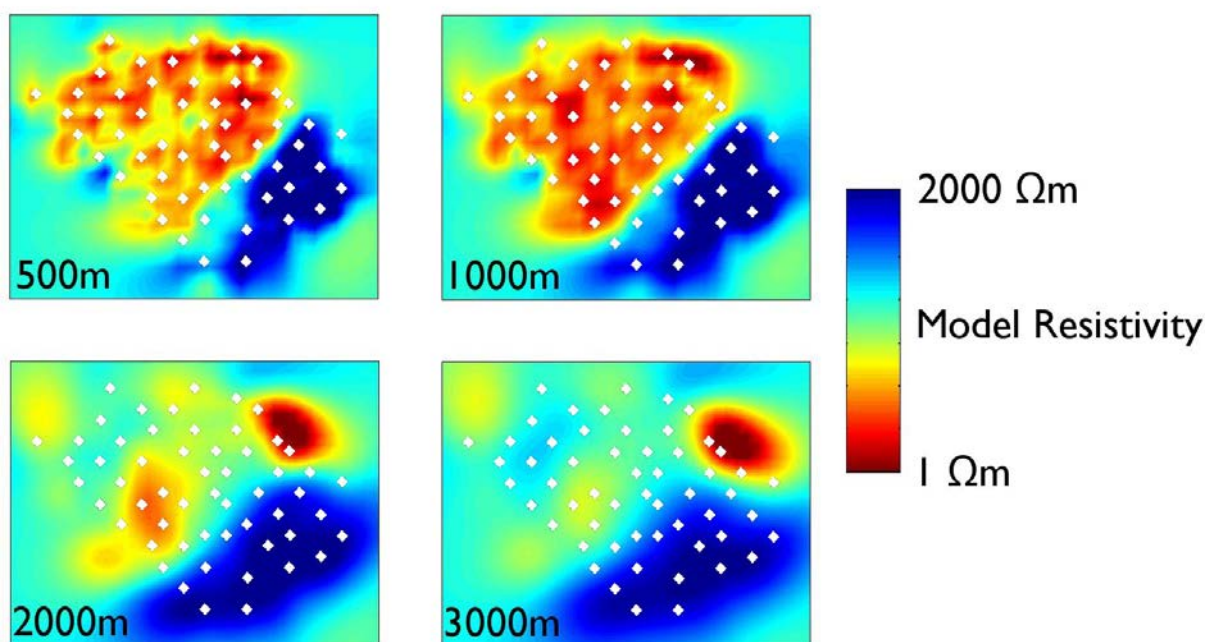


Figure 2.1.2.2.2. Depth slices from three dimensional resistivity inversion of onshore magnetotelluric soundings (white diamonds). Model misfit RMS 2.55.

Sections from 2D Resistivity Models for Rathlin Island Profiles RIE & RIN

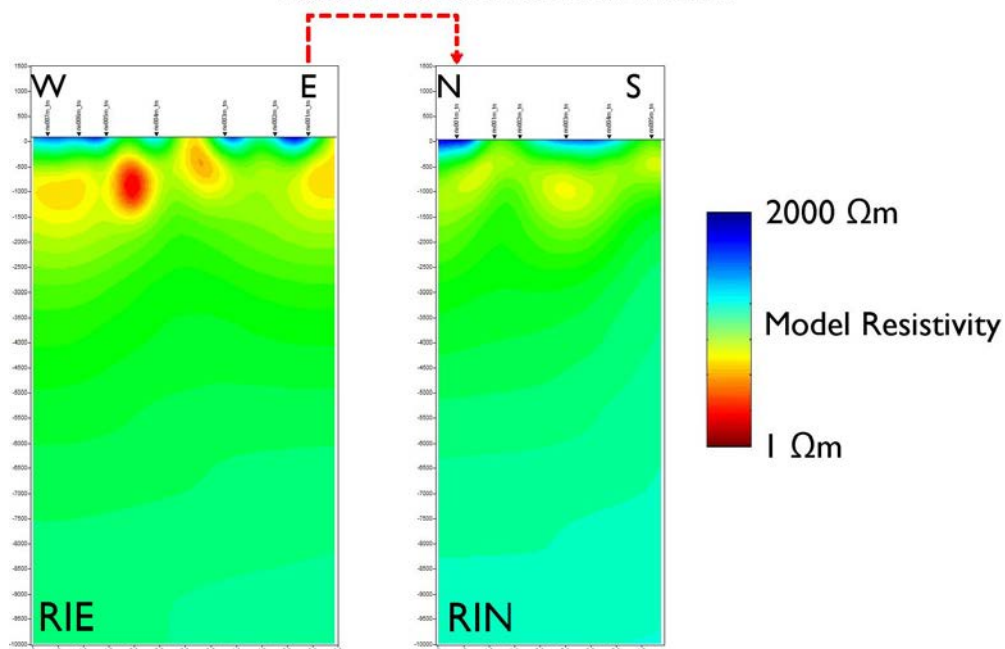


Figure 2.1.2.2.3. Profiles from two dimensional resistivity inversions of magnetotelluric soundings from Rathlin Island Profiles RIE and RIN. Models shown to 7km depth (no vertical exaggeration), and with misfits of 1.87 (RIE) and 1.76 (RIN). The two profiles intersect at site RIE001.

2.1.2.3 Donegal Seismic Area (NEW)

Delhay

The localised microseismicity in County Donegal suggests a possibility of secondary permeabilities in fault and fracture zones, which would be indicated by sub-vertical conductive zones in the generally resistive Cambrian metasedimentary country rock. As this seismic activity coincides with an area of elevated surface heat flow (from 2004 SEAI report on geothermal energy, Goodman et al.), an array of magnetotelluric soundings was planned and acquired in September 2013. A total of 51 combined MT and AMT, and 26 AMT-only soundings were acquired in an array aligned with regional fault structures. The processing of these data is in progress.

Locations of MT stations over the Lough Swilly Area

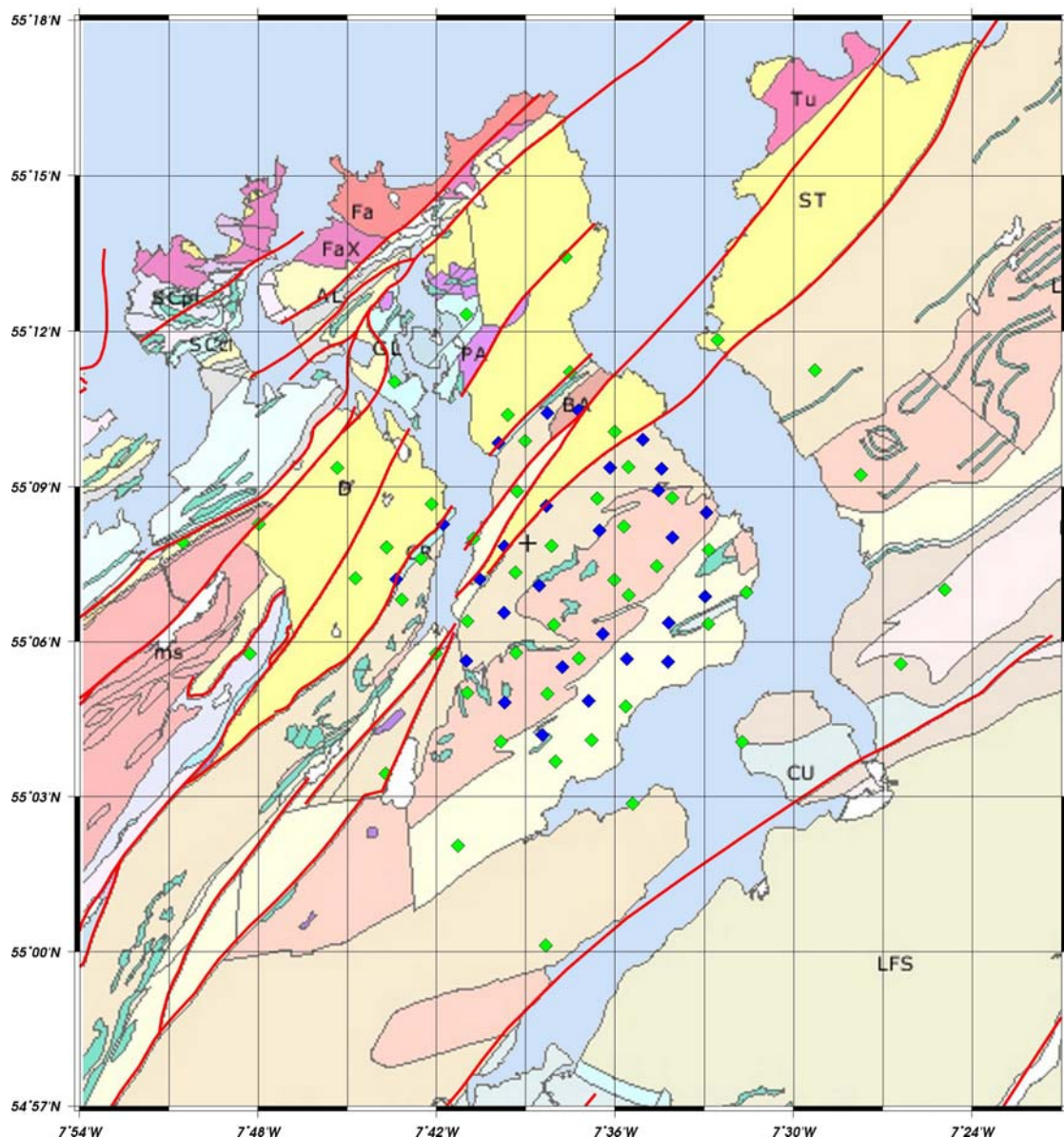


Figure 2.1.2.3.1. Magnetotelluric soundings over the Donegal seismic area. Soundings are indicated by green diamonds, with blue diamonds indicating AMT-only soundings.

2.1.3 Research Focus 3: Warm springs in Ireland

Blake, Jones, Dr. Tiernan Henry (NUIG)

The final AMT survey of the IRE THERM project was carried out over St. Gorman's Well warm spring site in Enfield, Co. Meath in October 2013. The survey followed the format of previous AMT surveys in Kilbrook, Co. Kildare and Lucan Co. Dublin and consisted of a grid of 37 AMT soundings with 200 m spacings. Recordings were made overnight in order to minimise anthropogenic noise effects and remote reference recordings were made for each sounding. Geophysical data acquisition for the investigation of the warm springs is now complete. The aim of these surveys is to identify any (electrically conductive) fluid conduit systems that may be associated with the springs and to provide an understanding of the observed association of the springs with major structural lineaments, such as the Iapetus Suture Zone that bisects Ireland.

Data from all three warm spring AMT surveys have been processed and modelling in 1D and 3D has commenced on St. Gorman's Well and Kilbrook springs. The data from St. Edmundsbury Spring, Lucan (AMT and controlled source surveys) are highly distorted by electromagnetic noise due to the site's proximity to Dublin city, so additional processing is required before modelling of this spring's data can begin.

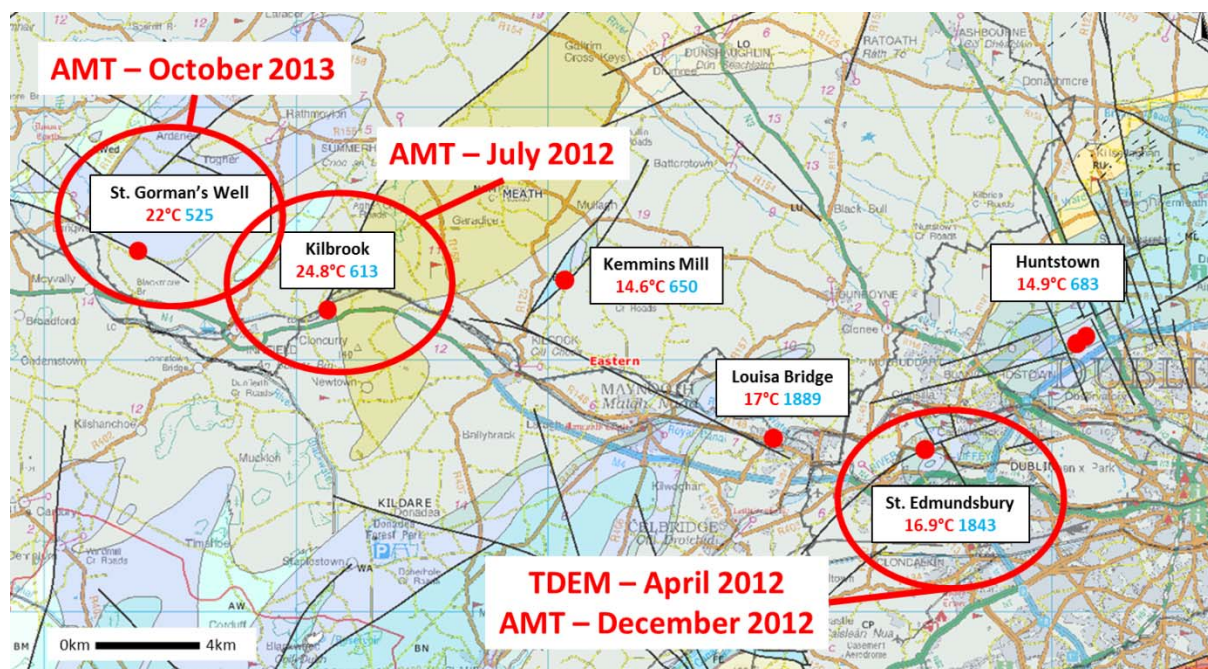


Figure 2.1.3.1. Six warm springs chosen for further investigation and geophysical surveys carried out to date. Maximum temperatures (red) and mean electrical conductivity values in $\mu\text{S}/\text{cm}$ (blue) from Burdon (1983a). Huntstown measurements collected July 2013.

The hydrochemical sampling and analysis programme commenced in July 2013 and is set to continue until the end of 2014. Six warm springs in Leinster were chosen for sampling (pictured above). Data loggers were installed in each of these locations to continuously monitor temperature and electrical conductivity fluctuations (15 minute sampling interval) and groundwater samples were collected from each spring in July 2013, October 2013 and January 2014. Sampling will continue in April and July 2014 in order to give five seasons of data. The hydrochemical results and the data from the loggers will be examined in conjunction with regional rainfall (see sample hydrograph for St. Gorman's Well below) and

available hydrogeological information in order to establish the nature of the relationship between the hydrological cycle and fluctuations in the hydrochemistry of the warm springs.

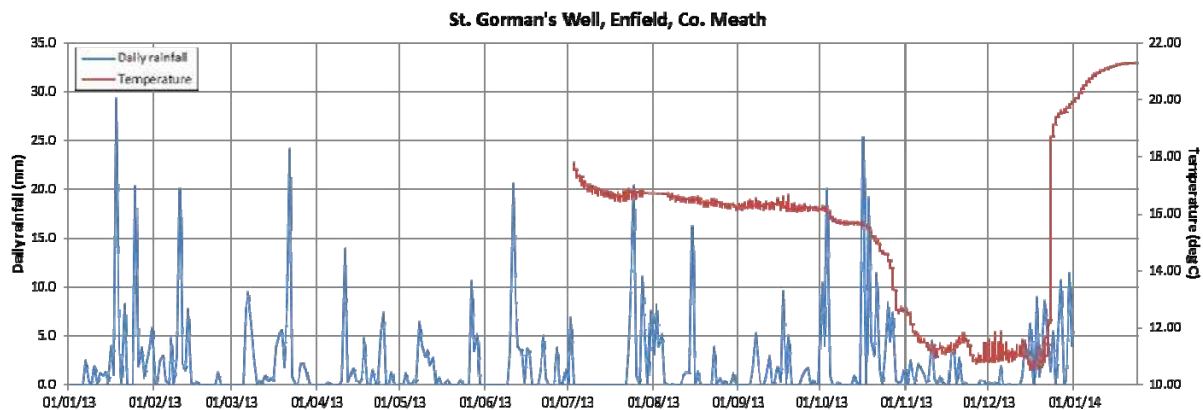


Figure 2.1.3.2. Continuous temperature data from St. Gorman's Well. Daily rainfall data from Dublin Airport synoptic station (provided by Met Eireann).

2.1.4 Research Focus 4: Heat production and heat distribution in Ireland's crust

Professor Stephen Daly, Nicola Willmot Noller, Tobias Fritschle (UCD)

Alan to complete from UCD input

2.1.5 Tool development

Voazar, Campanyà, Jones, Dr. Javier Fullea (CSIC, Madrid), Dr. Juan Carlos Afonso (Macquarie University, Sydney), Dr. Max Moorkamp (U Leicester, UK)

2.1.6 IRETherm publications and presentations

2.1.6.1 IRETherm publications

Fullea, J., M.R. Muller, A.G. Jones, and J.C. Afonso (2014), The lithosphere-asthenosphere system beneath Ireland from integrated geophysical-petrological modeling - II: 3D thermal and compositional structure. *Lithos*, **189**, 49-64, doi:10.1016/j.lithos.2013.09.014.

Jones, A.G., J.C. Afonso, J. Fullea, and F. Salajegheh (2014), The lithosphere-asthenosphere system beneath Ireland from integrated geophysical-petrological modeling - I: Observations, 1D and 2D hypothesis testing and modeling. *Lithos*, **189**, 28-48, doi:10.1016/j.lithos.2013.10.033.

2.1.6.2 IRETherm presentations

56th Irish Geological Research Meeting, Derry, Northern Ireland, 1-3 March.

Blake, S., M.R. Muller, A.G. Jones, Tiernan Henry, Alastair Allen, and the IRETherm team (2013), IRETherm: Multi-disciplinary investigation of Irish warm springs and their potential for geothermal energy provision.

Delhaye, R., M.R. Muller, A.G. Jones, D. Reay and the IRETherm team (2013), The IRETherm project: Assessment of the Rathlin Basin as a possible geothermal aquifer.

Farrell, T., A.G. Jones, M.R. Muller, M. Feely, and the IRETherm team (2013), IRETherm: A Magnetotelluric study of the geothermal energy potential of Irish radiothermal granites.

Jones, A.G., M.R. Muller, J.S. Daly, M. Long, J. Fulla, J. Vozar, S. Blake, R. Delhaye, T. Farrell, T. Fritschle, N. Willmot Noller, T. Waters, A. Allen, T. Henry, M. Feely, N. O'Neill, G. Jones, N.H. Hunter Williams, M. Lee, D. Reay, and R. Pasquali (2012), Progress in Deep Geothermal Energy Research in Ireland: an IRETherm Update for 2012.

33rd IAH (International Association of Hydrogeologists) Annual Conference, Tullamore, 23-24 April

Blake, S., M.R. Muller, A.G. Jones, T. Henry, A. Allen, and the IRETherm team (2013), IRETherm: Multi-disciplinary investigation of Irish warm springs and their potential for geothermal energy provision.

Geothermal Association of Ireland conference, Kilkenny, 13th November

Blake, S., M.R. Muller, A.G. Jones, T. Henry, A. Allen, and the IRETherm team (2013), IRETherm: Multi-disciplinary investigation of Irish warm springs and their potential for geothermal energy provision.

Farrell, T.F., A.G. Jones, M.R. Muller, M. Feely, and the IRETherm team (2013), IRETherm: The geothermal energy potential of Irish radiothermal granites.

Delhaye, R., A.G. Jones, C. Brown, D. Reay, M.R. Muller, and the IRETherm team (2013), The IRETherm project: Magnetotelluric investigation of Rathlin Island and Rathlin Basin for hydrothermal reservoir potential.

American Geophysical Union Fall meeting, San Francisco, USA, 9-13 December

Delhaye, R., A.G. Jones, D. Reay and the IRETherm Team (2013), The IRETherm project: Assessment of the Rathlin Basin as a possible geothermal aquifer.

Farrell, T.F., A.G. Jones, M.R. Muller, M. Feely, and the IRETherm team (2013), IRETherm: Magnetotelluric studies of radiothermal granites in Ireland.

Others

Jones, A.G., M.R. Muller, J. Fulla, J. Vozar, S. Blake, R. Delhaye, T. Farrell and the IRETherm Team (2013), IRETherm: Magnetotelluric Assessment of Geothermal Energy Potential of Hydrothermal Aquifer, Radiothermal Granite and Warm Spring Targets in Ireland. Contributed paper at: EGU, Vienna, Austria, 8-12 April.

Jones, A.G., J. Vozar, S. Blake, R. Delhaye, T. Farrell, J. Campaña, M. Muller, J. Fulla, and the IRETherm team (2013), IRETherm: Geothermal energy potential of hydrothermal aquifer, radiothermal granite and warm spring targets in Ireland. Contributed paper at: International Association of Geomagnetism and Aeronomy conference, Merida, Mexico, 26-31 August.

Vozar, J., A.G. Jones, S. Blake, R. Delhaye, T. Farrell, M. Muller, Ch. Yeomans Ch. and the IRETherm Team (2013), Electromagnetic survey of Dublin Basin southern margin. GAI Conference, Kilkenny, 13 November.

Jones, A.G., J.S. Daly, A. Allen, R. Goodman, N.H. Hunter Williams, M. Lee, D. Reay, M. Feely, P. Hanly, R. Pasquali, N. Piana Agostinetti, S. Lebedev, M. Long, J. Fulla, J. Vozar, J. Campaña, S. Blake, M. de Block, R. Delhaye, T. Farrell, T. Fritschle, N. Willmont Noller, T. Waters, (Muller, M., Yeomans Ch.) (2013), IRETherm: Research and Exploration Challenges in Assessing Ireland's Deep Low-Enthalpy Geothermal Energy Potential: Overview, Status Quo and Quo Vadimus. GAI Conference, Kilkenny, 13 November, invited oral presentation.

Campañà, J., and A.G. Jones (2013), The generalized Archie's law applied in geothermal situations. GAI conference, Kilkenny (Ireland), Poster.

2.2 SAMTEX: Southern African Magnetotelluric Experiment

A.G. Jones,
Alan to complete

SAMTEX Publications:

- Jones, A.G.**, S. Fishwick, R.L. Evans, **M.R. Muller**, and **J. Fulla** (2013), Velocity-conductivity relations for cratonic lithosphere and their application: Example of Southern Africa. *Geochemistry, Geophysics, Geosystems*, **14**, No. 4, 806-827, doi:10.1002/ggge.20075, ISSN: 1525-2027.
- Khoza, D.**, **A.G. Jones**, **M.R. Muller**, R.L. Evans, S.J. Webb, **M.P. Miensopust**, and the SAMTEX team (2013), Tectonic model of the Limpopo belt: Constraints from magnetotelluric data. *Precambrian Research*, **226**, 143-156, doi:10.1016/j.precamres.2012.11.016.
- Khoza, D.**, **A.G. Jones**, **M.R. Muller**, R.L. Evans, **M.P. Miensopust**, and S.J. Webb (2013), Lithospheric structure of an Archean craton and adjacent mobile belt revealed from 2D and 3D inversion of magnetotelluric data: example from southern Congo craton in northern Namibia. *Journal of Geophysical Research - Solid Earth*, **118**, Issue 8, 4378–4397, doi:10.1002/jgrb.50258

SAMTEX Presentations:

2.3 IRCSSSEM

A.G. Jones, Dr. Joan Campnayà, Dr. Xenia Ogaya

Alan to edit

The IRECCSEM (Irish carbon capture and storage assessment using EM methods) project, funded by SFI, initiated as required by SFI in April, 2013. The PDF and PhD positions were advertised, and applications assessed. The PDF competition yielded two very strong applicants, and the PDF position was awarded to Dr. Joan Campaña, and a one-year PDS (Post-Doctoral Scholarship) position awarded to Xenia Ogaya, both commencing on April 1st, 2014. The PhD competition did not yield a suitable candidate, and this is problematic as the next cycle of available students is not until summer, 2014 when fieldwork will commence. Nevertheless, the plan is to advertise the PhD position in February/March, with the hope that a successful candidate can be found and can start by July, 2014.

2.4 WAXI: West African Exploration Initiative

Dr. Florian Le Pape, Professor A.G. Jones

The WAXI-2 MT survey comprises a single 500-km-long east-west profile crossing southern Burkina Faso and northern Ghana (**Fig. 2.4.1**). The MT data were collected between February and May 2013. Both broadband (BBMT, crustal penetrating) and long period (LMT, upper mantle penetrating) magnetotelluric instruments were used. The LMT stations are separated by around 30 km on average, and the BBMT instruments define approx. 10 km spacing.

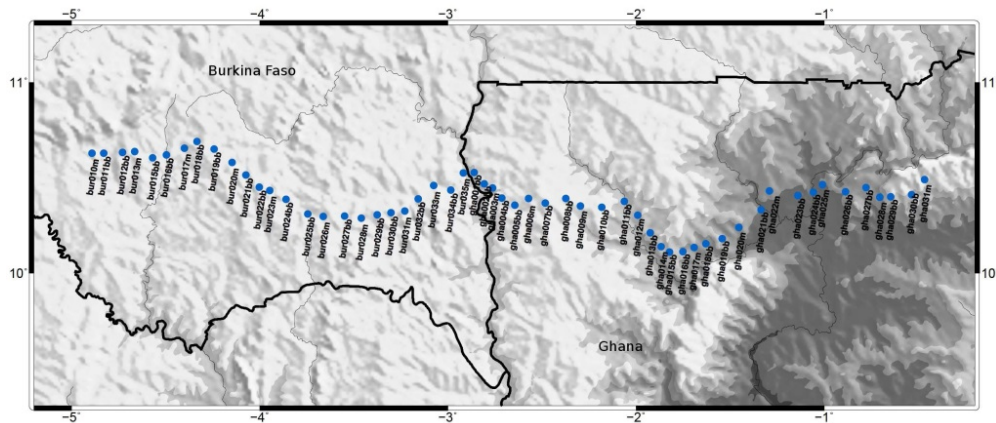


Figure 2.4.1. WAXI magnetotelluric stations layout across Burkina Faso and Ghana with locations of both merged stations (m) and broadband-only stations (bb).

Below is shown the preliminary preferred 2D model for the WAXI data with a focus on shallow structure over 60 km and large scale lithospheric anomalies (**Fig. 2.4.2**). The colour scale is broader for the shallow structure model (to 100,000 Ωm cf. to only 10,000 Ωm for the mantle model) in order to highlight lateral contrasts. Only the isotropic 2D model is plotted here. The 2D modelling shows a very interesting correlation with the main surficial geological structures (*Baratoux et al., 2011*). The main geological belts of western Burkina Faso can be clearly seen at depth on the MT profile. Structures located on the Houndé and Lawra belts appear particularly strongly resistive and correlate very well with the surficial geological map. In north-eastern Ghana, the Bole Nangodi belt corroborates with the transition from a resistive upper mantle in the west to a more conductive mantle to the east right beneath the Moho. Furthermore, the lithospheric structure of southern Burkina Faso and the most western part of northern Ghana appears more resistive compared to the rest of northern Ghana. The electrical lithosphere-asthenosphere boundary beneath BF is likely to be located around 250 km and shallows to the east of the profile.

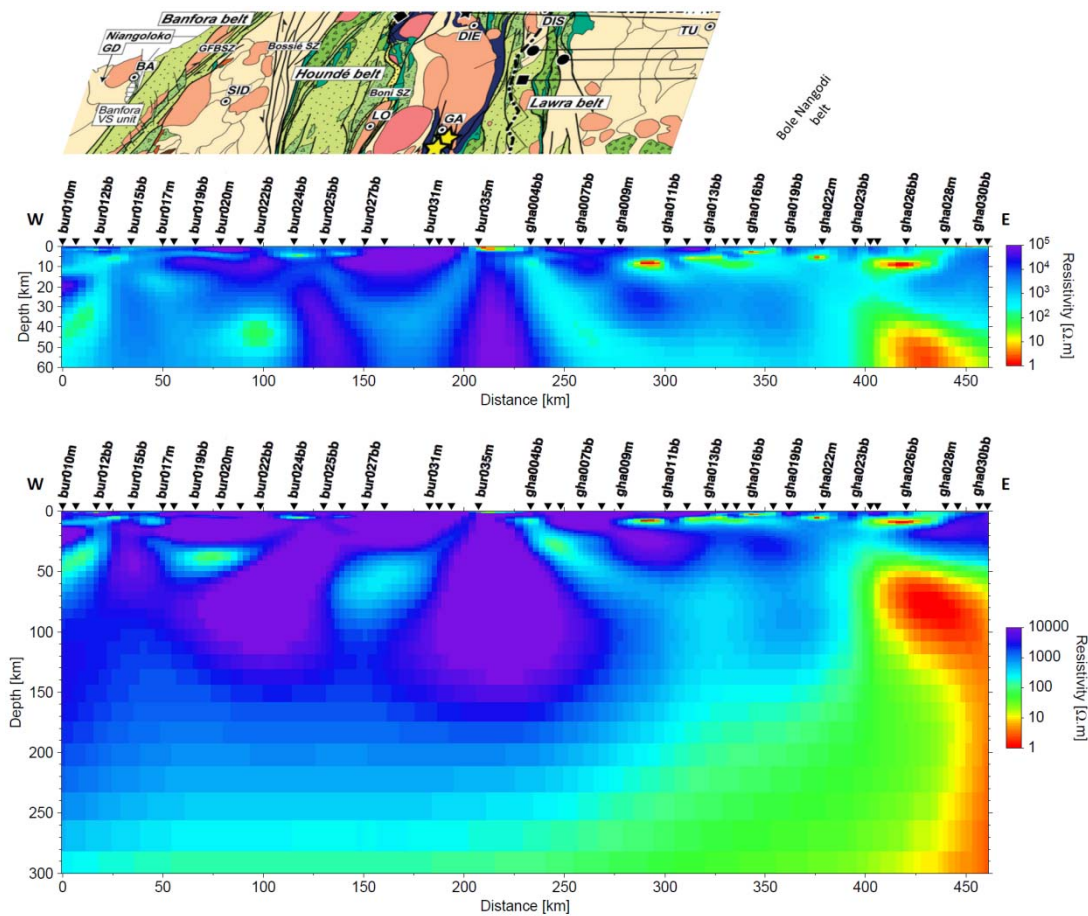


Figure 2.4.2. 2D isotropic resistivity model of WAXI data revealing shallow structures and deep lithospheric anomalies. The colour scale is changed for the shallow model to highlight lateral contrasts. Geological map from Baratoux et al. (2011). The profile crosses the cities of Banfora (BA), Sidéradougou (SID), Loropèni (LO) and Gaoua (GA).

The area covered by the WAXI MT data is defined by a very old and therefore complex geological setting, and the dimensionality analysis performed on the data highlight a significant 3D signature for several areas of the profile. The preliminary 2D anisotropic inversions are quite consistent with the isotropic results but the uncertainties in the strike direction leave some ambiguity in the models. For instance, the main feature that is still ambiguous is the strong conductive anomaly in the eastern part of the profile beneath 40 km present on both anisotropic and isotropic models. This anomaly is not consistent for adjacent 2D geoelectric strike orientations. Therefore, due to the uncertainties on the strike direction, the interpretation of this structure in the 2D model is quite complex. Furthermore, more than likely a significant conductor exists in this location at a depth just below the Moho but its total depth extent is not quantifiable due to lack of penetration through it. The 3D modelling of the WAXI data is becoming the main focus from now on.

2.5 INDEPTH

A.G. Jones, J. Vozar (PDF), F. Le Pape (PhD), with colleagues from China University of Geosciences Beijing, the University of Alberta, Cornell University, Stanford University, and INDEPTH collaborators

2.5.1 1D, 2D and 3D deep-probing electromagnetic studies and petro-physical modelling of the Tibetan Plateau

Vozar, Jones, Le Pape

We continue research with deep-probing multi-dimensional electromagnetic studies of the central Tibetan Plateau focused on the Banggong-Nujiang Suture and the central Tibetan Plateau geometries. The deep magnetotelluric sounding shows two different lithospheres. The resistive and thick edge of the Indian lithosphere was observed below Lhasa Terrane. The estimated LAB or upper mantle conductive layer was estimated from 200 km to 250 km (2-D modelling). The weaker and thinner Tibetan lithosphere is imaged below Qiangtang Terrane with conductive upper mantle at depths of about 150 km. Presence of a north-south elongated conductive body in the upper part of lithospheric mantle infers the existence of pervasive melt and possible fragmentation of upper part of Indian lithosphere. The 3-D modelling exhibits regional resistive and conductive structures with a similar orientation to the Shuanghu Suture, Tanggula Mountains and strike-slip faults such as the BengCo-Jiali Fault in the south. The orientation of crustal structures is perpendicular to convergence direction in this area (**Figure 2.5.1.1**). The GRACE satellite data from the region show that the deepest lower-crustal conductors are correlated to areas with maximum Moho depth

The paper with results of deep isotropic and anisotropic 2D modelling and 3D models of central Tibet were submitted in JGR. Now the paper is in the resubmitting process.

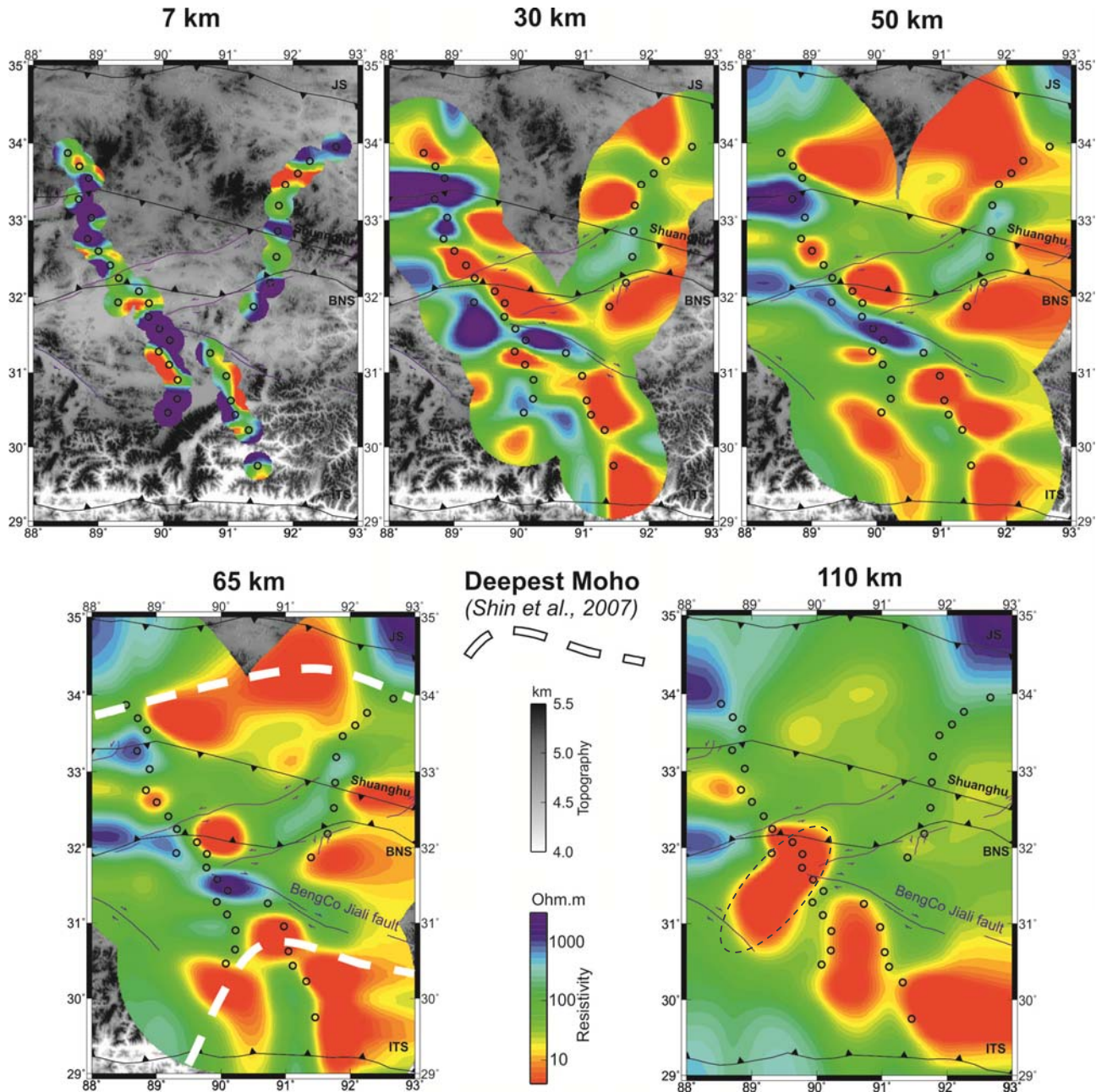


Figure 2.5.1.1. Horizontal slices for selected final 3-D inversion model at depths 7 km (near surface effects), 30 km (middle crust), 50 km, 65 km (lower crust) and 100 km (upper lithospheric mantle). The white dashed lines represent deepest Moho beneath Tibetan plateau from satellite gravimetric data. \rightleftarrows Conjugate strike-slip faults. \circ Lithospheric mantle conductor.

Alongside with MT studies we have been performing the integrated geophysical-petrological modeling of the MT and surface-wave data using the software package LitMod. Our results suggest an 80-120 km-thick, dry lithosphere in the central part of the Qiangtang Terrane. The presence of small amounts of water (<0.02 wt%) in the lithospheric-mantle for the Lhasa Terrane is required to fit the MT responses. Such a small amount of water dramatically affects the resistivity but has no influence on the seismic velocities. Three different proton conduction models for olivine conductivity and two water partition coefficients are tested. The Yoshino model needs too high bulk water content in the lithosphere (743ppm) to fit MT

data, where expected maximum values in similar lithospheric-mantles are less than 190 ppm. Our results favour a moderately wet underthrust Indian lithospheric-mantle, probably as a result of the dehydration processes, and LAB depth about 180 km

2.5.2 Tibetan Plateau's northern boundary

Le Pape, Jones, Vozar

In order to improve understanding of the anisotropic distribution of melt previously revealed by our 2D anisotropic modelling of INDEPTH III and IV MT data, a variant approach on 3D inversion of 2D profiles was investigated to explore and improve lateral resolution. In addition to the apparent surficial deformation associated with the sinistral strike-slip Kunlun fault, the 3D modelling of the INDEPTH MT data reveals that complex deformation processes are occurring at mid-crustal depths in northern Tibet. The 3D results, supported by synthetic modelling, particularly confirm and highlight the presence of separate north-south intrusions of conductive material crossing the Kunlun fault into the more resistive Kunlun-Qaidam block. We are also focusing on different approaches for melt estimations in order to quantify the proportion of flow that goes to the north. Finally, since both INDEPTH IV MT and seismic profiles share the same location, we are carrying out some qualitative comparison of the resistivity and seismic properties of the INDEPTH IV line.

INDEPTH Publications:

- Vozar, J., A.G. Jones, F. Le Pape,** and W. Wei (2014), Three-dimensional structures and geometries of central Tibetan Plateau from INDEPTH magnetotelluric data, *J. Geophys. Res.*, Submitted.
- Wei, W, **F. Le Pape, A.G. Jones, J. Vozar,** H. Dong, M.J. Unsworth, S. Jin, G. Ye, J. Jing, L. Zhang, and C. Xie (2014), Northward Channel flow in Northern Tibet revealed from 3D magnetotelluric modelling, *Physics of the Earth and Planetary Interiors*, Submitted.

INDEPTH Presentations:

- Le Pape, F., A.G. Jones, J. Vozar,** W. Wei, H. Dong, M.J. Unsworth, S. Jin, G. Ye, J. Jing, L. Zhang, and C. Xie (2013), Changes in the crustal resistivity structure of the Tibetan Plateau beneath the Kunlun fault, Contributed paper at: AGU, San Francisco, USA, 9-13 December.
- Vozar, J., J. Fullea, A.G. Jones, M. Agius,** and **S. Lebedev** (2013), Geophysical and petro-physical investigation of the lithosphere-asthenosphere boundary in central Tibet, IGRM, Derry, Northern Ireland, 1-3 March.
- Vozar, J., A.G. Jones,** and **F. Le Pape** (2013), Geoelectrical structures and their geometries in central Tibetan Plateau from INDEPTH magnetotelluric data. EGU, Vienna, Austria, 7-12 April.
- Vozar, J., A.G. Jones,** and **F. Le Pape** (2013), Geoelectrical structures and their geometries in central Tibetan Plateau from INDEPTH magnetotelluric data. IAGA, Merida Yucatan, Mexico, 26-31 August.
- Vozar, J., A.G. Jones,** and **F. Le Pape** (2013), Geoelectrical structures and their geometries in central Tibetan Plateau from INDEPTH magnetotelluric data. AGU Fall Meeting, San Francisco, USA, 9-13 December.
- Vozar, J., J. Fullea,** and **A.G. Jones** (2013), The lithospheric water content estimations from geophysical and petro-physical investigations in central Tibet. AGU Fall Meeting, San Francisco, USA, 9-13 December.

2.6 TopoMed: Plate re-organization in the western Mediterranean: Lithospheric causes and topographic consequences

A.G. Jones, Duygu Kiyan, with Dr. J. Fullea (CSIC, Madrid), Dr. J. Ledo (U. Barcelona), Dr. Agata Sinicalchi (U. Bari)

The PICASSO (Program to Investigate Convective Alboran Sea System Overturn) project, and the concomitant TopoMed (Plate reorganization in the western Mediterranean: Lithospheric causes and topographic consequences) project aim to develop a better understanding of the three-dimensional internal structure of the crust and the lithosphere of the Alboran Sea, Betics, Rif, Atlas Mountain belt and surrounding areas in the western Mediterranean. The land-based Magnetotelluric (MT) survey's objective of TopoMed is to provide new electrical conductivity constraints on the crustal and lithospheric structures of the Atlas Mountains, and to test the hypotheses for explaining the observation of a “missing” mantle root inferred from surface heat flow, gravity and geoid anomalies, elevation and seismic data modelling (i.e. Zeyen et al., 2005; Teixell et al., 2005; Fullea et al., 2010). The MT survey across the Atlas Mountains region began in September, 2009 and ended in February, 2010. The survey comprises acquisition of broad-band (crustal probing) and long period (mantle probing) MT data along two profiles: a N-S oriented profile crossing the Middle Atlas through the Central High Atlas to the east (profile MEK) and a NE-SW oriented profile crossing the western High Atlas towards the Anti Atlas in the west (profile MAR) (Figure 2.6.1.).

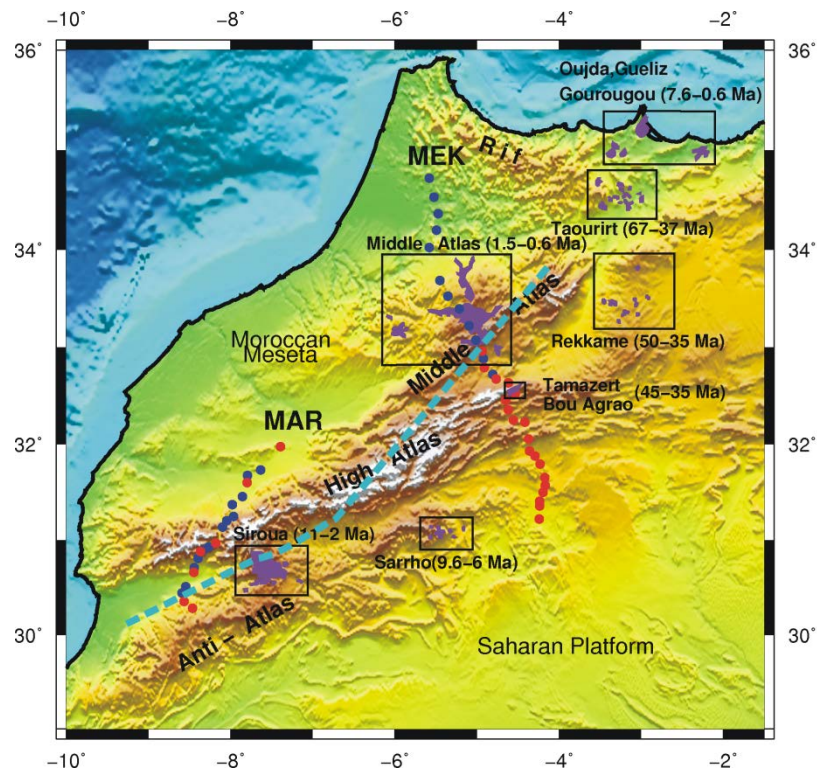


Figure 2.6.1. Details of Moroccan Atlas system (Middle Atlas, High Atlas and Anti-Atlas) and location of Cenozoic volcanic centers (purple polygons). Periods of volcanic activity are compiled from Missenard & Cadoux (2011). The solid circles represent the location of MT stations. Blue dashed line shows the axis of lithospheric thinning as evidenced by Missenard et al. (2006), Fullea et al. (2010) and the so-called Morocco Hot Line (de Lamotte et al., 2009).

We present the results from three-dimensional (3-D) MT inversion of two single MT profile data employing the parallel version of Modular system for Electromagnetic inversion (ModEM; Egbert & Kelbert, 2012) code. The distinct conductivity difference between the Middle-High Atlas (conductive) and the Anti-Atlas (resistive) correlates with the South Atlas Front fault, the depth extent of which appears to be limited to the uppermost mantle (approximately 55 km) (**Figure 2.6.2.**). In all inverse solutions, the crust and the upper mantle show resistive signature ($750\ \Omega\text{m} - 1,000\ \Omega\text{m}$) beneath the Anti-Atlas which is the part of stable West African Craton. For the first time, the electrical resistivity distribution in the crust and in the upper mantle of Western High Atlas has been studied. Our 3-D model (**Figure 2.6.3.**) shows that conductive ($1\text{-}20\ \Omega\text{m}$) western High Atlas is confined by two resistive basins ($>1,000\ \Omega\text{m}$), the Souss basin to the south and the Haouz basin to the north. At the southern boundary of the western High Atlas, the conductor is located at the shallower depth and it is deepening to the north.

Within the framework of TopoMed project, based on synthetic data sets from a profile, we also examined the importance of aligning both inversion and data coordinate systems with quasi-2-D geo-electrical strike direction in 3-D inverse modelling to map the right geometry and shape of the oblique conductive structures (Kiyani et al., 2014, *in press*).

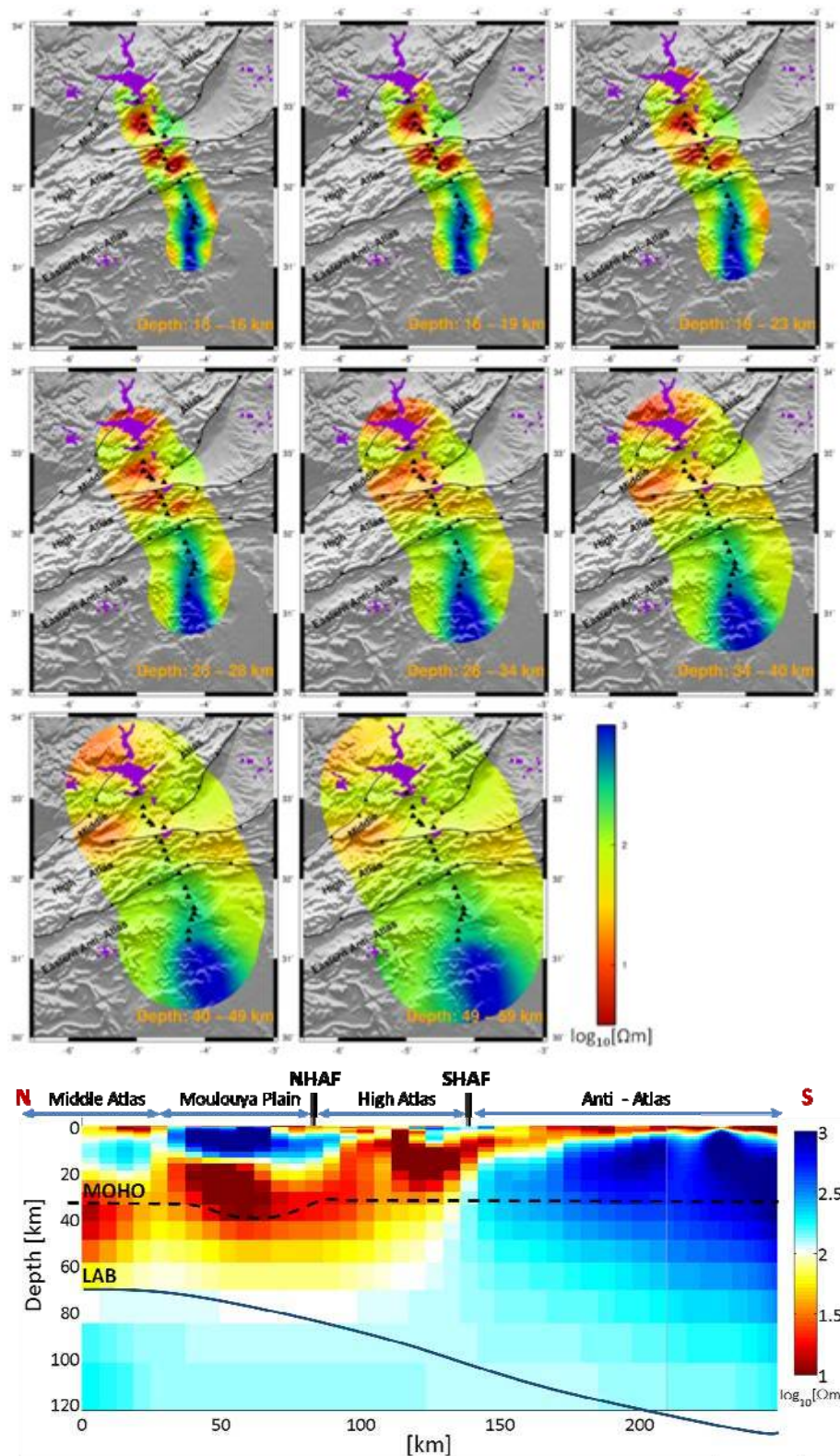


Figure 2.6.2. Plan view of the preferred 3-D electrical resistivity model obtained from the final inversion at depths: middle crust (13-16 km, 16-19 km, and 19-23 km), lower crust (23-28 km; 28-34 km) and lithospheric mantle (34-40 km; 40-49 km; 49-59 km). The triangles indicate the location of MT stations along the MEK profile. The part of the model which is well constrained by the data is shown only. At the bottom, representative cross section from the preferred model along the profile is presented. Superimposed crust-mantle boundary (MOHO) and lithosphere-asthenosphere boundary (LAB) geometries are from previous works in the

study area: Ayarza et al. (2005) and Fullea et al. (2010), respectively. NHAF: North Atlas Front Fault; SHAF: South Atlas Front Fault.

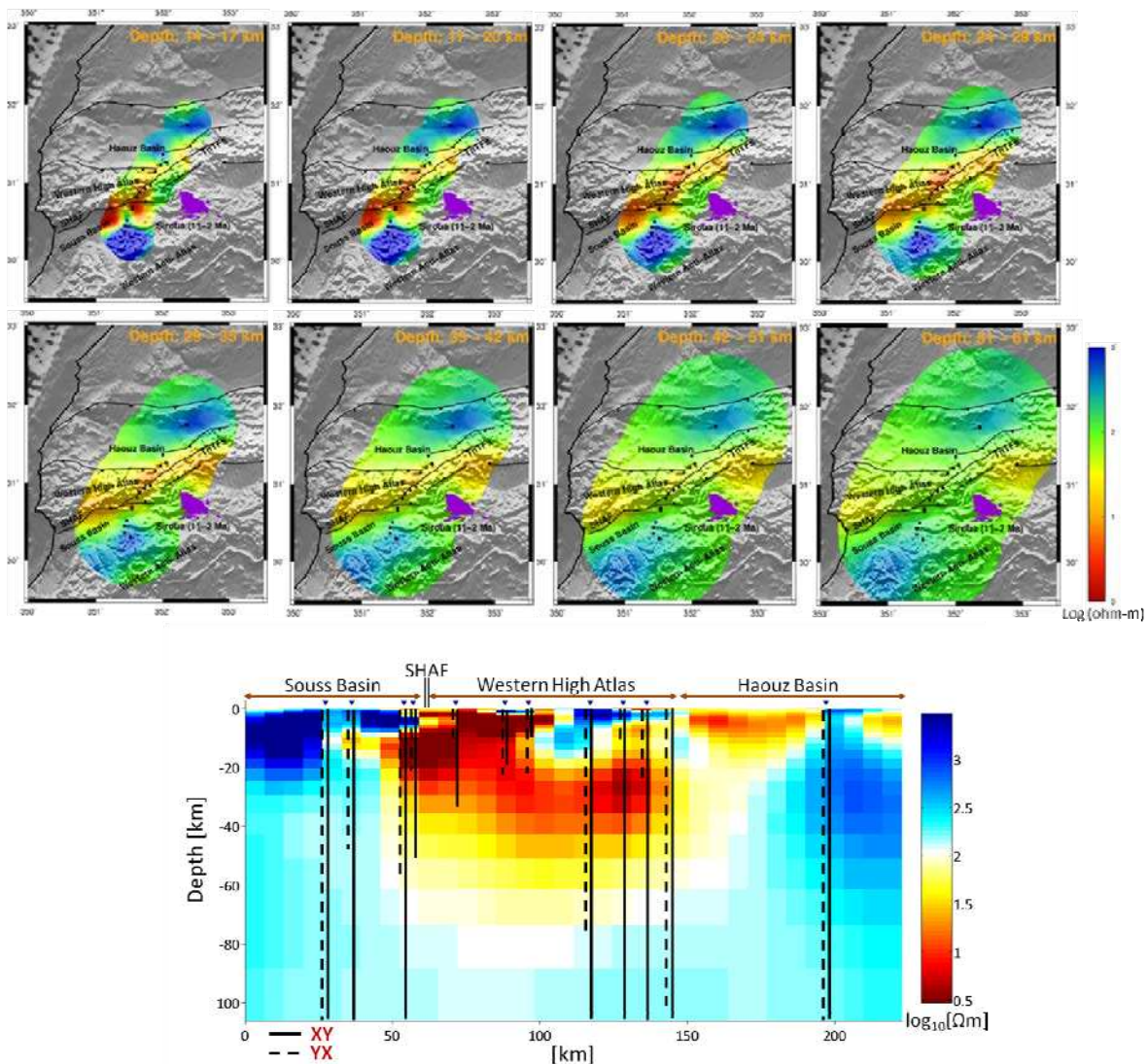


Figure 2.6.3. Plan view of the preferred 3-D electrical resistivity model obtained from the final inversion at depths: middle crust (14-17 km; 17-20 km), lower crust (20-24 km; 24-29 km; 29-35 km) and lithospheric mantle (35-42 km; 42-51 km; 51-61km). The squares indicate the location of MT stations along the MAR profile. At the bottom, representative cross section from the preferred model along the profile is presented. The approximate Niblett-Bostick penetration depths (Jones, 1983b) of two modes (XY and YX) are plotted on top of the model.

Working Group Meeting:

TopoMed Working Meeting held in Montpellier, 12th -15th May, 2013.

TopoMed Publications:

Kiyan, D., A.G. Jones, and J. Vozar (2013), The inability of magnetotelluric off-diagonal impedance tensor elements to sense oblique conductors in 3-D inversion, *Geophysical Journal International*, published online, 17 December 2013, doi:10.1093/gji/ggt470, in press.

TopoMed Presentations:

- Kiyan, D., A.G. Jones, J. Fulla, J. Ledo, A. Siniscalchi, and G. Romano (2013)**, Crustal and uppermost mantle structures of the Atlas Mountains of Morocco inferred from electromagnetic imaging. Contributed paper at: IAGA XIIth Scientific Assembly, Merida Yucatan, Mexico, 29-31 August.
- Kiyan, D., A.G. Jones, J. Fulla, J. Ledo, A. Siniscalchi, and G. Romano (2013)**, Three-dimensional magnetotelluric imaging of crustal and uppermost mantle structures of the Atlas Mountains of Morocco. Contributed paper at: EGU, Vienna, Austria, 8-12 April.
- Kiyan, D., A.G. Jones, J. Fulla, J. Ledo, A. Siniscalchi, and G. Romano (2013)**, Crustal and uppermost mantle structure of the Atlas Mountains of Morocco revealed from 3-D inversion of magnetotelluric data. Contributed paper at: AGU Fall Meeting, San Francisco, 9-13 December.

2.7 Multi-parameter modelling/inversion

Dr. Eric Mandolesi, Professor A.G. Jones

A new image-driven inversion framework based on the information theory concept of *mutual information* has been developed and tested. The mutual information constraint enhances the robustness of the inversion results leading the inversion algorithm to a more reliable solution whenever the reference model provides coherent information about the subsurface (Mandolesi and Jones 2013, accepted paper). The data integration method allowed a better constraint on model parameters unconstrained by one method (in this case MT) alone, as proven by a case-study from Central Europe.

Publication:

Mandolesi, E., and A.G. Jones (2013), Magnetotelluric Inversion based on Mutual Information, *Geophysics Journal International*, Submitted Dec 2013, Accepted Feb 2014, in revision.

2.8 SIMER: Simulation of Electromagnetic response of real Rocks

Dr. Eric Mandolesi, Professor A.G. Jones, with Dr. Max Moorkamp (U. Leicester, UK), Professor Andrea Tommasi (U. Montpellier II, France)

Phase One of SIMER began with the analysis of the response of a random three dimensional media to a single frequency exciting field. The preliminary analysis required the computation of thousands of responses from a random media built of 50x50x20 blocks, that represents a two-phase material. These preliminary simulations allowed the selection of the optimal parameters to design a meaningful numerical experiment, since both the probabilities that describe the distribution of the two phases in the material, the cell length and background electrical conductivity play a decisive role in the electromagnetic response.

The comparison of the data modelled with the prediction from the Hashin-Shtrikman bounds highlighted an abrupt increment in the electrical conductivity value far before the conductive phase network could be considered perfectly connected. From this evidence it is possible to infer that from field data perspective the inductive nature of the electromagnetic field plays a major role in the conduction mechanism in the real rocks. (Mandolesi et al., 2013, AGU Fall Meeting).

Further investigation will include a study on the scalability of the distribution mechanism using statistical approaches.

Presentation:

Mandolesi, E., M. Moorkamp, and A.G. Jones (2013), A numerical study of the influence of interconnected conductive paths in electrically resistive rocks, AGU Fall Meeting 2013, San Francisco, USA (poster).

2.9 Magnetotelluric theory and tool development

2.9.1 Electrical anisotropy

2.9.2 Distortion effects

2.9.3 Inter-station transfer functions

Dr. Joan Campanya

A new methodology for processing magnetotelluric (MT) data, site processing using Inter-station transfer functions (SPIT) (Campanyà et al., 2014), is already implemented for processing audiomagnetotellurics (AMT), broadband magnetotelluric (BBMT) and long period magnetotelluric (LMT) data. Three different MT processing algorithms (Birrp (Chave and Thompson, 2004), EMTF (Egbert, 2002) and Maxim Smirnov, 2003) have been adapted to SPIT. This method was developed to improve the results when the acquired magnetic fields were truncated, but has more possibilities like improve the processing in noisy areas, improves the statistics used to obtain the final results and modify the MT surveys getting more out of the available instruments. All this advantages are being applied in IRE THERM project and will be implemented in IRECCSEM project.

The Inter-station transfer functions have been also used for modelling the subsurface. The main work has been focused on improving the existing software (ModEM, Egbert and Kelbert, 2012) by implementing the Horizontal Magnetic Tensor (HMT). The program is ready to be used for IRE THERM and IRECCSEM projects. The use of the HMT opens new possibilities for characterization of the subsurface, obtaining MT models from different combinations of independent MT data: Z, TIP, HMT, Z_TIP, Z_HMT, TIP_HMT, Z_TIP_HMT. Structures present in all models will therefore be more reliable. Several tests have been done testing the properties of the HMT and determining in which situations is worth using it. Results from the tests show that HMT is mainly affected by the structures below the sites and less affected by lateral geoelectrical bodies, making it as a good complement with the TIP data, which is mainly affected by lateral structures. Two other important properties are that using HMT the high electrical resistivity structures are better constrained than only using Z data and that the reference site for HMT should not be on top of the target structures (Campanyà et al., 2013)

References:

Campanyà .J, J. Ledo, A.G. Jones, P. Queralt, A. Marcuello, M. Liesa, J.A. Munoz (2013), The role of different magnetotelluric tensor relationships in detecting partial melt in continental collision zones: results from synthetic models and real data. AGU conference, San Francisco, US. Poster.

- Campanyà, J., J. Ledo, P. Queralt, A. Marcuello, A.G. Jones (2014), A new methodology for processing magnetotelluric (MT) data: Site Processing using Inter-station Transfer-functions (SPIT). *Geophys. J. Int.* (Under review).
- Chave, A.D., and D.J. Thompson (2004), Bounded influence estimation of magnetotelluric response functions. *Geophys. J. Int.*, 157, 988-1006.
- Egbert, G.D. (2002), Processing and interpretation of the electromagnetic induction array data. *Surv. in Geophys.*, 23, 207-249.
- Egbert, G.D., and A. Kelbert (2012), Computation recipes for electromagnetic inverse problems. *Geophys. J. Int.*, 189, 251-267.
- Smirnov, M.Y. (2013), Magnetotelluric data processing with a robust statistical procedure having a high breakdown point. *Geophys. J. Int.* 152, 1-7.

2.9.4 Porosity-permeability relations

Dr. Joan Campanya

Campanyà has developed a new program to calculate (by Marquardt inversion) the connectivity of the rocks from porosity/conductivity samples. The program uses the n phases Archie's law suggested by Glover (2010). This program has been used to create a database of the connectivity of the Irish rocks using different available data of porosity and conductivity. The work is now focus on determine the permeability values of the target rocks from porosity, electrical conductivity and cementation factor values. We have been using different approaches and data published in the bibliography, mostly focused on data from Gomez et al. (2010). The influence of each parameter in the used approaches was tested, showing which parameters can create more instability when determine the permeability values. These results will be used as a source of preliminary information within IRETherm and IRECCSEM areas of study, where the used approaches will be calibrated using MT models and the boreholes information.

References:

- Glover, P.W.J. (2010), A generalized Archie's law for n phases. *Geophysics*. Vol. 75, No. 6, P.E247-E265
- Gomez, C.T., J. Dvorkin, T. Vanorio (2010), Laboratory measurements of porosity, permeability, resistivity, and velocity on Fontainebleau sandstones, *Geophysics*. Vol. 75, No. 6 P.E191-E204

Presentation:

Campanyà, J., and A.G. Jones (2013), The generalized Archie's law applied in geothermal situations. GAI conference, Kilkenny (Ireland), Poster.

2.10 Three-dimensional modelling and inversion

2.11 Other electromagnetic research

2.11.1 New Zealand geothermal activity

Christina Walter (U. Auckland, New Zealand), A.G. Jones

Christina to compile

2.11.2 MaSca (Magnetotellurics in Scandes)

Dr. Maxim Smirnov (U. Oulu), Dr. Toivo Korja (U. Oulu), A.G. Jones

Presentation:

2.11.3 Electrical Moho

Jones was invited to contribute to a special issue of *Tectonophysics* dedicated to the 100 year anniversary of Andrija Mohorovičić's 1910 paper that identified a seismic discontinuity that usefully defines the crust-mantle boundary from a seismological perspective. Calculations by Jones showed how difficult it is to detect a change in electrical conductivity unless special conditions are met.

Publication:

Jones, A.G. (2013), Imaging and observing the Electrical Moho, *Invited Review, Tectonophysics, "Moho" special issue*, doi: 10.1016/j.tecto.2013.02.025, in press.

2.11.4 Canada

A mega-paper (Jones et al., 2013) describing the results of 30 years of MT observations across Canada by the whole Canadian EM Induction community during LITHOPROBE and other programmes was finally completed and submitted to *Canadian Journal of Earth Sciences*. Data from over 6,5000 sites are mapped in various ways, showing (i) correlations with anisotropy directions inferred from crustal stress (inferred by borehole breakouts), lithospheric mantle fossil structures (inferred by SKS directions), and asthenospheric flow (plate motion directions), and (ii) correlations with thermal models of Canada's lithosphere. Through combining thermal model data with estimated resistivities at the same locations and depths, an estimate is made of the water content in olivine, showing at 100 km that the cratons are dry and the younger areas not completely dry. Surprisingly, at 200 km all parts of the mantle can be explained by dry mantle minerals at the temperatures suggested by the thermal models – there is no need to invoke water in the mantle.

Jones, A.G., J. Ledo, I.J. Ferguson, J.A. Craven, M.J. Unsworth, M. Chouteau, and J.E. Spratt (2013), The electrical resistivity of Canada's lithosphere and correlation with other parameters: Contributions from LITHOPROBE and other programmes. *Canadian Journal of Earth Sciences*, accepted on 4th November, 2013, subject to minor revision.

Other publications:

Adentunji, A.Q., I.J. Ferguson, and **A.G. Jones** (2013), Crustal and lithospheric scale structures of the Precambrian Superior-Grenville margin. *Tectonophysics*, submitted 12th June.

Spratt, J., T. Skulski, J.A. Craven, **A.G. Jones**, D. Snyder, and **D. Kiyan** (2013), Magnetotelluric investigations of the lithosphere beneath the central Rae Craton, mainland Nunavut, Canada, *Journal of Geophysical Research*, submitted 26 March 2013, in revision.

2.11.5 Other contributions

Publications

Invited Presentations

Other Presentations

2.12 Main international collaborations

- U. Barcelona: Professors J. Ledo, P. Queralt, A. Marcuello, A. Mari
- U. Bari: Prof. A. Sinichalchi
- U. Leicester: Drs. S. Fishwick, M. Moorkamp, A. Avdeeva
- U. Montpellier: Profs. A. Tommasi, S. Demouchy
- U. Oulu: Prof. T. Korja, Dr. M. Smirnov
- China University of Geosciences Beijing: Profs. W. Wei, S. Jin, G. Ye
- Geological Survey of Canada: Mr. J. Craven, Dr. D. Snyder, Ms. J. Spratt
- WHOI: Drs. A.D. Chave, R.L. Evans
- Memorial University, St John's, Newfoundland: Professor Colin Farquharson
- Icelandic Geosurvey ISOR, Reykjavik, Iceland

3 Petrological-geophysical modelling

Group Leader: Senior Professor Alan G. Jones

3.1 Correlation of electromagnetic data with other geoscientific data

Alan to edit

Joint modelling/inversion must begin from a standpoint of expecting a correlation between different physical or physio-chemical parameters. The relationship between velocity and conductivity has been explored over the last few years by Jones and colleagues, culminating in the paper in press in *Geochemistry, Geophysics, Geosystems*. Having this background in place, formal methods can now proceed.

Publication:

Jones, A.G., S. Fishwick, R.L. Evans, *M.R. Muller*, and *J. Fulla* (2013), Velocity-conductivity relations for cratonic lithosphere and their application: Example of Southern Africa. *Geochemistry, Geophysics, Geosystems*, in press.

Invited Presentations

3.2 Water in olivine

Alan to complete

3.3 Modelling Ireland's lithosphere

3.3.1 In two-dimensions (2D)

Alan to edit

3.4 Probabilistic Inversion

Alan to edit

Working with Afonso and colleagues, the group has developed a probabilistic inversion approach that derives likely composition, temperature, pressure and water content from surface observables.

Publications:

Afonso, J.C., **J. Fullea**, W. L. Griffin, Y. Yang, **A.G. Jones**, J.A.D. Connolly, and S.Y. O'Reilly (2013), 3D multi-observable probabilistic inversion for the compositional and thermal structure of the lithosphere and upper mantle. I: a priori petrological information and geophysical observables. *Journal of Geophysical Research - Solid Earth*, in press.

Afonso, J.C., **J. Fullea**, Y. Yang, J.A.D. Connolly, and **A.G. Jones** (2013), 3D multi-observable probabilistic inversion for the compositional and thermal structure of the lithosphere and upper mantle. II: General methodology and resolution analysis. *Journal of Geophysical Research - Solid Earth*, in press.

Presentation:

3.5 Meyer-Neldel Rule

A.G. Jones

Alan to write

3.6 Other petrological-geophysical modelling activities

Alan to edit

Other petrological-geophysical modelling activities are described elsewhere in this Annual Report, including in South Africa (Section 2.2), Tibet (Section 2.3), Morocco (Section 2.6), and Mongolia (Section **Error! Reference source not found.**).

Invited presentations

Presentations

4 Geodynamic research activities

Group Leader: Professor Zdenek Martinec

4.1 Mass-density Green's functions for the GOCE gravitational gradient tensor

Four different forms of the tensor Green's function for the gravitational gradient tensor, derived in this article, give a theoretical basis for geophysical interpretations of the GOCE-based gravitational gradients in terms of the Earth's mass-density structure. The first form is an invariant expression of the tensor Green's function that can be used to evaluate numerically the gravitational gradients in different coordinate systems (e.g., Cartesian). The second form expresses the gravitational gradients in spherical coordinates

(ϑ, φ) with the origin at the north pole as a series of tensor spherical harmonics. This form is convenient to apply when the GOCE data are represented in terms of the gravitational potential as a scalar spherical harmonic series, such as the GOCO03S satellite gravity model. The third form expresses gravitational gradients in spherical coordinates (ψ, α) with the pole at the computation point. The fourth form then expresses the corresponding isotropic kernels in a closed form. The last two forms are used to analyse the sensitivity of the gravitational gradients with respect to lateral distribution of the Earth's mass-density anomalies. They additionally provide a tool for evaluating the omission error of geophysically modelled gravitational gradients and its amplification when the bandwidth-limited GOCE-based gravitational gradients are interpreted at different heights above the Earth's surface. We show that the omission error of the bandwidth-limited mass-density Green's functions for gradiometric data at the GOCE satellite's altitude does not exceed 1% in amplitude when compared to the full-spectrum Green's functions. However, when evaluating the bandwidth-limited Green's functions at lower altitudes, their omission errors are significantly amplified. In this case, we show that the short-wavelength content of the forward-modelled gravitational gradients generated by an *a priori* density structure of the Earth must be filtered out such that the omission error of the GOCE-based gravitational gradients (i.e., the signal that has not been modelled from the GOCE data) is equal to the omission error of the forward-modelled gravitational gradients. Only after performing such filtering can the GOCE-based gravitational gradients at low altitudes be interpreted in terms of the Earth's density structure. Both the closed and spherical-harmonic forms of the Green's functions allow a direct interpretation in terms of the minimum lateral extent of the Earth that needs to be considered in a regional model constrained by gravitational gradients if the full information provided by the Green's functions is to be retained. We show that this extent (i) is smallest for the vertical-vertical Green's function and (ii) linearly increases with increasing computation-point height. The spectral forms of the gravitational gradients are further used to calculate the sensitivity of the GOCE-based gravitational gradients to the depth of density anomalies, expressed in terms of the harmonic degree of the internal mass-density anomaly. We show that the largest gravitational gradient response is obtained for shallow mass anomalies, and is further amplified as the harmonic degree increases.

Publication:

Martinec, Z. (2013), Mass-density Green's functions for the gravitational gradient tensor at different heights. *Geophys. J. Int.*, (in press, on line access since January 3, 2014), doi: 10.1093/gji/ggt495.

Presentations:

Martinec, Z. (2013), A refined model of sedimentary rock cover over the Congo basin from the interpretation of GOCE gradiometric data. EGU General Assembly, Vienna, Austria, 7-12 April.

Martinec, Z., B. Vermeersen, W. van der Wal, P. Novak, J. Sebera, O. Baur, D. Tsoulis, N. Sneeuw, and R. Haagmans (2013), Interpreting the GOCE Gravitational Gradients over the Congo Basin. ESA Living Planet Symposium, Edinburgh, UK, 9-13 September.

Novak, P., J. Sebera, M. Valko, M. Sprlak, O. Baur, D. Tsoulis, **Z. Martinec**, N. Sneeuw, W. van der Wal, B. Vermeersen, and R. Haagmans (2013), Towards a Better Understanding of the Earth's Interior and Geophysical Exploration Research. ESA Living Planet Symposium, Edinburgh, UK, 9-13 September.

Sebera, J., P. Novak, M. Valko, M. Sprlak, O. Baur, D. Tsoulis, **Z. Martinec**, N. Sneeuw, B. Vermeersen, W. van der Wal, J. Bouman, M. Fuchs, and R. Haagmans (2013), High-

Resolution Grids of Gravitational Gradients from GOCE. ESA Living Planet Symposium, Edinburgh, UK, 9-13 September (poster).

4.2 Antarctic ice-mass balance 2003 to 2012

We present regional-scale mass balances for 25 drainage basins of the Antarctic Ice Sheet (AIS) from satellite observations of the Gravity and Climate Experiment (GRACE) for time period January 2003 to September 2012. Satellite gravimetry estimates of the AIS mass balance are strongly influenced by mass movement in the Earth interior caused by ice advance and retreat during the last glacial cycle. Here, we develop an improved glacial-isostatic adjustment (GIA) estimate for Antarctica using newly available GPS uplift rates, allowing us to more accurately separate GIA-induced trends in the GRACE gravity fields from those caused by current imbalances of the AIS. Our revised GIA estimate is considerably lower than previous predictions, yielding an estimate of apparent mass change of $53 \pm 18 \text{ Gt yr}^{-1}$. Therefore, our AIS mass balance of $-114 \pm 23 \text{ Gt yr}^{-1}$ is less negative than previous GRACE estimates. The northern Antarctic Peninsula and the Amundsen Sea sector exhibit the largest mass loss ($-26 \pm 3 \text{ Gt yr}^{-1}$ and $-127 \pm 7 \text{ Gt yr}^{-1}$, respectively). In contrast, East Antarctica exhibits a slightly positive mass balance ($26 \pm 13 \text{ Gt yr}^{-1}$), which is, however, mostly the consequence of compensating mass anomalies in Dronning Maud and Enderby Land (positive) and Wilkes and George V Land (negative) due to interannual accumulation variations. In total, 6 % of the area constitutes about half the AIS imbalance, contributing $151 \pm 7 \text{ Gt yr}^{-1}$ (ca. 0.4 mm yr^{-1}) to global mean sea-level change. Most of this imbalance is caused by ice-dynamic speed-up expected to prevail in the near future.

Publication:

Sasgen, I., H. Konrad, E.R. Ivins, M.R. van den Broeke, J. Bamber, **Z. Martinec**, and V. Klemann (2013), Antarctic ice-mass balance 2003 to 2012: regional reanalysis of GRACE satellite gravimetry measurements with improved estimate of glacial-isostatic adjustment based on GPS uplift rates. *The Cryosphere*, **7**, 1499--1512, doi:10.5194/tc-7-1499-2013.

Presentation:

Martinec, Z., and I. Sasgen (2013), Weak formulation of the sensitivity equations for glacial isostatic adjustment. EGU General Assembly, Vienna, Austria, 7-12 April (poster).

4.3 Interpretation of GOCE data over Congo basin

We aim to interpret the vertical gravity and vertical gravity gradient of the GOCE-GRACE combined gravity model over the south-eastern part of the Congo basin to refine the published model of sedimentary rock cover. We use the GOCO03S gravity model and evaluate its spherical harmonic representation at or near the Earth's surface. In this case, the gradiometry signals are enhanced {as compared to the original measured GOCE gradients at satellite height} and better emphasize the spatial pattern of sedimentary geology.

To avoid aliasing, the omission error of the modelled gravity induced by the sedimentary rocks is adjusted to that of the GOCO03S gravity model. The mass-density Green's functions derived for the a priori structure of the sediments show a slightly greater sensitivity to the GOCO03S vertical gravity gradient than to the vertical gravity. Hence, the refinement of the sedimentary model is carried out for the vertical gravity gradient over the basin, such that a few anomalous values of the GOCO03S-derived vertical gravity gradient are adjusted by refining the model. %This maximizes the signal-to-noise ratio and minimizes the errors %due

to the downward continuation of the gravity field. We apply the 5-parameter Helmert's transformation, defined by 2 translations, 1 rotation and 2 scale parameters that are searched for by the steepest descent method.

The refined sedimentary model is only slightly changed with respect to the original map, but it significantly improves the fit of the vertical gravity and vertical gravity gradient over the basin. However, there are still spatial features in the gravity and gradiometric data that remain unfitted by the refined model. These may be due to lateral density variation that are not contained in the model, a density contrast at the Moho discontinuity, lithospheric density stratifications or mantle convection.

In a second step, the refined sedimentary model is used to find the vertical density stratification of sedimentary rocks. Although the gravity data can be interpreted by a constant sedimentary density, such a model does not correspond to the gravitational compaction of sedimentary rocks. Therefore, the density model is extended by including a linear increase in density with depth. Subsequent L_2 and L_∞ norm minimization procedures are applied to find the density parameters by adjusting both the vertical gravity and the vertical gravity gradient.

We found that including the vertical gravity gradient in the interpretation of the GOCO03S-derived data reduces the non-uniqueness of the inverse gradiometric problem for density determination. The density structure of the sedimentary formations that provide the optimum predictions of the GOCO03S-derived gravity and vertical gradient of gravity consists of a surface density contrast with respect to surrounding rocks of 0.24-0.28 g/cm³ and its decrease with depth of 0.05-0.25 g/cm³ per 10 km. Moreover, the case where the sedimentary rocks are gravitationally completely compacted in the deepest parts of the basin is supported by L_∞ norm minimization. However, this minimization also allows a remaining density contrast at the deepest parts of the sedimentary basin of about 0.1 g/cm³.

Publications:

Martinec, Z., and J. Fullea (2013), A refined model of sedimentary rock cover in the south-eastern part of the Congo basin from GOCE gravity and vertical gravity gradient observations. *Int. J. Appl. Earth Observation & Geoinformation*, (submitted, June 11, 2013; major revision Sept. 6, 2013).

Fullea, J., J. Rodríguez-González, M. Charco, Z. Martinec, A. Negredo, and A. Villaseñor (2013), Upper mantle structure under the Atlantic-Mediterranean transition zone: new constraints from GOCE mission and other potential field data. *Int. J. Appl. Earth Observation & Geoinformation*, (submitted, June 13, 2013; major revision December 2, 2013).

Presentation:

Martinec, Z. (2013), A refined model of sedimentary rock cover over the Congo basin from the interpretation of GOCE gradiometric data. EGU General Assembly, Vienna, Austria, 7-12 April.

4.4 A benchmark study for geoid model computation codes

We report on testing the UNB (University of New Brunswick) software suite for accurate regional geoid model determination by use of Stokes-Helmert's method against an Australian Synthetic Field (ASF) as "ground truth". This testing has taken several years and has led to

discoveries of several significant errors (larger than 5mm in the resulting geoid models) both in the UNB software as well as the ASF. It was our hope that, after correcting the errors in UNB software, we would be able to come up with some definite numbers as far as the achievable accuracy for a geoid model computed by the UNB software. Unfortunately, it turned out that the ASF contained errors, some of as yet unknown origin, that will have to be removed before that ultimate goal can be reached. Regardless, the testing has taught us some valuable lessons, which we describe in this paper. As matters stand now, it seems that given errorless gravity data on 1' by 1' grid, a digital elevation model of a reasonable accuracy and no topographical density variations, the Stokes-Helmert approach as realised in the UNB software suite is capable of delivering an accuracy of the geoid model of no constant bias, standard deviation of about 25 mm and a maximum range of about 200 mm. We note that the UNB software suite does not use any corrective measures, such as biases and tilts or surface fitting, so the resulting errors reflect only the errors in modelling the geoid.

Publication:

Vanicek, P., R. Kingdon, M. Kuhn, A. Ellmann, W.E. Featherstone, M.C. Santos, **Z. Martinec**, C. Hirt, and D. Avalos (2013), Testing Stokes-Helmert geoid model computation on a synthetic gravity field: experiences and shortcomings, *Studia Geophys. Geod.*, **57**, 369-400.

4.5 The adjoint sensitivity method of global electromagnetic induction for downward continuation of secular magnetic variations

Martinec (Geophys. J. Int., 136, 1999) developed a time-domain spectral-finite element approach for the forward modelling of vector electromagnetic induction data as measured on ground-based magnetic observatories or by the CHAMP satellite. We use the same time and space representations of magnetic induction vector and designed a new method of computing the sensitivity of the ground-based or CHAMP magnetic induction data to a magnetic field prescribed at the core-mantle boundary, which we term the adjoint sensitivity method. The forward and adjoint initial boundary-value problems, both solved in the time domain, are identical, except for the specification of prescribed boundary conditions. The respective boundary-value data on the ground or at the satellite's altitude are the X magnetic component measured by a vector magnetometer for the forward method and the difference between the measured and predicted Z magnetic component for the adjoint method. The squares of the differences in Z magnetic component summed up over the time of observation and all spatial positions of observations determine the misfit. Then the sensitivities of observed data, that is the partial derivatives of the misfit with respect to the parameters characterizing the magnetic field at the core-mantle boundary, are then obtained by the surface integral over the core-mantle boundary of the product of the adjoint solution multiplied by the time-dependent functions describing the time variability of magnetic field at the core-mantle boundary, and integrated over the time of observation.

Presentation:

Hagedoorn, J.M., and **Martinec, Z.** (2013), Downward continuation of the Earth's geomagnetic field through an electrically conducting mantle: first application of the adjoint sensitivity method. EGU General Assembly, Vienna, Austria, 7-12 April (poster).

4.6 The deformational response of a coupled thermomechanical ice sheet model and a viscoelastic solid Earth model

We apply a coupled thermomechanical ice sheet -- self-gravitating viscoelastic solid Earth model (SGVEM), allowing for the dynamic exchange of ice thickness and bedrock deformation, in order to investigate the effect of viscoelastic deformation on ice dynamics and vice versa. In a synthetic glaciation scenario, we investigate the interaction between the ice sheet and the solid Earth deformation, the glacial-isostatic adjustment (GIA), accounting for an atmospheric forcing dependent on the ice sheet surface altitude. We compare the results from the coupled model to runs with a simple, but common solid Earth parametrization consisting of an elastic lithosphere and a relaxing asthenosphere (ELRA), as well as to a rigid Earth without any deformation. We find that the deformational behaviour of the SGVEM on ice dynamics (i.e. stored ice volume, ice thickness and velocity field) is comparable to the ELRA for an optimal choice of the parameters in steady state, but feature differences in the transient behaviour. Beyond the ice sheet, in the region of peripheral forebulge, the differences in the transient surface deformation between ELRA and SGVEM are substantial, demonstrating the inadequacy of the ELRA model for interpreting constraints on GIA in the periphery of the ice sheet, such as sea level indicators and GPS uplift rates.

Publication:

Konrad, H., M. Thoma, I. Sasgen, V. Klemann, K. Grosfeld, D. Barbi, and **Z. Martinec** (2013), The deformational response of a viscoelastic solid Earth model coupled to a thermomechanical ice sheet model. *Surv. Geophys.*, (accepted October 13, 2013).

Presentation:

Konrad, H., I. Sasgen, M. Thoma, V. Klemann, K. Grosfeld, and **Z. Martinec** (2013), Ice sheet and ice shelf simulations with a fully coupled ice sheet -- solid Earth model. IAG symposium on 'Reconciling Observations and Models of Elastic and Viscoelastic Deformation due to Ice Mass Change', Ilulissat, Greenland, 30 May - 2 June.

4.7 A benchmark study for global 3-D electromagnetic computation codes

Global electromagnetic (EM) induction studies have been the focus of increasing attention during the past few years. A primary stimulus for this interest has been increased quality, coverage and variety of the newly available data sets especially from recent low-Earth-orbiting satellite missions. The combination of traditional ground-based data with satellite-borne measurements presents intriguing opportunity to attack the most challenging problem of deep EM studies: the recovery of 3-D variations of electrical conductivity in the Earth's mantle. But the reliable inference of deep-Earth electrical properties depends on the accuracy and efficiency of the underlying forward modelling solutions used to model 3-D electromagnetic induction in a heterogeneous sphere. Several 3-D forward solvers have been proposed over the last decade, which are based on staggered-grid finite difference, integral equation, finite element, and spherical harmonic-finite element approaches. However, there has been no systematic intercomparison amongst the solvers. The goal of this research is to conduct such a study in order to explore the relative merits of the different approaches when confronted with a set of synthetic models designed to probe the numerical accuracy of each. The results of the intercomparison are presented along with performance metrics to help assess the computational costs associated with each solution.

Publication:

Kelbert, A., A. Kuvshinov, J. Velimsky, T. Koyama, J. Ribaud, J. Sun, **Z. Martinec**, and C.J. Weiss (2013), Global 3-D electromagnetic forward modeling: A benchmark study. *Geophys. J. Int.*, (accepted January 21, 2014).

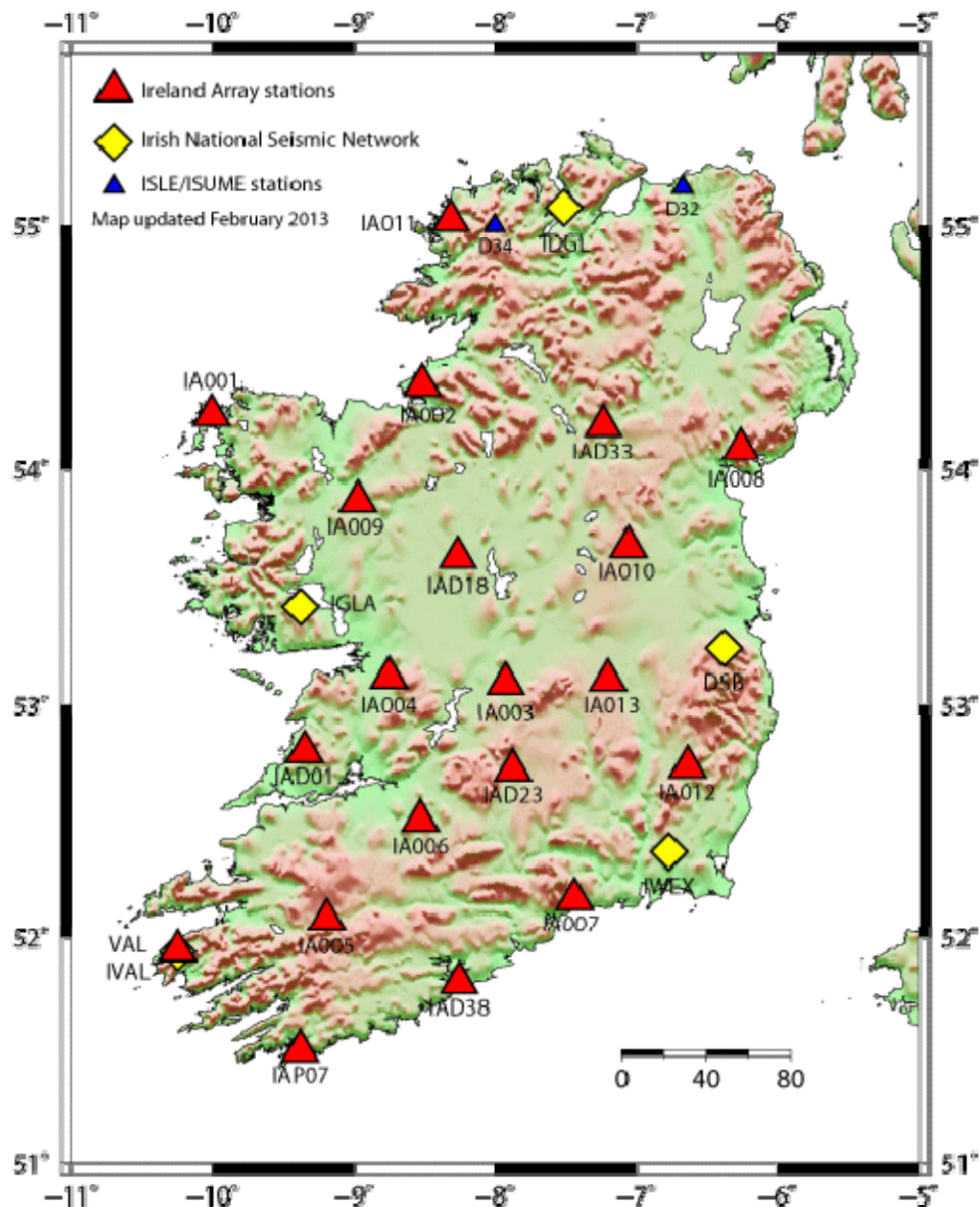
5 Seismology and geodynamics

Group Leader: Assistant Professor Sergei Lebedev

5.1 Ireland Array

Sergei Lebedev, Clare Horan, Andrew Schaeffer, Peter Readman, Nicola Piana Agostinetti, Andrea Licciardi, Louise Collins, Matthew Agius, Franz Hauser, Brian O'Reilly, Tom Blake





Ireland Array is a major broadband seismometer deployment that has been a collaboration of all seismologists in the Geophysics Section. The stations were installed using savings in existing seismology grants, with this major new facility now helping us to attract new funding. In 2013, data collection and station maintenance have continued. The dense coverage of the entire country with the stations of Ireland Array is now enabling detailed imaging Ireland's subsurface and monitoring of its seismicity, in both basic and applied studies. The imaging is beginning to reveal Ireland's deep structure and evolution at a new level of detail. The first research project using Ireland Array data—imaging the Moho and crustal structure across Ireland with teleseismic receiver functions—is being completed at DIAS by Andrea Licciardi and co-workers, with a paper in preparation.

Presentations:

- Licciardi, A., S. Lebedev, and N. Piana Agostinetti** (2013), Imaging Ireland's crust with teleseismic receiver functions, with applications to geothermal research (talk). Irish Geological Research Meeting, Derry, 2 March.
- Licciardi, A., S. Lebedev, and N. Piana Agostinetti** (2013), Moho depth and crustal anisotropy in Ireland from teleseismic receiver functions (Poster). EGU General Assembly, Vienna, Austria, 7-12 April.
- Lebedev, S., C. Horan, A.J. Schaeffer, P.W. Readman, M.R. Agius, L. Collins, N. Piana Agostinetti, A. Licciardi, J. Adam, F. Hauser, B.M. O'Reilly, and T. Blake** (2013), Ireland Array: Probing the crust and mantle beneath Ireland and North Atlantic (Poster). Atlantic Ireland Conference, Dublin, 11 November.
- Lebedev, S., B.M. O'Reilly, N. Piana Agostinetti, and C.J. Bean** (2013), Establishing Baseline Seismicity of the Irish Frontier Basins: Understanding seismic hazard and regional crustal structure offshore Ireland using new broadband seismometer arrays onshore (Poster). Atlantic Ireland Conference, Dublin, 11 November.

5.2 Global seismic tomography

A. Schaeffer, S. Lebedev

Heterogeneity of the composition and physical state of the rocks within the Earth is reflected in variations in seismic-wave speeds at depth. This seismic heterogeneity can be observed in a number of different ways, each yielding a complementary perspective on the Earth's bulk properties, structure, and dynamics. A surface-wave dispersion diagram, constructed from millions of fundamental and higher-mode dispersion measurements around the world, shows variability around global averages for all modes and all frequencies that are included in it, with the largest variations seen for the fundamental-mode phase and group velocities at short periods (less than 30 and 40 s, respectively) that sample the highly heterogeneous crust and uppermost mantle. Seismic tomography turns large sets of measurements into models of three-dimensional wave speed variations at depth. Global shear-wave speed models have been in agreement since 1990s regarding heterogeneity in the upper mantle at thousands-of-kilometres scales. The rapid recent increase in global data sampling facilitated an increase in the tomographic resolution, and a number of today's models show close agreement in the upper 200 km of the mantle at much shorter, hundreds-of-kilometres scale lengths. Greater disagreements between different models remain in the mantle transition zone. Our new model SL2013sv, constrained by an unprecedentedly large new dataset of multimode waveform fits, demonstrates increased resolution compared to other existing models for a variety of features; it captures regional scale heterogeneity globally, within both the upper mantle and the crust. A global stack of shear-velocity profiles extracted from SL2013sv shows a monotonic decrease in the amplitude of wavespeed variations with depth, mirrored by a decrease in RMS variations in SL2013sv and other current models, from largest in the top 150–200 km to much smaller below 250 km. Regionalization of SL2013sv by means of cluster analysis, with no a priori information, provides an accurate tectonic regionalization of the entire Earth. The three oceanic and three continental types that naturally come out of the clustering differ by the age of the deep lithosphere. The results give a new perspective on the “depth of tectonics”—the depths down to which shear speed profiles (and, by inference, geotherms) beneath oceanic and continental regions of different ages are different. Old oceanic plates are underlain by higher shear-wave speeds compared to young and intermediate-age oceans down to 200 km depth. At 200–250 km, all type-average mantle profiles converge, except for the Archean craton profile that shows distinctly higher velocities down to 250–280 km depths.

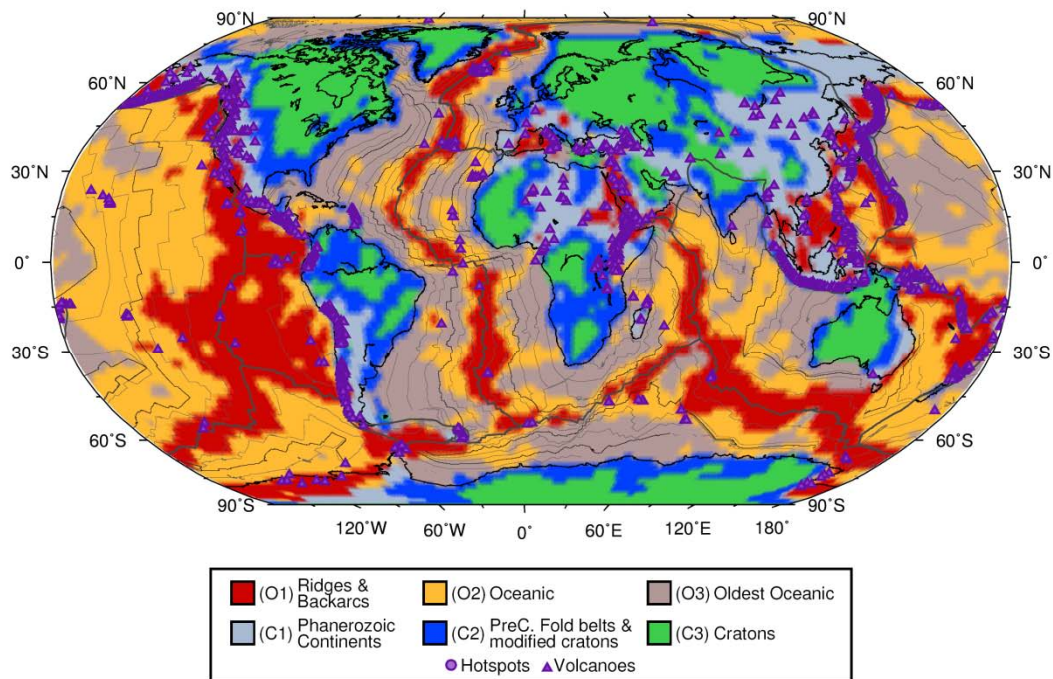


Figure 5.2.1. Tectonic regionalization of the Earth computed from the model SL2013sv using the *k-means* clustering.

Publications:

Schaeffer, A.J., and S. Lebedev (2013), Global shear-speed structure of the upper mantle and transition zone. *Geophys. J. Int.*, **194**, 417-449. [WINNER, GJI Student Author Award for best paper, 2013 (A. Schaeffer).]

Schaeffer, A. J., and S. Lebedev (2013), Global heterogeneity of the lithosphere and underlying mantle: A seismological appraisal based on multimode surface-wave dispersion analysis, shear-velocity tomography, and tectonic regionalization. Invited Review in: "The Earth's Heterogeneous Mantle," Springer, accepted September 9, 2013.

Presentations:

Schaeffer, A.J., and S. Lebedev (2013), Heterogeneity and dynamics of the Earth's upper mantle and crust (Talk). 56th Irish Geological Research Meeting, University of Ulster, Derry, March.

Schaeffer, A.J., and S. Lebedev (2013), Heterogeneity of the Earth's upper mantle, from waveform inversion of over one million broadband seismograms (Poster). EGU General Assembly, Vienna, Austria, 7-12 April.

Lebedev, S., and A. Schaeffer (2013), Seismic tomography meets millions of waveforms: Exploiting data redundancy to control errors and increase resolution (Talk). 4th QUEST workshop, Benodet, France, 19-24 May.

Schaeffer, A., and S. Lebedev (2013), Heterogeneity and anisotropy of the Earth's upper mantle and crust (Poster). 4th QUEST workshop, Benodet, France, 19-24 May.

Lebedev, S. (2013), Global and regional upper-mantle tomography: Exploring the structure and dynamics of tectonic plates. Invited seminar, University of Southern California, Los Angeles, 6 December.

5.3 Seismic anisotropy of the Earth's mantle

A. Schaeffer, S. Lebedev, in collaboration with T. Becker (USC), M. Long (Yale), C. Conrad (U. Hawaii)

Deformation within the Earth's crust and mantle often results in crystallographic preferred orientations that produce measurable seismic anisotropy. Shear wave splitting measurements are an unambiguous indicator of the presence of seismic anisotropy; however, they suffer from poor depth resolution (integrated measurement from CMB to surface), in addition to being geographically limited (measurements only made at seismometer locations). The analysis of surface wave propagation also provides insight into the azimuthal variations in wave-speed, but with significantly better depth resolution. Thanks to the rapid increase in the number of seismic stations around the world, increasingly accurate, high-resolution 3D models of azimuthal anisotropy can be calculated using surface-wave tomography. Our new global, azimuthally anisotropic model of the upper mantle and the crust is constrained by a very large waveform fit dataset (>900,000 vertical-component seismograms). Automated, multimode waveform inversion was used to extract structural information from surface and S wave forms, yielding resolving power from the crust down to the transition zone. Our unprecedentedly large waveform dataset, with complementary high-resolution regional arrays (including USArray) and global network sub-sets within it, produces improved resolution of global azimuthal anisotropy patterns. The model also reveals smaller scale patterns of 3D anisotropy variations related to regional lithospheric deformation and mantle flow, in particular in densely sampled regions. In oceanic regions, the strength of azimuthal anisotropy is a function of depth, spatial position with respect to the spreading ridge, and of the orientation of the current and fossil spreading directions. In continental regions, azimuthal anisotropy is more complex. Reconciling complementary observations given by shear wave splitting, surface-wave array analysis, and large-scale, global 3D models offers new insights into the mechanisms of continental deformation and the architecture and evolution of the lithosphere.

Quantitative joint analysis of anisotropy mapped by tomography and geodynamic models is another component of this project, undertaken together with geodynamicists. The targets of this collaboration are the origin of azimuthal seismic anisotropy and the plate tectonics and mantle dynamics beneath oceans.

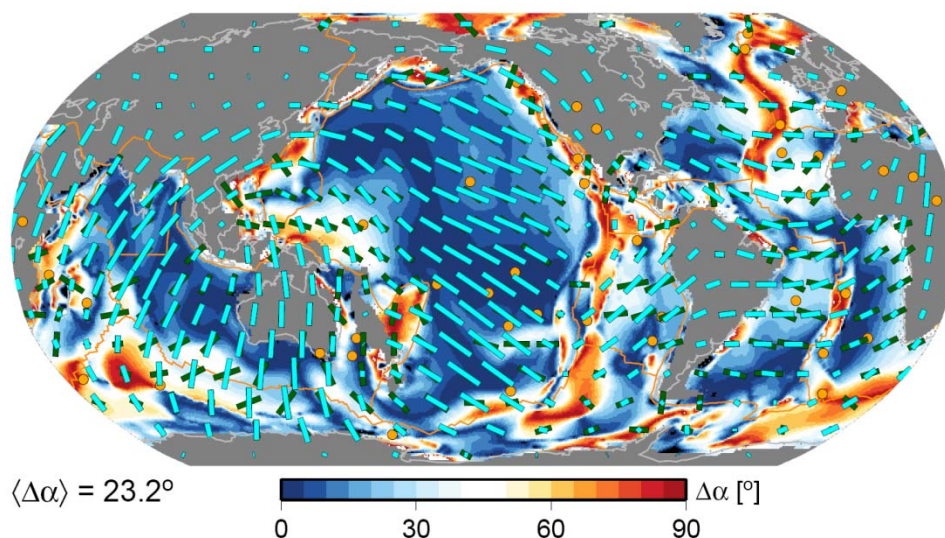


Figure 5.3.1. A comparison at 200-km depth of azimuthal anisotropy (cyan, Schaeffer and Lebedev, 2013) and the best-fit LPO fabric geodynamic model of Becker, based on mantle flow (dark green sticks). Background

colours show the absolute angular misfit; legend specifies the global, tomography-anomaly weighted mean. All misfit metrics are computed for oceanic plates only, while tomography is shown globally (Becker et al., work in progress).

Presentations:

Schaeffer, A.J. (2013), Heterogeneity and anisotropy of the Earth's upper mantle: from global to regional scales. School of Geological Sciences, University College Dublin, January.

Schaeffer, A., and S. Lebedev (2013), Global variations in azimuthal anisotropy of the Earth's upper mantle and crust (Poster, 9 December). AGU Fall Meeting, San Francisco, 9-13 December.

Campbell, L., M.D. Long, T.W. Becker, and **S. Lebedev** (2013), Complex seismic anisotropy beneath Germany from shear wave splitting and surface wave models (Poster, 9 December). AGU Fall Meeting, San Francisco, 9-13 December.

5.4 Lithospheric structure of North America

A. Schaeffer, S. Lebedev

The deployment of the Earthscope USArray during the last decade has produced a very dense sampling of the central part of the North American continent (within the United States) with broadband seismic data. Regional tomography is now mapping the deep structure of the continent in great detail, in particular beneath the western US where the USArray deployment began. At the scale of the entire continent, however, the resolution of seismic imaging remains uneven, with much poorer coverage away from the footprint of the array than beneath it. Important questions regarding the deep structure, lateral extent and evolution of the North American Craton, most of it not covered by USArray, thus remain difficult to answer.

We computed a new model of the upper mantle beneath the entire North America by means of inversion of multimode waveform fits of 3/4 of a million vertical-component, broadband seismograms. Of these, almost 230 thousand are from the Transportable Array component of USArray, several tens of thousands from other USArray-affiliated stations, and the rest from global networks and other arrays. Automated multimode waveform inversion was used to extract accurate structural information from surface and S wave forms, yielding resolving power from the crust down to the transition zone.

Our unprecedentedly large waveform dataset, with highly complementary USArray and global-network sub-sets within it, produces improved resolution for a variety of features in North American upper mantle, compared to other available models. The internal structure and boundaries of the North American Craton are resolved in more detail than previously. Sharp northern boundaries of the cratonic lithosphere are observed to closely follow the coastline, with North America's and Greenland's lithospheric roots clearly separated. The boundary of the craton in western Canada closely follows the Rocky Mountain Front, whereas in eastern North America, where multiple episodes of continental rifting are superimposed, the boundary largely coincides with the western extent of the Appalachian orogenic front. Within the continent, relatively low-velocity lithosphere is found beneath the failed Mid-Continental Rift. High velocities at depth between the Great Bear Arc and Beaufort Sea provide convincing new evidence for the enigmatic, recently proposed "MacKenzie Craton", not exposed anywhere at the surface.

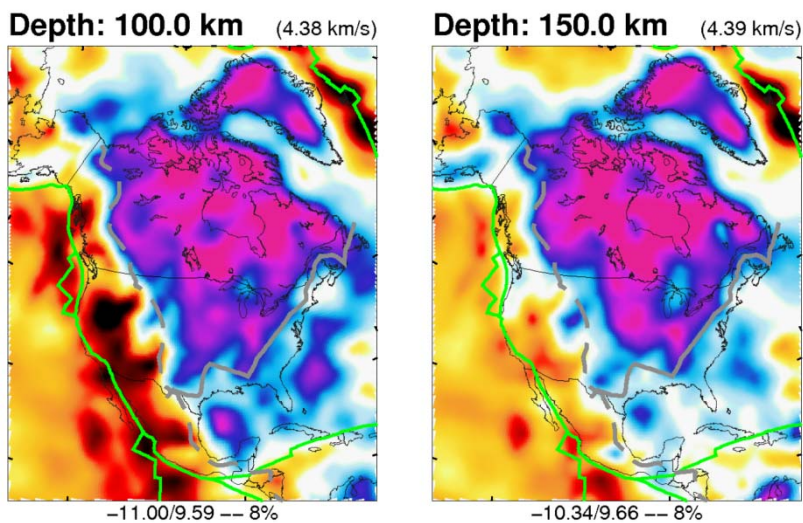


Figure 5.4.1. Shear-wave speeds beneath North America at 100 and 150 km depths. Mantle reference velocity is indicated in brackets at the top right of each map. The same linear colour scale is used; the absolute minimum and maximum percentage and the saturation limit of the scale are indicated beneath each map. Major plate boundaries are plotted in green, and the boundaries of the Proterozoic stable continent as grey lines, with the western boundary being the Rocky Mountain Front (dashed) and the eastern boundary being the ancient rifted continental margin (solid).

Publication:

Schaeffer, A.J., and S. Lebedev (2013), Imaging the North American continent using waveform inversion of global and USArray data. *Earth Planet. Sci. Lett.*, in revision.

Presentation:

Schaeffer, A.J., and S. Lebedev (2013), Heterogeneity and anisotropy of the North American upper mantle, imaged using multimode waveform tomography. Invited talk, GSC GEM Diamonds Project, University of British Columbia, Robson Square, Canada, February.

Lebedev, S., and A.J. Schaeffer (2013), Lithospheric Structure of the North American Continent Imaged With Earthscope USArray and Global Data (Poster). AGU Fall Meeting, San Francisco, 9-13 December.

5.5 Structure and evolution of the Arctic region

S. Lebedev, A. Schaeffer

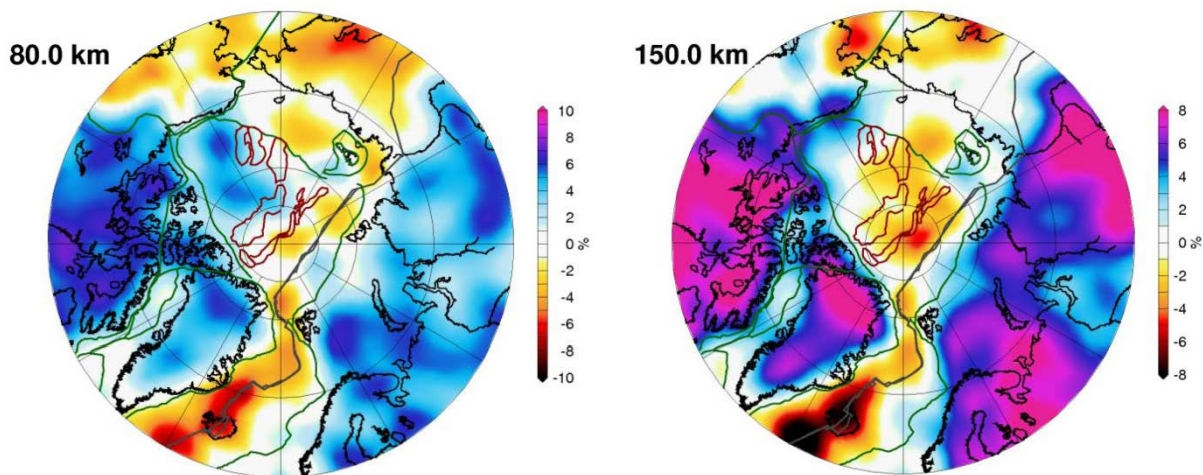


Figure 5.5.1. Shear-wave speed distributions at 80 and 150 km depths beneath the Arctic region.

Lateral variations in seismic velocities in the upper mantle, mapped by seismic tomography, reflect primarily the variations in the temperature of the rock at depth. Seismic tomography thus reveals lateral changes in the temperature and thickness of the lithosphere; it maps deep boundaries between tectonic blocks with different properties and with different age of the lithosphere.

Our new global, 3D tomography provides improved resolution of the lithosphere across the whole of the Arctic region, compared to other available models. The most prominent high-velocity anomalies, seen down to 150-200 km depths, indicate the cold, thick, stable mantle lithosphere beneath Precambrian cratons. The northern boundaries of the Canadian Shield's and Greenland's cratonic lithosphere closely follow the coastlines, with the Greenland and North American cratons clearly separated from each other. In Eurasia, in contrast, continental crust underlain by cratonic lithosphere extends hundreds of kilometres north of the coast of the continent, beneath the Barents and eastern Kara Seas. The boundaries of the Archean cratons mapped by tomography indicate the likely offshore extensions of major Phanerozoic deformation fronts in northern Eurasia.

The old oceanic lithosphere of the Canada Basin is much colder and thicker than the younger lithosphere beneath the adjacent Amundsen Basin, north of the Gakkel Ridge. Beneath the slow-spreading Gakkel Ridge, the expected low-velocity anomaly associated with partial melting in the uppermost mantle is weaker than beneath faster-spreading ridges globally. South of the ridge, the Nansen Basin shows higher seismic velocities in the upper mantle beneath it, compared to the Amundsen Basin. At 150-250 km depth, most of the oceanic portions of the central Arctic (the Canada and Amundsen Basins) are underlain by a moderate low-velocity anomaly, characteristic of a warm asthenosphere similar to that beneath northern Pacific. Beneath Iceland and surroundings in the North Atlantic, the asthenosphere shows much lower velocities, probably indicating partial melting associated with the hotspot volcanism.

Presentation:

Lebedev, S. and A.J. Schaeffer (2013), Seismic tomography with millions of waveforms and global upper-mantle heterogeneity, with a zoom-in on the Arctic. Invited seminar, University of Oslo, Norway, 24 October.

Lebedev, S., and A.J. Schaeffer (2013), Seismic Tomography of the Arctic: Continental Cratons, Ancient Orogens, Oceanic Lithosphere and Convecting Mantle Beneath (Invited Talk, 9 December). AGU Fall Meeting, San Francisco, 9-13 December.

5.6 Surface-wave imaging of Asia

E. Neenan, S. Lebedev, A. Schaeffer, T. Blake

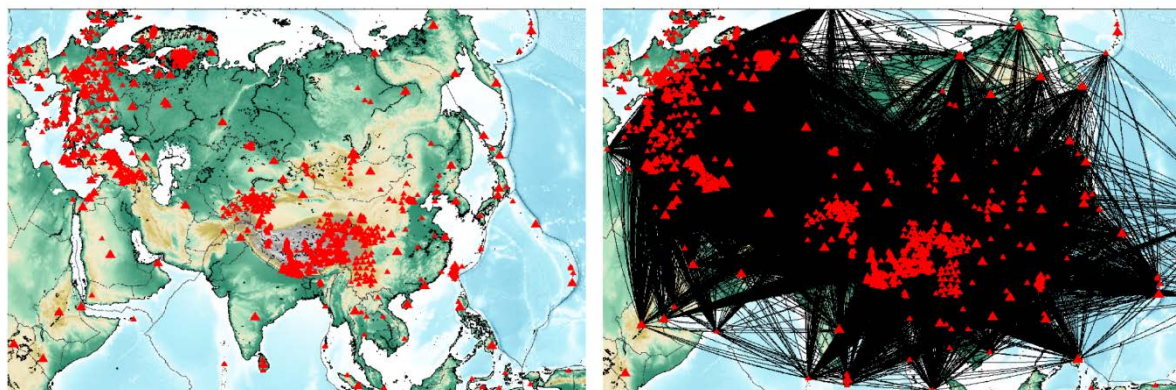


Figure 5.6.1. Distribution of 1221 stations from which the data have been collected (left) and the 135381 station-station paths (right) with data suitable for interstation measurements. Larger red triangles are permanent global network stations. Stations surrounding the continent have been included for better coverage of peripheral areas. Robust Rayleigh-wave dispersion curves have been measured for 112039 station pairs.

In this project, automated techniques for the inter-station measurement of surface-wave phase velocities are being applied to a very large data set, sampling the whole of Asia. The many thousands of new surface-wave dispersion curves measured will be inverted for tomographic phase-velocity maps. Seismic velocities and their anisotropy resolved by the tomography will reveal the structure and deformation within the tectonic plates and beneath them. The objective of the project is to build a whole-Asia model of surface-wave velocities that will provide a significant advance in resolution compared to the currently available models.

Asia—from the Eastern Mediterranean to the Far East and from India to the Arctic—includes diverse tectonic blocks, ranging from ancient, stable continental units to foldbelts that record Asia's tectonic assembly and evolution, and to the large zone of active continental collisions that stretches from Anatolia to Iran and to Tibet. Detailed seismic images of the lithosphere (the tectonic plate) at the scale of entire Asia will give us new insights into the fascinating geological processes that formed this enormous landmass. The high-resolution tomographic models can also be used for accurate modelling of seismic wave propagation in regions within Asia that are of particular interest for monitoring in the CTBTO framework.

The high resolution of the seismic models is being achieved through the application of accurate, automated new methods for surface-wave measurements to a very large data set (all of the publicly available broadband data). The hundreds of stations across Asia are being treated as a large, single array of stations.

The project represents MSc research of Emily Neenan, funded by a one-year grant from CTBTO, Vienna.

Presentations:

Neenan, E., A.J. Schaeffer, S. Lebedev, T. Blake, and T. Meier (2013), High-Resolution Mapping of Surface-Wave Velocities Across Asia Using Automated Inter-Station Measurements (Poster). CTBT Science Technology Conference, Vienna, 17-21 June.

Neenan, E., A.J. Schaeffer, S. Lebedev, T. Meier, and T.A. Blake (2013), Array Imaging at Continent Scale: Surface-Wave Imaging of Asia Using Automated, Broadband Interstation Measurements (Poster). AGU Fall Meeting, San Francisco, 9-13 December.

5.7 Regional seismic tomography of China

S. Lebedev, in collaboration with Drs. Li Zhao, Frederic Deschamps, Cedric Legendre (Institute of Earth Sciences, Academia Sinica, Taiwan)

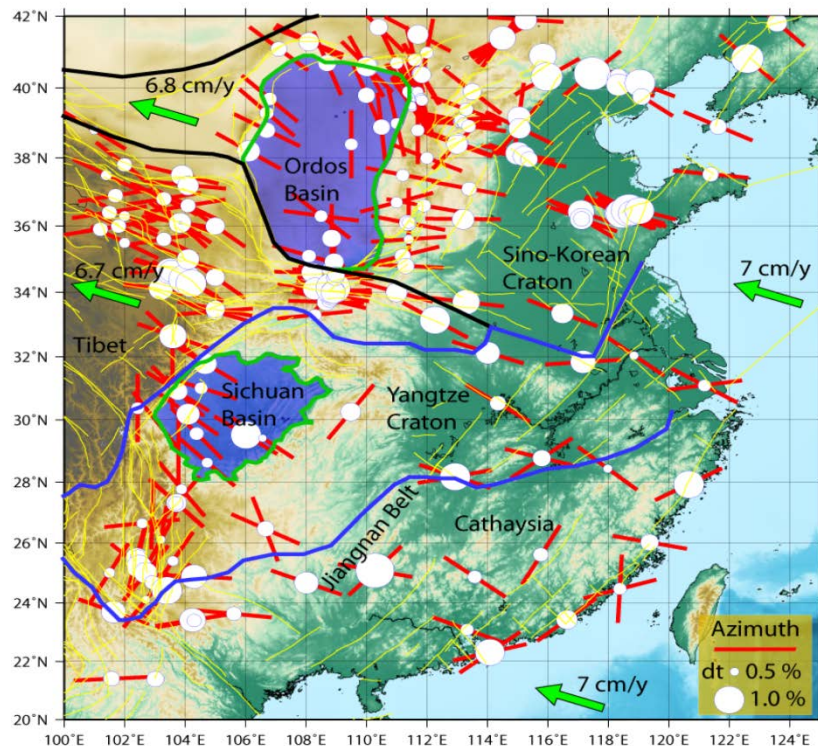


Figure 5.7.1. Topography, main tectonic units and published shear-wave splitting in eastern China (from Legendre et al., submitted manuscript). Most of seismic stations in the east are new and are being used in surface-wave imaging in this project.

The Phanerozoic assembly of China—from a multitude of continental blocks—and its spectacular tectonic evolution in the geologically recent past makes its lithospheric structure a fascinating object of study. The recent deployments of large, dense arrays of broadband seismic stations across much of China offer an opportunity of seismic imaging with resolution much higher than possible previously. In collaborative projects with colleagues in Taiwan and Beijing, Lebedev’s surface-wave imaging methods are being applied in SE and NE China, with the results providing new information on their crustal and upper-mantle structure. Isotropic, surface-wave, phase-velocity anomalies reveal the deep boundaries of intact cratonic blocks. The deep mantle keels are notably absent beneath both eastern Sino-Korean and eastern Yangtze cratons. Azimuthal anisotropy shows fabric that is a record of ancient lithospheric deformation and of recent asthenospheric flow, the latter a possible cause for some of the intra-plate basaltic volcanism in eastern China.

Presentations:

- Legendre, C.P., L. Zhao, F. Deschamps, **S. Lebedev**, and Q. Chen (2013), Anisotropic Maps of Rayleigh-wave Phase Velocity Beneath Eastern China (Poster, 25 June). AOGS 10th Annual Meeting, Brisbane, Australia, 24-28 June.
- Tian, Y., P. Legendre, L. Zhao, M. Wu, **S. Lebedev**, Q. Chen, and J. Ning (2013), Anisotropic Rayleigh-Wave Phase-Velocity Maps beneath North-eastern China (Poster, 13 December). AGU Fall Meeting, San Francisco, 9-13 December.
- Legendre, C.P., F. Deschamps, L. Zhao, **S. Lebedev**, and Q. Chen (2013), Rayleigh-wave Phase-velocity Maps beneath Eastern China (Poster, 13 December). AGU Fall Meeting, San Francisco, 9-13 December.

5.8 Seismic structure and evolution of Mongolia

S. Lebedev, in collaboration with Dr. Jiatie Pan and Prof. Wu (China Earthquake Administration, Beijing)

This collaborative project is focussed on the seismic imaging of central Mongolia using teleseismic and ambient-noise surface-wave measurements. The new data used in the project has been recorded by an array of wide-band seismic stations that has been operated by the China Earthquake Administration for the last 2 years. The goal of the project is to determine the isotropic and anisotropic structure of the crust and upper mantle and obtain new constraints on the enigmatic Phanerozoic assembly of Mongolia, in particular on the lithospheric deformation associated with the closure of the Mongol-Okhotsk Ocean and the subsequent orogeny. Dr Jiatie Pan (CEA) has been funded in China to come to DIAS to work on this project with Lebedev for 4 months. The project has been initiated with the arrival of Dr. Pan to DIAS on December 16, 2013.

5.8.1.1 Development of seismic imaging methods

S. Lebedev, in collaboration with Prof. T. Meier and his group at Univ. Kiel, Germany

The most exciting advance in the development of imaging methods has been the completion and testing of a fully automated technique for accurate, broadband, surface-wave dispersion measurements and the application of the technique to very large data sets, with eventual tomographic inversions.

Inter-station dispersion curves of Rayleigh and Love waves are measured by cross-correlating vertical and transverse component seismograms, respectively. The phase velocity curves are first computed from the phase of the filtered and weighted cross-correlation functions and then undergo a selection procedure. Segments of the phase velocity curve that (1) are reasonably close to a path-dependent background model, that (2) pass a smoothness criterion, and that (3) are sufficiently long are accepted. The final inter-station dispersion curve is computed by averaging all measurements at the same station pair for a large number of events. Comparison of average dispersion curves measured along the same inter-station path for the opposite propagation directions is a useful check and can reveal errors caused by off-path propagation and erroneous instrument response information.

The procedure has been applied to broad-band recordings at 286 permanent stations in central and northern Europe (1990-2012). It yielded a data set of high-quality, inter-station Rayleigh and Love dispersion curves in a very broad frequency band of about 10 s to 350 s, with low values of the standard deviation and the standard error (below 2% and 0.5%, respectively). The automated processing makes it possible to determine the phase velocities for different

sets of parameters for curve-smoothness selection criteria. Rough perturbations in the phase velocity curves result primarily from diffraction, mode interference and noise. Contrary to common belief, these effects do not bias the average phase velocities towards greater values, which indicate a random perturbation of the phase velocities by noise and complex non-plane wave propagation.

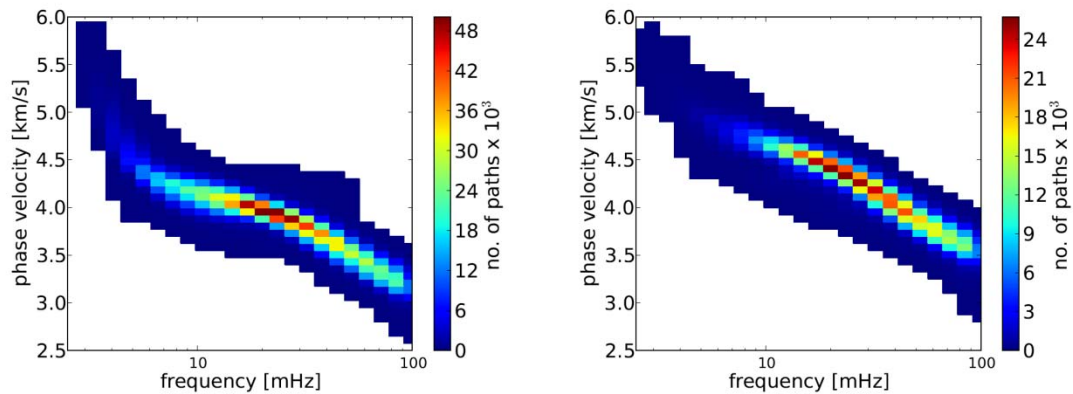


Figure 5.9.1. 2-D histograms of the automatically measured phase velocity curves of the central and northern Europe dataset (Soomro et al. 2013) for Rayleigh (a) and Love (b) waves. The colour scale shows the number of inter-station paths in a bin.

Presentations:

- Soomro, R.A., C. Weidle, **S. Lebedev**, L. Cristiano, and T. Meier (2013), Automated Inter-station Measurements of Fundamental Mode Phase Velocities, and Tomographic Inversion of Surface Waves for Central to Northern Europe (Talk, 7 March). Deutschen Geophysikalischen Gesellschaft, Leipzig, 4-7 March.
- Soomro, R., C. Weidle, **S. Lebedev**, L. Cristiano, and T. Meier (2013), Automated inter-station measurements of fundamental mode phase velocities, and tomographic inversion for Central and Northern Europe (Talk, 11 April). EGU General Assembly, Vienna, Austria, 7-12 April.
- Soomro, R.A., C. Weidle, **S. Lebedev**, L. Cristiano, and T. Meier (2013), Surface wave tomography of central and northern Europe from automated inter-station dispersion measurements (Poster, 11 December). AGU Fall Meeting, San Francisco, 9-13 December.

5.9 Structure and deformation of southern Africa's lithosphere

S. Lebedev, J. Adam, together with F. Sodoudi, F. Tilmann, R. Kind (GFZ Potsdam)

Joint analysis of S receiver functions and surface-wave anisotropy yields evidence for a thick and layered lithosphere beneath the Kalahari Craton. The results of the analysis show that frozen-in anisotropy and compositional changes can generate sharp Mid-Lithospheric Discontinuities (MLD) at depths of 85 and 150–200 km, respectively. A 50 km thick anisotropic layer, containing 3% S wave anisotropy and with a fast-velocity axis different from that in the layer beneath, can account for the first MLD at about 85 km depth. Significant correlation between the depths of an apparent boundary separating the depleted and metasomatised lithosphere, as inferred from published chemical tomography, and those of our second MLD suggest that it is a compositional boundary, most likely due to the modification of the cratonic mantle lithosphere by magma infiltration. The deepening of this

boundary from 150 to 200 km is spatially correlated with the surficial expression of the Thabazimbi-Murchison Lineament (TML), implying that the TML isolates the lithosphere of the Limpopo terrane from that of the ancient Kaapvaal terrane. Thus, the Kalahari lithosphere may have survived multiple episodes of intense magmatism and collisional rifting during the billions of years of its history, which left their imprint in its internal layering.

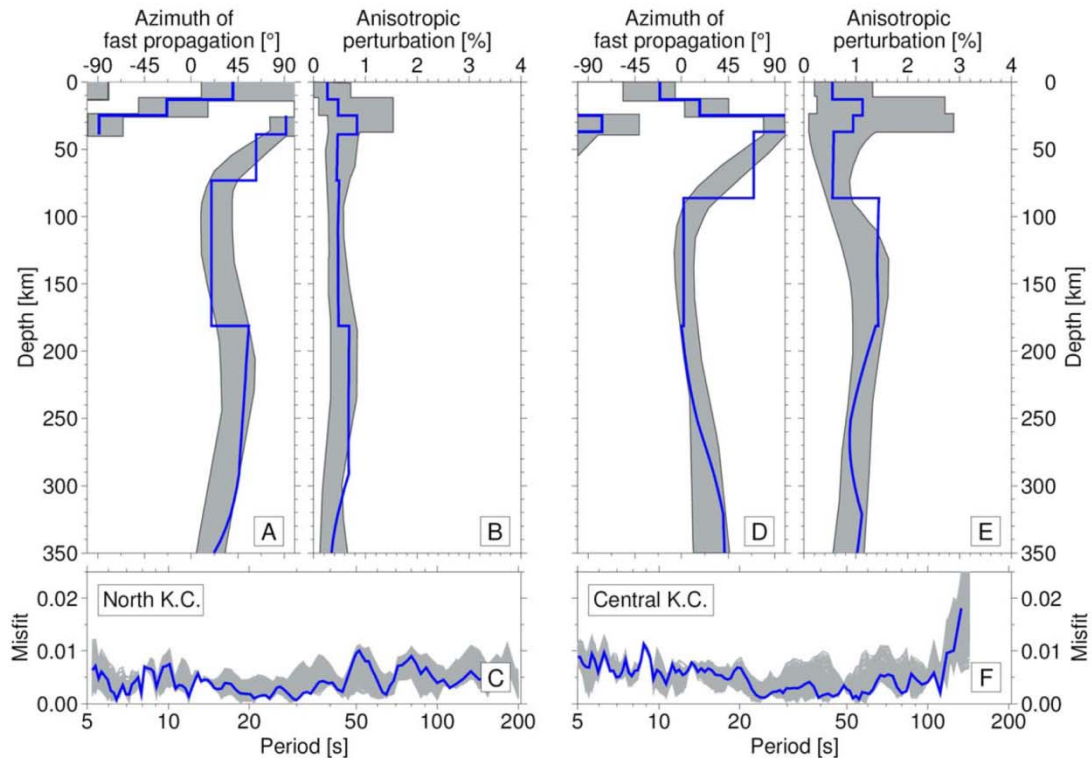


Figure 5.10.1. Azimuthal, shear-wave velocity anisotropy beneath the (a–c) northern and (d–f) central Kaapvaal Craton. The azimuth of fast propagation (a and d) is relative to North (0°), and the amplitude of anisotropy (b and e) is relative to the isotropic-average versus gray bands (a, b, d, e) enclose models that are smooth in the upper mantle and fit the data approximately equally well. Blue lines show the models in which the upper mantle down to 200 km was parameterized with two boxcar basis functions, with three discontinuities above, below, and between them which were allowed to move up and down during the inversion. Misfits for all the models are shown in c and f. The change in the fast-propagation azimuth around 80–90 km depth is present in all models that fit the data and is a robust result of the inversions.

Publication:

Soudoudi, F., X. Yuan, R. Kind, **S. Lebedev**, **J. Adam**, E. Kästle, F. Tilmann (2013), Seismic evidence for stratification in composition and anisotropic fabric within the thick lithosphere of Kalahari Craton. *Geochem. Geophys. Geosyst.*, **14**, 5393–5412, DOI: 10.1002/2013GC004955, 2013.

Presentations:

Adam, J., and **S. Lebedev** (2013), Shear velocity and anisotropy distributions beneath southern Africa's cratons: Lithospheric structure, deformation, LAB and other discontinuities (Talk). EGU General Assembly, Vienna, Austria, 7–12 April.

Muller, M., **J. Fulla**, **A.G. Jones**, **J. Adam**, **S. Lebedev**, and **N. Piana Agostinetti** (2013), Lithospheric-Mantle Structure of the Kaapvaal Craton, South Africa, Derived from Thermodynamically Self-Consistent Modelling of Magnetotelluric, Surface-Wave

Dispersion, S-wave Receiver Function, Heat-flow, Elevation and Xenolith Observations (Poster). EGU General Assembly, Vienna, Austria, 7-12 April.

Adam, J., and S. Lebedev (2013), Shear velocity and anisotropy distributions beneath southern Africa's cratons: Lithospheric structure, deformation, LAB and other discontinuities (Poster). Gordon Research Conference on Interior of the Earth, Mount Holyoke College, South Hadley, MA, USA, 2-7 June.

Sodoudi, F., X. Yuan, R. Kind, **S. Lebedev**, and F.J. Tilmann (2013), Seismic evidence for stratification in composition and anisotropic fabric within the thick lithosphere of Kalahari Craton (Poster). AGU Fall Meeting, San Francisco, 9-13 December.

Domingues, A., J. Chamussa, G.M. Silveira, S. Custodio, **S. Lebedev**, S.-J. Chang, A.M. Ferreira, and J.F. Fonseca (2013), Ambient Noise Tomography of the East African Rift System in Mozambique (Talk). AGU Fall Meeting, San Francisco, 9-13 December.

Muller, M.R., J. Fulla, A.G. Jones, J. Adam, S. Lebedev, and N. Piana Agostinetti (2013), Integrated Petrological Modelling of MT, Seismics, Heat Flow and Topography on the Kaapvaal Craton (Poster). AGU Fall Meeting, San Francisco, 9-13 December.

PhD Thesis:

Adam, J. M.-C., “Seismic structure and anisotropy in southern Africa’s lithosphere: Constraints from broad-band surface-wave dispersion” (supervisor: S. Lebedev). Trinity College Dublin, degree awarded April, 2013.

5.10 Seismic study of the structure and dynamics of Tibet

M. Agius, S. Lebedev

The lithospheric dynamics of Tibet is debated, with very different end-member models advocated to this day. Uncertainties over the anomalies in seismic tomography models contribute to the uncertainty of their interpretations, ranging from the subduction of India as far as northern Tibet to subduction of Asia there and to extreme viscous thickening of the entire Tibetan lithosphere. Within the lithosphere itself, a low-viscosity layer in the mid-lower crust is evidenced by many observations. It is still unclear, however, whether this layer accommodates a large-scale channel flow (which may have uplifted northern and eastern Tibet, according to one model) or if, instead, deformation within it is similar to that observed at the surface (which implies different uplift mechanisms).

Broad-band surface waves provide resolving power from the upper crust down to the asthenosphere, for both isotropic-average shear-wave speeds (proxies for composition and temperature) and the radial and azimuthal shear-wave anisotropy (indicative of the patterns of deformation and flow). We measured highly accurate Love- and Rayleigh-wave phase-velocity curves in broad period ranges (up to 5-200 s) for a few tens of pairs and groups of stations across Tibet, combining, in each case, hundreds to thousands of inter-station measurements, made with cross-correlation and waveform-inversion methods. Robust shear-velocity profiles were then determined by series of non-linear inversions, yielding depth-dependent ranges of shear speeds and radial anisotropy consistent with the data. Temperature anomalies in the upper mantle were estimated from shear-velocity ones using accurate petro-physical relationships. Azimuthal anisotropy in the crust and upper mantle was determined by surface-wave tomography and, also, by sub-array analysis targeting the anisotropy amplitude.

Our results show that the prominent high-velocity anomalies in the upper mantle are most consistent with the presence of subducted Indian lithosphere beneath large portions of Tibet.

Estimated thermal anomalies within the high-velocity features match those expected for subducted India. The morphology of India's subduction beneath Tibet is complex and shows pronounced west-east variations. Beneath eastern and north-eastern Tibet, in particular, the subducted Indian lithosphere appears to have subducted, at a shallow angle, hundreds of km NNE-wards.

Azimuthal anisotropy beneath Tibet is distributed in multiple layers with different fast-propagations directions, which accounts for the complexity of published shear-wave splitting observations. The fast directions within the mid-lower crust are parallel to the extensional components of the current strain rate field at the surface, consistent with similar deformation through the entire crust, rather than channel flow. Anisotropy within the asthenosphere beneath north-eastern Tibet (sandwiched between the Tibetan lithosphere above and the subducted Indian lithosphere below) indicates SSW-NNE flow, parallel to the direction of motion of the Indian Plate, including its subducted leading edge.

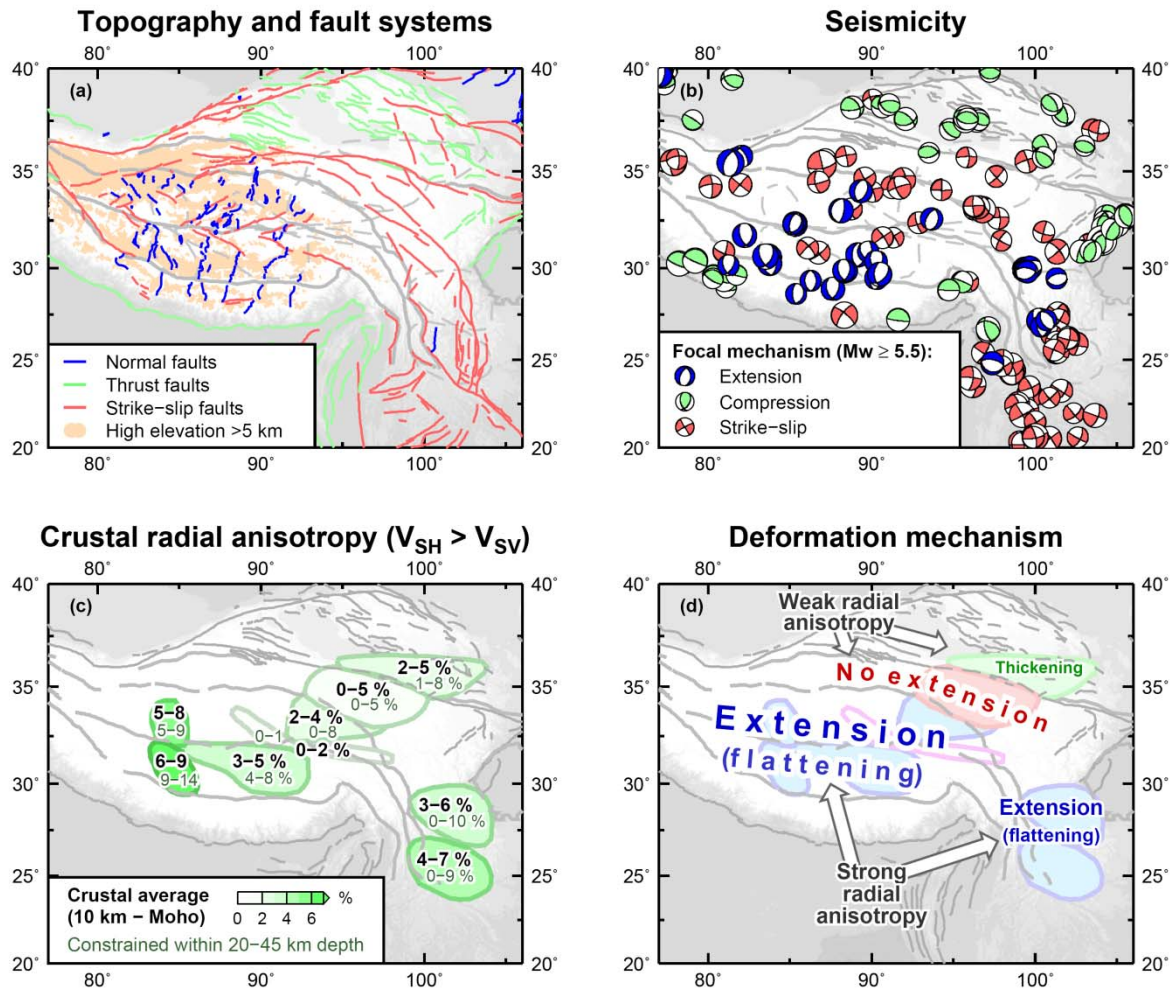


Figure 5.11.1. Deformation and radial anisotropy in the Tibetan crust. (a) Faults, colour-coded according to their type (normal, thrust, and strike-slip). Orange shade highlights regions of elevation higher than 5 km. (b) Focal mechanism of shallow earthquakes (<50 km depth) with moment magnitude >5.5. (c) Ranges of crustal-average radial anisotropy ($(V_{SH} - V_{SV})/V_{S(iso)}$), between 10 km depth and the Moho (bold, black numbers), and ranges of radial anisotropy constrained in the 20–45 km depth range (dark green numbers). (d) The correlation of the deformation regime and radial anisotropy within Tibetan crust.

Publication:

Agius, M.R., and S. Lebedev (2013), Tibetan and Indian lithospheres in the upper mantle beneath Tibet: Evidence from broadband surface-wave dispersion. *Geochem. Geophys. Geosyst.*, **14**, 4260–4281, DOI 10.1002/ggge.20274.

Presentations:

Agius, M.R., and S. Lebedev (2013), Subduction of the Indian lithosphere beneath Tibet and deformation of the Tibetan crust and mantle, imaged with broad-band surface waves (Talk), EGU General Assembly, Vienna, Austria, 7-12 April.

Agius, M.R., and S. Lebedev (2013), Deformation of Tibetan Crust and Mantle and the Uplift of the Plateau: Insights from Broadband Surface Waves (Poster). AGU Fall Meeting, San Francisco, 9-13 December.

PhD Thesis:

Agius, M.R., “The structure and dynamics of the lithosphere beneath Tibet from seismic surface-wave analysis” (supervisor: S. Lebedev). Trinity College Dublin, degree awarded April, 2013.

5.11 Geodynamic modelling of continental deformation

C. Tirel, S. Lebedev, in collaboration with J.-P. Brun (Rennes), E. Burov (Paris VI)

Since plate tectonics began on Earth, grandiose “subduction factories” have continually shaped the continents, accreting continental blocks and new crust at the convergent plate boundaries. An enigmatic product of subduction factories is the high-pressure to ultrahigh-pressure (HP-UHP) metamorphic crustal rocks, regurgitated to Earth’s surface, sometimes from depths as great as 200 km. The Aegean backarc domain comprises two continental blocks that underwent HP metamorphism during the subduction of the African plate. In this project, we have used thermomechanical numerical simulations to show that subduction of small continental-lithosphere blocks separated by oceanic domains, induces variations in the slab buoyancy, giving rise to episodic rollback-exhumation cycles. The single, self-consistent numerical model successfully reproduces the major structural patterns and pressure-temperature-time paths of HP rocks across the Aegean. It appears likely that the “caterpillar walk” of exhuming HP rock units, revealed by our simulations, is a fundamental mechanism behind HP exhumation globally.

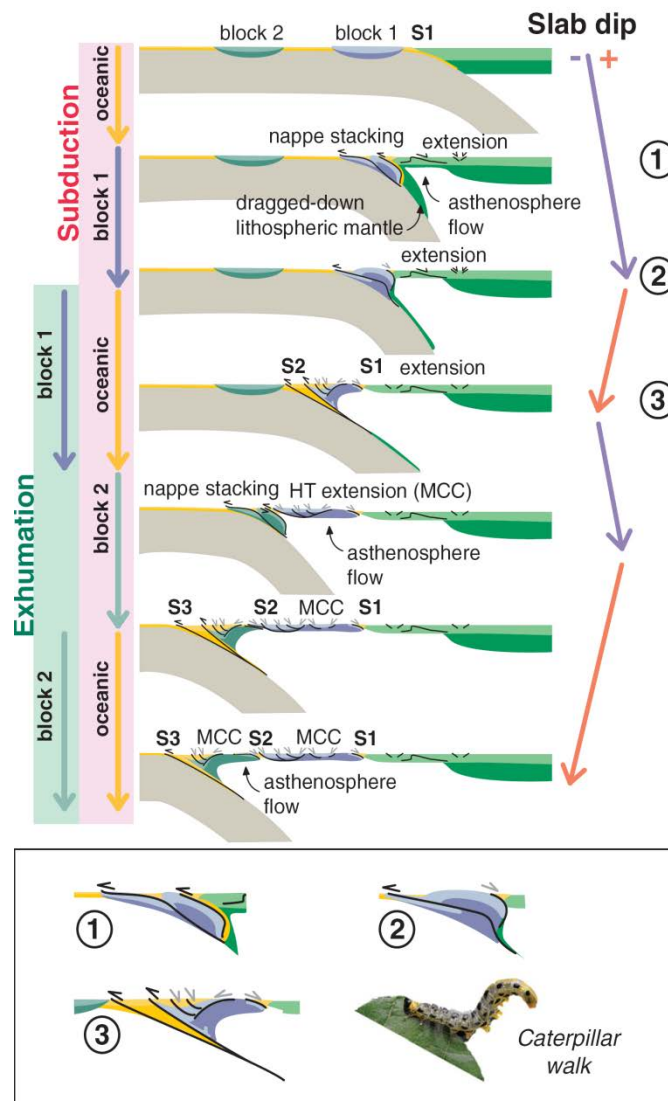


Figure 5.12.1. The relationship between the continental-block subduction and caterpillar-walk exhumation, slab dip changes, and crustal deformation. Numbers “1”, “2”, and “3” indicate turning buckles in the caterpillar walk of the exhuming crustal block. S—suture; HT—high-temperature; MCC—metamorphic core complex.

Publication:

Tirel, C., J.-P. Brun, E. Burov, M.J.R. Wortel, and **S. Lebedev** (2013), A plate tectonics oddity: Caterpillar-walk exhumation of subducted continental crust. *Geology*, **41**, 555-558.

5.12 Mapping the Moho with seismic surface waves

S. Lebedev, J. Adam, with T. Meier (Univ. Kiel)

A special issue of *Tectonophysics* has been published for the 100th anniversary of the discovery of the “Moho,” the crust-mantle boundary in the Earth. In an invited paper in this volume, Lebedev, Adam and Meier reviewed surface-wave studies of the Moho, with a focus on early work, analysed the resolution of the Moho depth offered by surface waves, and offered recommended strategies for the inversion of surface waves for the Moho properties.

This significant collection of papers on the Moho will also be published by Elsevier as a book.

Publication:

Lebedev, S., J. M.-C. Adam, and T. Meier (2013), Mapping the Moho with seismic surface waves: A review, resolution analysis, and recommended inversion strategies. *Invited Review, Tectonophysics*, "Moho" special issue, **609**, 377–394.

Presentation:

Lebedev, S., J. Adam, and T. Meier (2013), Mapping the Moho with seismic surface waves: Sensitivity, resolution, and recommended inversion strategies (Talk). EGU General Assembly, Vienna, Austria, 7-12 April.

5.13 Crustal anisotropy, patterns of mechanical weakness, and destructive earthquakes in Canterbury, New Zealand.

S. Lebedev, in collaboration with Bill Fry (GNS, New Zealand)

Low strain rate areas of the Earth are often host to long-recurrence but damaging earthquake cycles. In many cases, these events occur on reactivated and previously un-recognized faults. Noise-based imaging of seismic anisotropy is capable of revealing the seismic fabric of inherited structures as well as the preferred orientation of pervasive cracking in the upper crust, both features with a potential relationship to failure on faults, causing catastrophic earthquakes. By understanding the orientation of seismic weaknesses, seismic hazard in areas of low-strain rate can be better understood. The geometric relation of crustal anisotropy and the 3-D crustal stress tensor has the potential to qualitatively inform us of the location and/or orientation of large crustal earthquakes in regions with little previously recorded seismicity but known tectonic loading directions.

In this project, noise cross correlation techniques are used to measure surface wave dispersion. These measurements are inverted to solve for azimuthal anisotropy of fundamental mode Rayleigh waves in the Canterbury region of the South Island of New Zealand. The results of passive imaging show a distinct difference in magnitude and azimuth of surface-wave anisotropy at different depths within the crust across the region. The approximately east-west fast axis orientation at upper-crustal depths is likely to reflect the Cretaceous faulting of the impacting Chatham Rise and the approximately northeast-southwest fast axis orientation at lower-crustal depths – the present plate boundary strain direction. The upper-crust fast axis parallels the surface-rupturing Greendale Fault which gave rise to the ongoing destructive Canterbury earthquake sequence. The upper-crust azimuthal anisotropy measured using ambient noise is thus likely to reveal the dominant patterns of crustal weaknesses in regions like Canterbury, prone to low-recurrence but highly damaging earthquakes.

Publication:

Fry, B., F. Davey, D. Eberhart-Phillips, and **S. Lebedev** (2013), Depth variable crustal anisotropy, patterns of crustal weakness, and destructive earthquakes in Canterbury, New Zealand, *Earth Planet. Sci. Lett.*, in press.

5.14 Main collaborations

- University of Bergen, Norway (Profs. Henk Keers, Lars Ottemoller, Stephane Rondenay)
- University of British Columbia, Canada (Prof. Michael Bostock)
- University of Ottawa, Canada (Prof. Pascal Audet)
- University of Kiel, Germany (Prof. Thomas Meier, Dr. Christian Weidle)
- Ruhr University Bochum, Germany (Prof. Wolfgang Friederich)
- University College Dublin, Ireland (Prof. Chris Bean)
- Macquarie University, Australia (Drs. Juan Carlos Afonso and Yingjie Yang)
- University Paris VI, France (Prof. Evgeny Burov)
- University of Maryland, U.S. (Prof. Vedran Lekic)
- University of Southern California, U.S. (Prof. Thorsten Becker)
- Yale University, U.S. (Prof. Maureen Long)
- GNS (Geological and Nuclear Sciences), Wellington, New Zealand (Dr. Bill Fry)
- Utrecht University, the Netherlands (Profs. Jeannot Trampert, Rinus Wortel, Dr. Hanneke Paulssen)
- University of Potsdam, Germany (Dr. Brigitte Endrun)
- Université du Québec à Montréal, Canada (Prof. Fiona Darbyshire)
- Institute of Earth Sciences, Academia Sinica, Taiwan (Drs. Li Zhao, Frederic Deschamps, Cedric Legendre)
- University of Prague: Profs C. Matyska, O. Cadek, Drs. O. Soucek, J. Velimsky, L. Hanyk
- GFZ Potsdam: Drs I. Sasgen, V. Klemann, I. Roghuzina, J. Hagedoorn
- UNB Canada: Prof P. Vanicek
- University of Stuttgart: Profs E.W. Grafarend, N. Sneew
- Delft University: Prof B. Vermeersen, Dr W. van der Wal
- JPL USA: Dr E. Ivins
- University of Urbino: Prof G. Spada
- KTH Stockholm: Prof L. Sjoberg
- ETH Zurich: Prof A. Jackson, Dr. A. Kuvshinov
- University of Tokyo: Dr Y. Tanaka
- UWB Pilsen: P. Novak, J. Sebera
- British Antarctic Survey, UK: Prof R. Hindmarsh

6 Seismological and potential field activities

Group Leader: Assistant Professor Brian O'Reilly

6.1 PIMS (Porcupine Irish Margin Seismics)

B. M. O'Reilly

Detailed travel-time analysis of amphibious seismic data along the south-western Irish shelf region was finalised and used to link onshore structure with the highly extended crust that lies below the Porcupine Basin (**Figure 6.1.1**). Potential field data and public domain information have been evaluated and incorporated and used to link onshore structure. Full 1-D waveform calculations were successfully performed in the deep-water centre of the Porcupine Basin

where the Cretaceous to Recent seismic stratigraphy is very close to one-dimensional, robustly supporting the model in this region.

A proposal was submitted to the Irish Petroleum Infrastructure Programme as part of the government and industry initiated NAPSA program (see NAPSA). This was funded in December 2013 (352,627 EURO for over two years) and is presently scheduled to begin in the autumn time of 2014. It is designed to investigate the entire structure of the Porcupine Basin, using an integrated scientific approach, which will investigate and re-evaluate the crustal structure of the basin using a multitude of geological and geophysical tools and a very diverse range of academic and industry expertise. The aim of this project is a) to quantify variations in crustal geometry and seismic properties along the basin axis and towards mainland Ireland and b) to investigate the stratigraphic response to tectonic hyperextension and its potential impact on petroleum systems.

Ideas regarding the geological (potentially observable) consequences of a conceptual geological model for the growth of the Irish/British crust were developed. Initially, two hypothetical scenarios were investigated based on present ideas and using a simple quantitative approach. The amounts of tectonic uplift and rock exhumation are difficult to reconcile with general geological evidence observations. Although the results support the (previously formulated) concept of “incipient delamination” they indicate that stronger geological and geochronological constraints are required in order to test the concept. Future progress will be possible only with detailed multidisciplinary studies of geological processes over the time period (~350 – 410 million years) across the entire region.

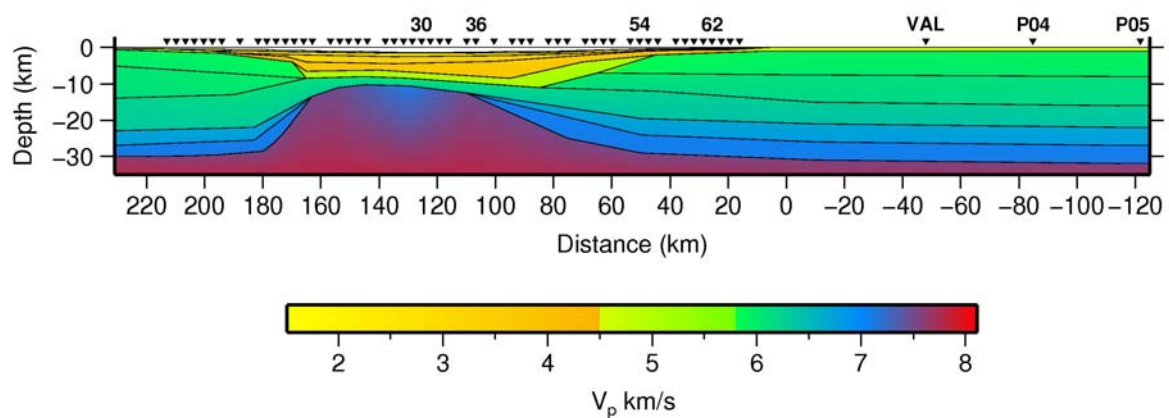


Figure 6.1.1. Crustal and sedimentary structure across the Porcupine Basin into southwest Ireland along the RAPIDS4 profile (see Figure 1 for location), and extended onshore Ireland. Vertical exaggeration is again 1:1.6. Numbered triangles (VAL, P04, and P05) are land stations used to record seismic energy sources at long offsets. Seismic velocities are indicated by bar scale: yellow tones are potential hydrocarbon rich sedimentary deposits, overlying highly thinned crust (green to blue tones).

6.2 TRIM (Tobi Rockall Irish Margins)

B. M. O'Reilly, and colleagues from University College Dublin, the University of Ulster and Durham

A presentation entitled “Deep-water geomorphology of the glaciated Irish margin from high-resolution marine geophysical data” summarising the final result of the TRIM project was given at the EGU General Assembly. The TRIM study integrated TOBI side-scan sonar data with high-resolution multibeam bathymetry and backscatter data. It resulted in a detailed geomorphological interpretation of the northwest Irish continental margin and an improved

understanding of the effects of glacial forcing on the morphology and sediment architecture of the shelf and slope region west of Ireland. Based partly on the research results obtained from this project a proposal was submitted to the Irish Shelf Programme Study Group (ISPSG) of the Petroleum Infrastructure Programme (PIP) to establish baseline seismicity of the Irish Frontier Basins, due to tectonic crustal earthquakes and/or induced slope failure. The proposed project was designed to answer key questions regarding seismic hazard, which is important for future exploration and development of hydrocarbon deposits as well as being of societal importance.

Presentation:

Sacchetti, F., S. Benetti, A. Georgiopoulou, P. Shannon, **B. O'Reilly**, P. Dunlop, R. Quinn, and C. Ó Cofaigh (2013), Deep-water geomorphology of the glaciated Irish margin from high-resolution marine geophysical data. Geophysical Research Abstracts Vol. 15, European Geophysical Union General Assembly, April.

6.3 ISUME (Irish Seismological Upper Mantle Experiment)

P. W. Readman, B. M. O'Reilly, S. Lebedev and G. Polat,

The final integration of the ISLE/ISUME data, acquired since 2003, with the collective data from the Ireland-Array and SIM-CRUST projects was completed during the year. Gulten Polat (the ISUME student) completed her analysis of teleseismic shear wave splitting and surface waves. She submitted her PhD thesis to University College Dublin, which was entitled “Investigating seismic anisotropy of Ireland from Shear wave splitting and Surface wave tomography”.

6.4 NAPSA (North Atlantic Petroleum Systems Assessment group)

B. M. O'Reilly, and colleagues from Memorial University, Newfoundland, University College Dublin, Memorial University, Newfoundland and Geotarctic Canada.

The objective of NAPSA is to foster research collaboration between Irish and Atlantic Canadian researchers that will lead to the establishment of funded scientific projects to enhance our understanding of the petroleum geology of the North Atlantic basins. The longer-term goal is to promote research that leads to increased petroleum exploration and development, with projects also fostering basic research to enhance the growth of scientific knowledge. NAPSA is designed to increase knowledge of and to quantify the potential of the North Atlantic petroleum systems within the North Atlantic conjugate margin and sedimentary basin assemblage that encompasses North America and Western Europe.

A two-year government funded study was completed in 2013. It has resulted in the development of a new kinematic plate tectonic reconstruction between Ireland and Canada (**Figure 6.4.1.**) and has also improved understanding about the evolution of this tectonically complex basin and margin system. The project is part of a long-term research program to acquire strategic new geological and geophysical data on both sides of the Atlantic and develop research efforts.

The project team, which was led by GeoArctic Ltd, included researchers from the Dublin Institute for Advanced Studies (DIAS), University College Dublin (UCD), Memorial University of Newfoundland (MUN), the University of Liverpool, the Geological Survey of Canada (GSC), and others. The project was jointly funded by the Irish Shelf Petroleum Studies Group (ISPSG) of the Petroleum Infrastructure Programme and Nalcor Energy (on

behalf of the Offshore Geoscience Data Program with the Government of Newfoundland and Labrador). Newly awarded research funding to DIAS (see PIMS) is part of this grander research endeavour.

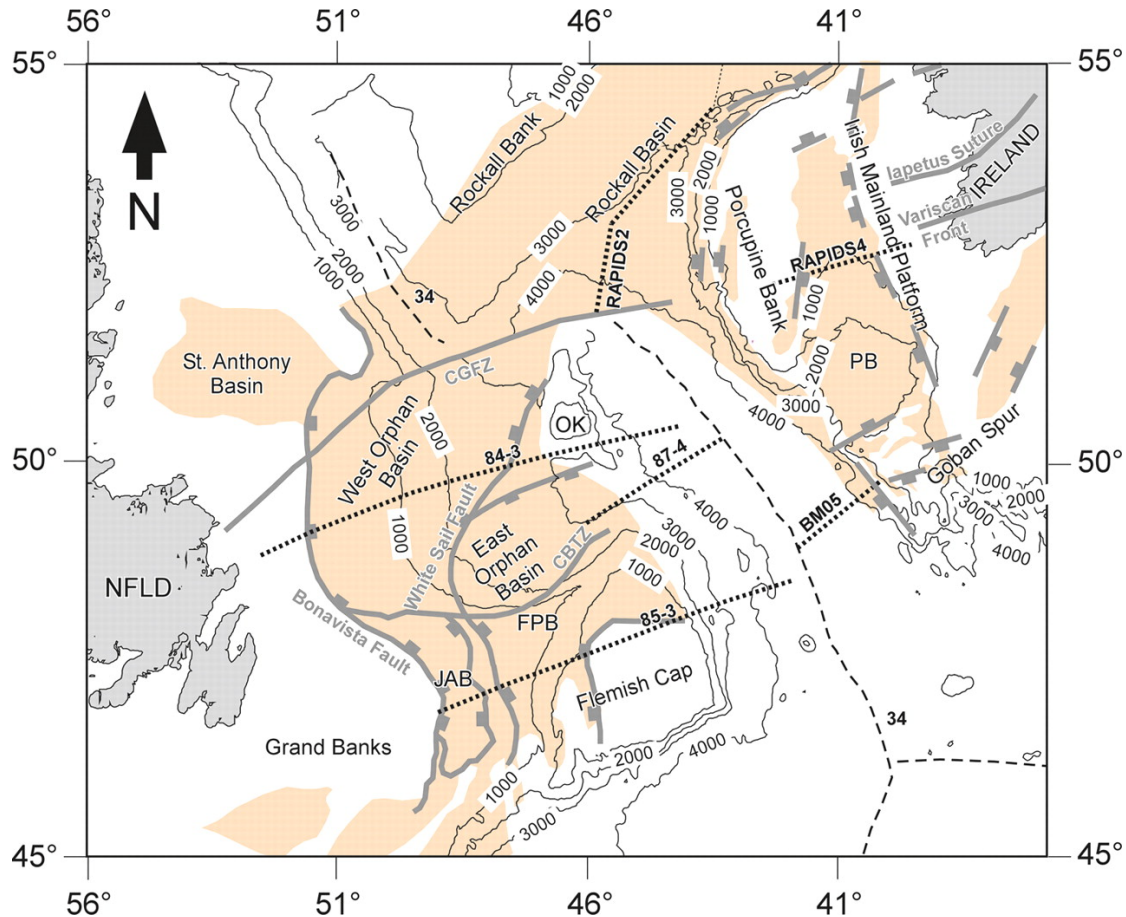


Figure 6.4.1. Preliminary plate tectonic reconstruction of the Irish and Newfoundland continental margins and basins at late Cretaceous geological time. This is based primarily on the results of gravity field studies and the results of deep-crustal seismological studies on both sides of the Atlantic. The grey lines represent the major fault systems whose activity controlled the formation of the major Mesozoic sedimentary systems, the extent of which are marked in pale orange.

Publication:

Geoartec Ltd and the NAPSA Project Team (2013), A New Kinematic Plate Reconstruction between Ireland and Canada. Final Project Report to the Governments of Ireland, Newfoundland and Labrador.

6.5 Collaborations

- UCD School of Geological Sciences: ISUME, TRIM, PIMS
- University of Birmingham, PIMS
- Applied Geophysics Unit, NUI Galway, ISUME
- University of Ulster (Colrairie), TRIM
- Memorial University, St Johns, Newfoundland, NAPSA
- University of Liverpool, NAPSA
- University of Durham, TRIM

7 Seismic imaging of the Irish crust for geothermal energy

Dr. Nicola Piana Agostinetti, Andrea Licciardi, Sergei Lebedev

7.1 Project overview

The project “Seismic imaging and monitoring of the upper crust: exploring the potential low-enthalpy geothermal resources of Ireland” (SIM-CRUST) is funded by SFI under the “Starting investigator Research Grant” program (SIRG). The aim of the project is the passive seismic exploration of the Irish crust to better understand its geothermal potential. Details of the seismic structure of the shallow crust (e.g. seismic anisotropy) are fundamental to assess key parameters for a geothermal site (e.g. rock porosity). To obtain such ambitious goal, different passive seismic techniques are used, from local earthquakes tomography to high-frequency receiver function, to ambient noise dispersion analysis. Local earthquakes tomography (LET) exploits the information brought to the surface by seismic waves generated by (natural) microseismicity and it has been mainly used to reconstruct 3D P-velocity models of the shallow crust. Receiver function (RF) analysis is based on the recording of P-to-s and S-to-p converted phases generated by teleseismic waves crossing a seismic discontinuity. Seismic anisotropy and sharp S-velocity discontinuity at depth are the main targets of RF analysis. Ambient noise is routinely used to compute the S-wave dispersion curve for different station pairs, from which S-velocity models can be retrieved.

The project is focused on two main target areas, the Lough Swilly area (Co. Donegal) and the Dublin basin, where two dense seismic arrays will be deployed for three years. Lough Swilly has been struck by a number of low-magnitude earthquakes in the last ten years and microseismicity should be relevant in the area. In the Dublin basin, a borehole for geothermal exploration has been drilled along the southern slope. Thus, complementary data are available and will be used to assess the resolution of our techniques. Both regions partially overlap with the area investigated by IREITHERM project and results from seismic and magneto-telluric studies will be compared. To extend the analysis to a broader area, seismic data recorded during temporary deployment in the last ten years (ISLE, Ireland Array) will be analyzed.

7.2 Fieldwork updates

The deployment of 4 broadband seismic stations in the Dublin basin has been concluded in August 2013. In the last few years, this area has been the subject of an increasing interest in the context of geothermal potential assessment. This network is planned to be operative for two years, providing enough data for a detailed high frequency receiver function analysis of the upper crust. This will help in better constrain the fine structure, composition and presence of fluids in the first 5-10 km of the crust.

The seismic network in Co. Donegal has been continuously operated during 2013. The quality of the seismic signals recorded has been routinely checked. Such analysis suggested the re-deployment of one station, already done. Moreover, a new station has been deployed in the most promising area for microseismicity. The seismic network in Co. Donegal partially overlaps the area investigated using MT in the framework of the IREITHERM project.

7.3 Results update

We computed teleseismic receiver functions at 34 broadband seismic stations in Ireland, integrating permanent and temporary networks. This allowed us to achieve an unprecedented

seismic coverage of the island, which we exploited in a regional-scale study of Ireland's crust. Through the application of a classic and widespread receiver functions method we obtained first-order maps of Moho depth and Vp/Vs ratio across Ireland. These outputs are meant to provide robust basis for further geophysical studies on Ireland. These results are reported in a manuscript submitted to *Geophysical Journal International*.

A code for reversible-jump Markov chain Monte Carlo to solve the Local Earthquake Tomography inverse problem has been developed and tested on data from the EGS site in Soultz (induced seismicity) and is going to be tested on natural seismicity recorded in Italy in the geothermal site of the Larderello-Travale area. The algorithm has been presented in a manuscript submitted to *Geophysical Journal International*.

Teleseismic data recorded at the geothermal site of the Larderello-Travale area have been processed to reconstruct the fine-scale (<250m) seismic structure of such important area, from a geothermal point of view. Results will be presented at the next general assembly of the European Geophysical Union (Vienna, April 2014).

7.4 Publications and meeting abstracts

SIM-RUST Publications:

- Spada, M., I. Bianchi, E. Kissling, **N. Piana Agostinetti** and S. Wiemer (2013), Combining controlled-source seismology and receiver function information to derive 3-D Moho topography for Italy, *Geophys. J. Int.*, **194**, 2, 1050-1068.
- Sun, D., M.S. Miller, **N. Piana Agostinetti**, P. D. Asimow, and D. Li (2013), Modeling high frequency waves in the slab beneath Italy, *Earth Pla. Sci. Lett.*, in press.
- Govoni, A., A. Marchetti, P. De Gori, M. Di Bona, F.P. Lucente, C. Chiarabba, A. Nardi, L. Margheriti, L. Improta, **N. Piana Agostinetti**, R. Di Giovambattista, D. Latorre, M. Anselmi, M.G. Ciaccio, M. Moretti, C. Castellano, and D. Piccinini (2013), The 2012 Emilia seismic sequence (Northern Italy): imaging the thrust fault system by accurate aftershocks location, submitted to *Tectonophysics*.
- Piana Agostinetti, N.** (2013), The structure of the Moho in the Northern Apennines and evidence for an incipient slab tear fault. Submitted to *J. of Geodynamics*.
- Rosenbaum, G., and **N. Piana Agostinetti** (2013), Crustal and upper mantle response to lithospheric tear faulting: the Livorno-Sillaro Lineament in the northern Apennines. Submitted to *Tectonics*.
- Piana Agostinetti, N.**, G. Giacomuzzi, and A. Malinverno (2013), Local 3D earthquake tomography by trans-dimensional Monte Carlo sampling, Submitted to *Geophys J. Int.*
- Licciardi, A.**, and **N. Piana Agostinetti** (2013), Moho depth and Vp/Vs in Ireland from teleseismic receiver functions analysis, Submitted to *Geophys J. Int.*

SIM-CRUST Presentations:

- Rosenbaum, G. and **N. Piana Agostinetti** (2013), Crustal and upper mantle response to lithospheric tear faulting: the Livorno-Sillaro Lineament in the northern Apennines, EOS trans. AGU, Fall meeting suppl, Abstract T33B-2622.
- Chiarabba, C., G. Giacomuzzi, I. Bianchi, **N. Piana Agostinetti**, and J. Park (2013), Velocity contrasts in the mantle: changing the paradigm of the Apennines, EOS trans. AGU, Fall meeting suppl, Abstract DI33A-2213.
- Licciardi, A.**, L. Chiaraluce, and **N. Piana Agostinetti** (2013), Crustal Structure and Moho Geometry around the Alto Tiberina Fault (Northern Apennines) from Receiver Functions, EOS trans. AGU, Fall meeting suppl, Abstract S31C-2356.

- Miller, M.S., D. Sun, and **N. Piana Agostinetti** (2013), Detecting slab structure beneath the Mediterranean, *Geophysical Research Abstracts*, 15, EGU2013-1852.
- Licciardi, A., S. Lebedev, and N. Piana Agostinetti** (2013), Moho depth and crustal anisotropy in Ireland from teleseismic receiver functions, *Geophysical Research Abstracts*, 15, EGU2013-9755-1
- Muller, M., J. Fullea, A.G. Jones, J. Adam, S. Lebedev, and N. Piana Agostinetti** (2013), Lithospheric-Mantle Structure of the Kaapvaal Craton, South Africa, Derived from Thermodynamically Self-Consistent Modelling of Magnetotelluric, Surface-Wave Dispersion, S-wave Receiver Function, Heat-flow, Elevation and Xenolith Observations. EGU General Assembly, Vienna, Austria.
- Piana Agostinetti, N.** (2013), Geothermal exploration via passive seismic analysis, Ireland Geological Research Meeting, Derry.
- Licciardi, A., and N. Piana Agostinetti** (2013), Receiver functions analysis for Vs profiles and Moho depth estimations. The Alto Tiberina Near Fault Observatory (TABOO) Workshop, Ancona, Italy.
- Licciardi, A.** (2013), Structure of the crust with teleseismic Receiver Functions: a multiscale approach. PhD introductory talk, University College Dublin, Dublin, Ireland.
- Licciardi, A., and N. Piana Agostinetti** (2013), Crustal structure of Ireland from receiver-function analysis. Atlantic Ireland 2013 Conference, Dublin, Ireland.

8 Irish Geoscience Graduate Programme (IGGP)

Professor Alan G. Jones, Caroline Moloney

IGGP continues to grow offering higher quality courses to Post Graduates. DIAS is contributing 13 courses of the 27 currently on the IGGP website, and most will be presented in 2013 and 2014 and we are currently setting up new course for 2015.

DIAS 001	Applied Geophysical Methods from First Principles , Dr. B.M. O'Reilly, 2 - 5 April 2013
DIAS 002	Seismology for Non-Seismologists , Dr. M. Muller, 12 - 15 March 2013
DIAS 003	Time Series Analysis , Prof. G. Mitchum (U Southern Florida), 19 - 22 March 2013
DIAS 004	Magnetotellurics , Prof. A.G. Jones, 17 -21 February 2014
DIAS 005	Computational Statistics , Dr. A.D. Chave (WHOI), 11 – 15 November 2013
DIAS 006	Glacial Isostasy and Sea Level Change , Prof. G. Spada (Rome), 19-21 February 2013
DIAS 007	Monte Carlo approach to geophysical inverse problem , Dr. N. Piana Agostinetti, 25 - 27 March 2013
DIAS 007	Introduction to Linux , Philippe Grange, 21 October 2013
DIAS 008	Introduction to FORTRAN95/2003 , Dr. E. Mandolesi, 29 - 30 November 2013
DIAS 008	Advanced Programming in FORTRAN95/2003 , Dr. T. Kalscheuer, 18 - 22 November 2013
DIAS 009	Short course on Seismic Reflection Data Processing , Dr. R. Hardy (Tonnta

DIAS School of Cosmic Physics; Geophysics Section
2013 Annual Report – Part 2

	Energy), 04 -06 November 2013
DIAS 010	Rotation of the Earth , Prof. Z. Martinec, 24 - 28 June 2013
DIAS 011	Tensor Calculus , Prof. Z. Martinec, 6 – 7 May 2013
DIAS 012	Introduction to GMT – A. Schaeffer, 04 – 07 March 2014
DIAS 013	Fundamentals of Geophysical Inversion Methods – Dr. M. Yedlin, April - May 2015
GSI/GSNI	3D Visualisation & Research opportunities with Geological Surveys, TELLUS & INFOMAR datasets – Dr. K. Verbruggen - Spring 2014
NUIM 001	ArcGIS for Geoscientists - Level 1 Introductory Course – Dr. G. Scott, 26 – 30 May 2014
NUIM 002	ArcGIS for Geoscientists - Level 2 Advanced Course – Dr. G. Scott, 03 – 06 June 2014
NUIG 001	Fluid Inclusions: Study methods and Interpretations – Prof. M. Feely, 05 - 09 May 2014
NUIG 002	The Geochemical/Geoscience Applications of Terrestrial/Volcanic Dust – Prof. P. Croot, February 2014
NUIG 003	Balancing the Hydrological Equation - Introduction to Hydrology and Hydrogeology – Dr. T. Henry, 25 – 29 November 2013
UCD 001	Basic Maths and Physics: tools for the geoscientist , Prof. C. Bean, 25 – 28 March 2013
UCC 001	Petroleum Geology and Basin Analysis , Dr D. Jarvis and Prof. B. Williams, 17 -20 March and 24 – 27 March 2014
UCC 002	Hydrogeology and Engineering Geology , E. McCarthy and Prof. A. Wheeler, 28 th October – 16 th December – Tues 4-5; Weds 10-11; Weds 3-5 (no longer possible to block teach)
UCC 003	Exploration Structural Geology for Hydrocarbon Exploration , Dr. M. Cooper and Dr. P. Meere, 09 -13 December 2013
UCC 004	Exploration Structural Geology for Mineral Exploration , Dr. P. Meere, 04 – 07 March 2014
UCC 005	Coal Exploration , Dr. L. Thomas and Prof. A. Wheeler, 19 - 21 March 2014
UCC 006	Geotechnical Investigation of Soils and Rock , E. McCarthy and Prof. A. Wheeler, 07 – 15 January 2014
UCC 007	Exploration Methods and Professional Development , G. Earls and Prof A. Wheeler, 25 – 29 November 2013

Following the success of IGGP and resolution at the resource issues, additional modules are being proposed leading to development of IGGP as a virtual geosciences graduate school. It is now imperative to keep this valuable programme afloat and to seek funding to continue on the position of the IGGP Administrator beyond the end of the Griffith award (2015).

Interest has already been expressed from bodies outside Ireland in access to IGGP modules. These could also be made available to other geoscientists in Ireland as part of continuing professional development. Income can be obtained, from these sources.

IGGP modules are also suitable in many cases as parts of taught MSc programmes, particularly if these were available by cooperation between several institutions.

The issue of costs must be addressed if IGGP is to develop, not only between universities but also between the universities in which the student is registered and any outside body mounting a module. Bodies such as Geological Surveys, Associations or Institutes cannot be expected to subsidise IGGP when universities accrue significant fee income/resources for registered PhD students.

IGGP has obtained sanction to pay for the presentation of modules by post-doctoral fellows for 2011-2014 only. In the long term universities must help to cover these costs.

Finally, it was with great regret that we announce that Professor M. Kennedy (Ben) passed away very suddenly last July, 2013. Along with Professor Alan Jones, they worked tirelessly to make Irish Geoscience Graduate Programme (IGGP) possible, and we acknowledge this great work and in Ben's memory, are even more determined to grow the programme, to improve its content offering and will seek funding to maintain it past 2015 for the continued benefit of Geoscience Post Graduates everywhere, but primarily on the island of Ireland.

9 The Irish National Seismic Network (INSN)

Tom Blake, Clare Horan, Louise Collins

The INSN seismic station network continued to function without any major problems in recording seismic data and its near real-time transmission to the seedlink server in DIAS. The development of the station ILTH is currently under-way and the seismic bunker itself has been completed, we are now awaiting the installation of the electrics and installation of the data transfer communications. In 2013 the strongest teleseismic event recorded by the network was a Mag 7.8 in Awaran, Pakistan and the nuclear test in North Korea. (See table below).

The routine analysis of seismic events recorded by the INSN is now confined to local events with the automatic trigger system being checked each morning and any events reviewed and logged to the Seiscomp3 database. All data from the previous day is scanned and any local events are analysed, located and logged also. Seismograms of significant events are put on the web-page.

Notable events recorded at INSN stations in 2013

Date	Time	Latitude	Longitude	Magnitude	Location
13 th February	02:57:51	41.308 N	129.076 E	5.4	North Korea Nuclear test
16 th April	10:44:20	28.107 N	062.053 E	7.7	Iran / Pakistan border
24 th May	05:44:49	54.874 N	153.281 E	8.3	Sea of Okhotsk, Russia
29 th May	03:16:27	52.879 N	004.764 W	3.8	Irish Sea, off Welsh coast

26 th June	22:28:01	52.893 N	004.722 W	2.8	Irish Sea, off Welsh coast
24 th September	11:29:47	26.951 N	065.501 E	7.7	Pakistan
4 th December	11:29:47	51.45 N	008.72 W	2.6	South of Courtmacsherry, Cork

9.1 Local Seismic Events:

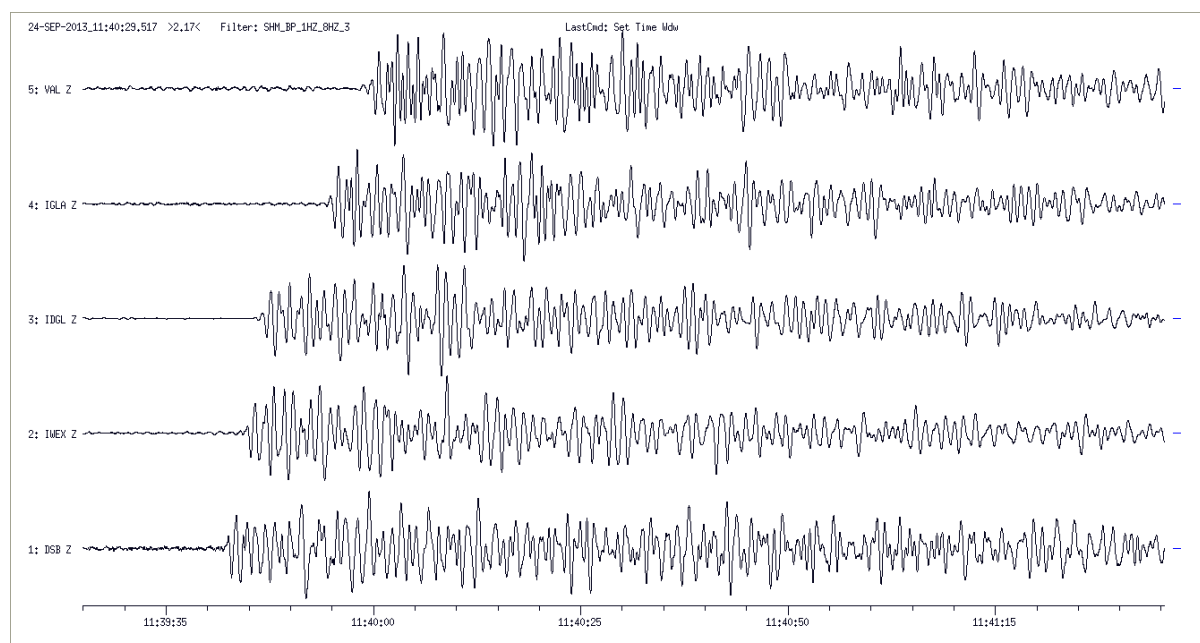


Figure 9.1.1. Of particular interest were the recent local events recorded by the network. Several local earthquakes were recorded by the INSN during the summer the largest of which was a Mag 3.8 off the Welsh coast and felt by many people on the east coast of Ireland.

Earthquake off Welsh Coast, felt in Ireland

On 29th May, 2013 at 03:16:27.8 UTC an earthquake Mag ML3.8 occurred in the Irish Sea, off the Welsh Coast, location 52.879N, 4.764W and depth 11 Km. The [Irish National Seismic Stations](#) recorded the event. There has been some felt reports in Dublin, Wicklow and Wexford. If you felt this event please fill out our [questionnaire](#).

The earthquake location is approximately 15 km west of the magnitude 5.4 earthquake that occurred on the Llyn peninsula on 19 July 1984. The latter quake was the largest ever recorded earthquake on mainland Britain and was felt throughout Ireland's east coast, Wales and England. Aftershocks from the quake measured up to 4.3 on the Richter scale and some structural damage resulted along the east coast of Ireland.

[DIAS press release for Welsh Coast event.](#)

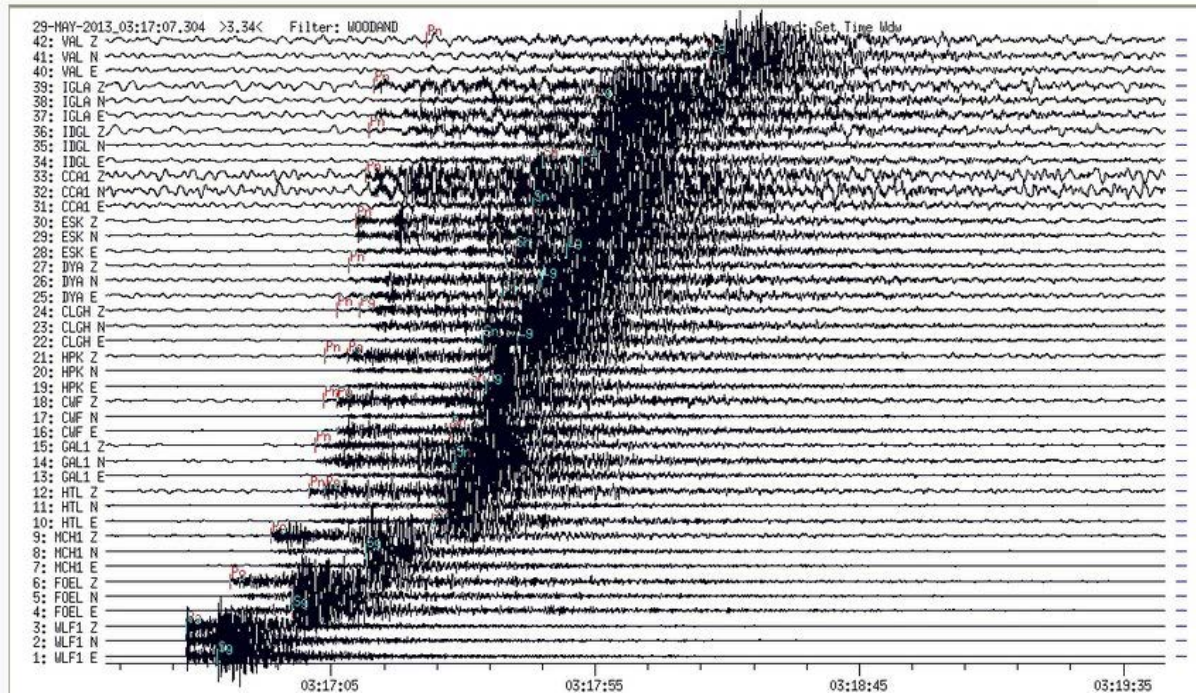


Figure 9.1.2.

9.2 Teleseismic Events:

9.2.1 Earthquake in Pakistan 24-9-2013

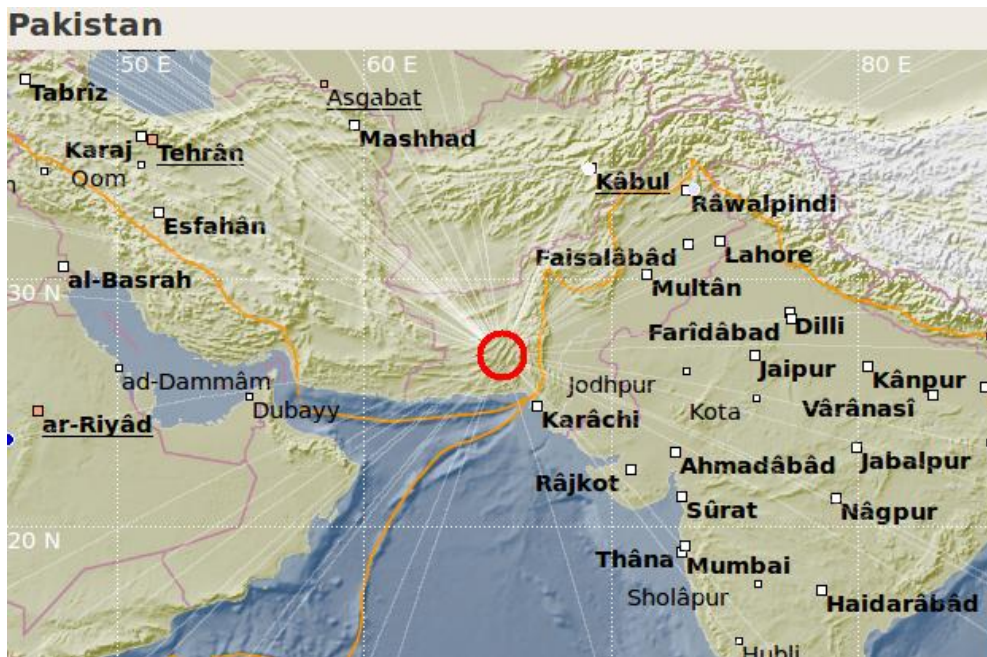


Figure 9.2.1.1.

A major M7.7 earthquake occurred in the Balochistan region of Pakistan on 24th September at 11:29 UTC (16:29 local time), 290km north of Karachi, in a mostly rural area. The earthquake was felt in Pakistan and as far away as New Delhi in India, United Arab Emirates and Oman. In the first 24 hours after the main shock, five aftershocks >M5 have been recorded.

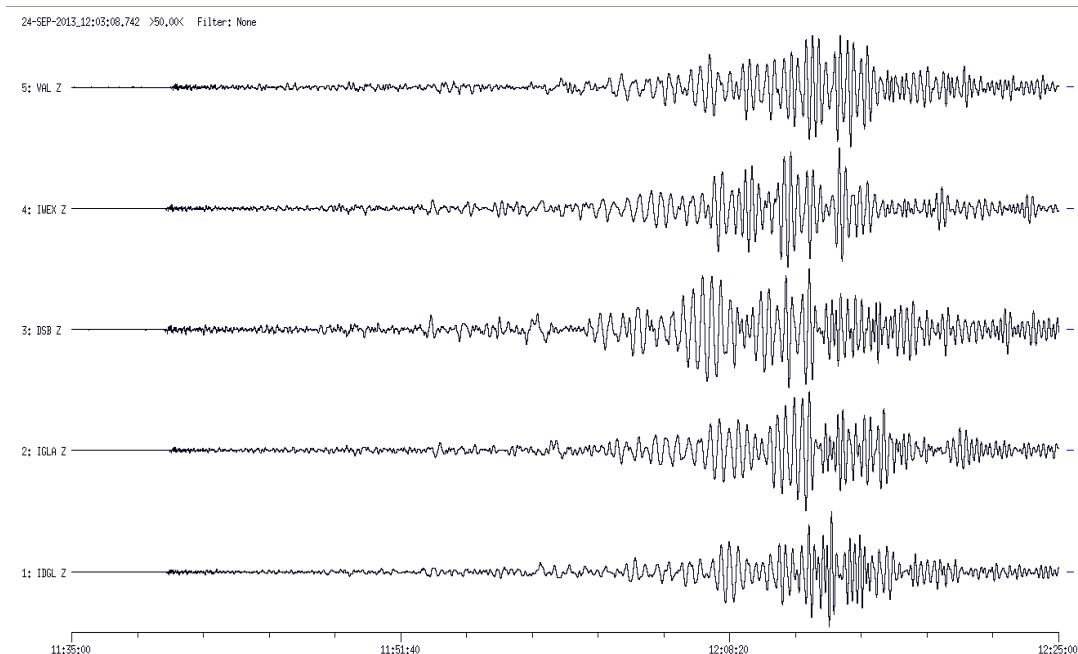


Figure 9.2.1.2. Image of the seismic traces of the main event recorded on the stations of INSN.

Blake gave an invited speaker address to the Open University Geological Society Annual Meeting, at DCU in July entitled “Irish National Seismic Network (INSN) and CTBTO - Monitoring – a wave of opportunity”.

There was a field trip to the INSN and NDC HQ in DIAS as part of the Open University Geological Society Annual Meeting, to help this year in July in Dublin City University (DCU). Over 20 participants were treated to a brief lecture on the workings of the INSN and the role of the NDC in CTBTO.

The Embassy of Japan in Ireland has invited the INSN in DIAS to co-sponsor a one day Science and Technology Symposium in February 2014 to be held in DIAS, Burlington Road. The guest speaker will be Dr Yoshiyuki Kaneda, Project Leader of the Earthquake and Tsunami Research Project for Disaster Prevention at the Japan Agency for Marine-Earth Science and Technology (JAMSTEC), on the topic, "The forefront of earthquake and tsunami observation research, based on lessons learned from the Great East Japan Earthquake".

The routine analysis of seismic events recorded by the INSN network is now confined to local events:

1. The automatic trigger system is checked each morning and any events are reviewed and logged to the Seiscomp3 database.
2. Data from the previous day is scanned and any local events are analysed, located and logged.
3. Teleseismic events are noted but not analysed or reported. Seismograms of significant events are put on web-page.
4. It is planned to liaise with quarries and mines to identify man made events and mark them as such in the data base.
5. Selected information from the database will be put on the website (local seismic non man made events).

9.3 North East Atlantic Mediterranean Tsunami Warning Group (NEAMTWG)

Tom Blake

Blake represents DIAS at the annual NEAMTWG meetings. Currently, France is prepared to act as the regional Early Tsunami Warning agency for both the Mediterranean and the North East Atlantic.

10 Irish National Magnetotelluric Observatory (INMTO)

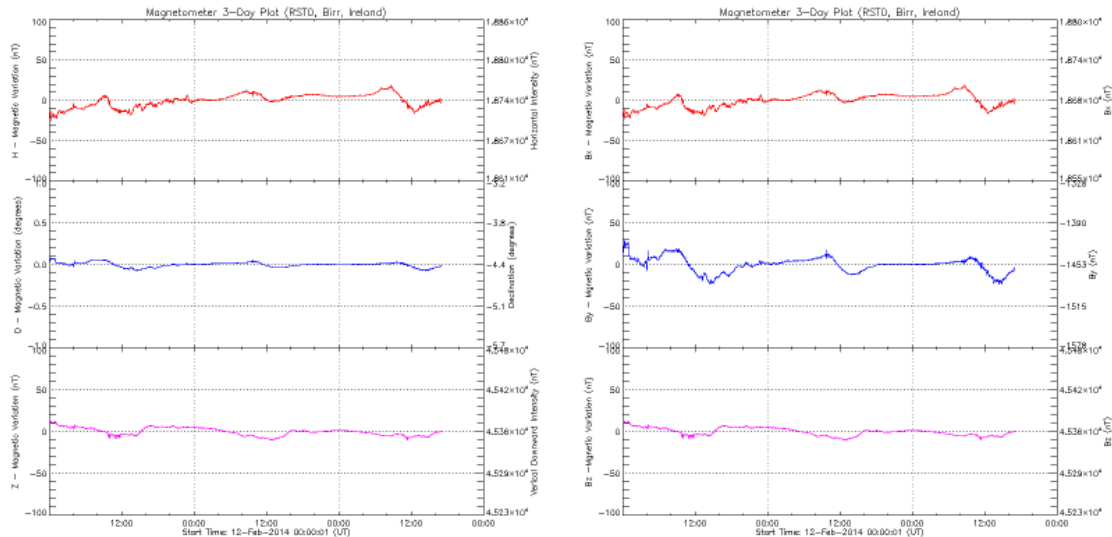
A.G. Jones, C. Hogg

The INMTO, as part of the Rosse Solar-Terrestrial Observatory (RSTO) at Birr Castle, is currently only recording magnetic fields and plans are underway for installation of the electric field array. The data are available in real-time (<http://www.rosseobservatory.ie/data>).

In March / April 2014, a large scale electrode array will be deployed creating a large scale magnetotelluric observatory. Following this step, a more permanent structure will be built to house the magnetometer with the objective of reaching International Observatory standard.

Currently the data is been used to calculate real-time local K-index values (a measure of how disturbed the Earth's magnetic field is) in real-time.

Earth's magnetic field at RSTO from DIAS/TCD magnetometer



Geomagnetic activity from RSTO K-Index

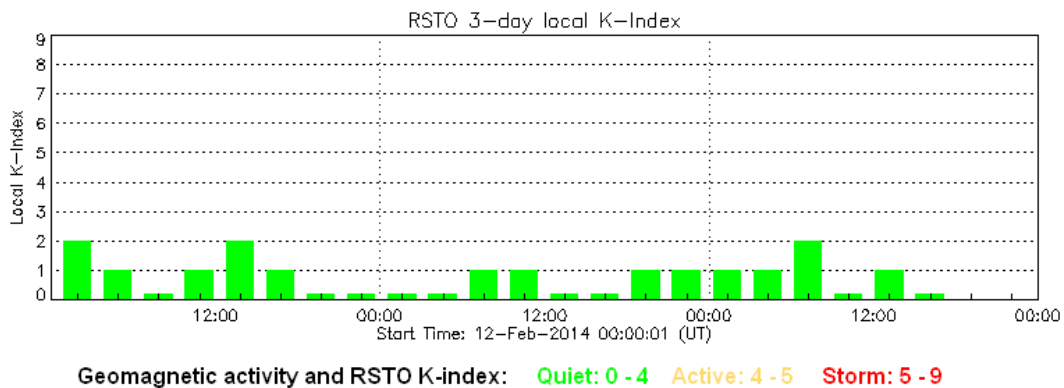


Figure 10.1.

11 CTBTO - Comprehensive Nuclear-Test-Ban Treaty Organisation, National Data Centre (NDC).

Tom Blake

The NDC continued to raise its profile and that of the CTBTO throughout the year. One event in particular brought the NDC to the attention of the public and in particular the media.

On Feb 12, 2013, the Irish National Seismic Network (INSN) recorded an unusual seismic event in the Democratic People's Republic of Korea (DPRK). The DPRK claimed that it had conducted yet another nuclear test, the third within the last seven years.

Initial estimates showed that this event measured Mag 4.9, and occurred at 02.58 GMT approx. It was located in the region of the previous North Korean nuclear tests of 2006 and

2009. The South Korean defence ministry has provided preliminary yield estimates for the test of between 6 - 7 kilotons.

The picture shows the energy generated by the nuclear test arriving at our stations in DSB Dublin and IDGL Donegal, approx 11 minutes after the time of detonation.

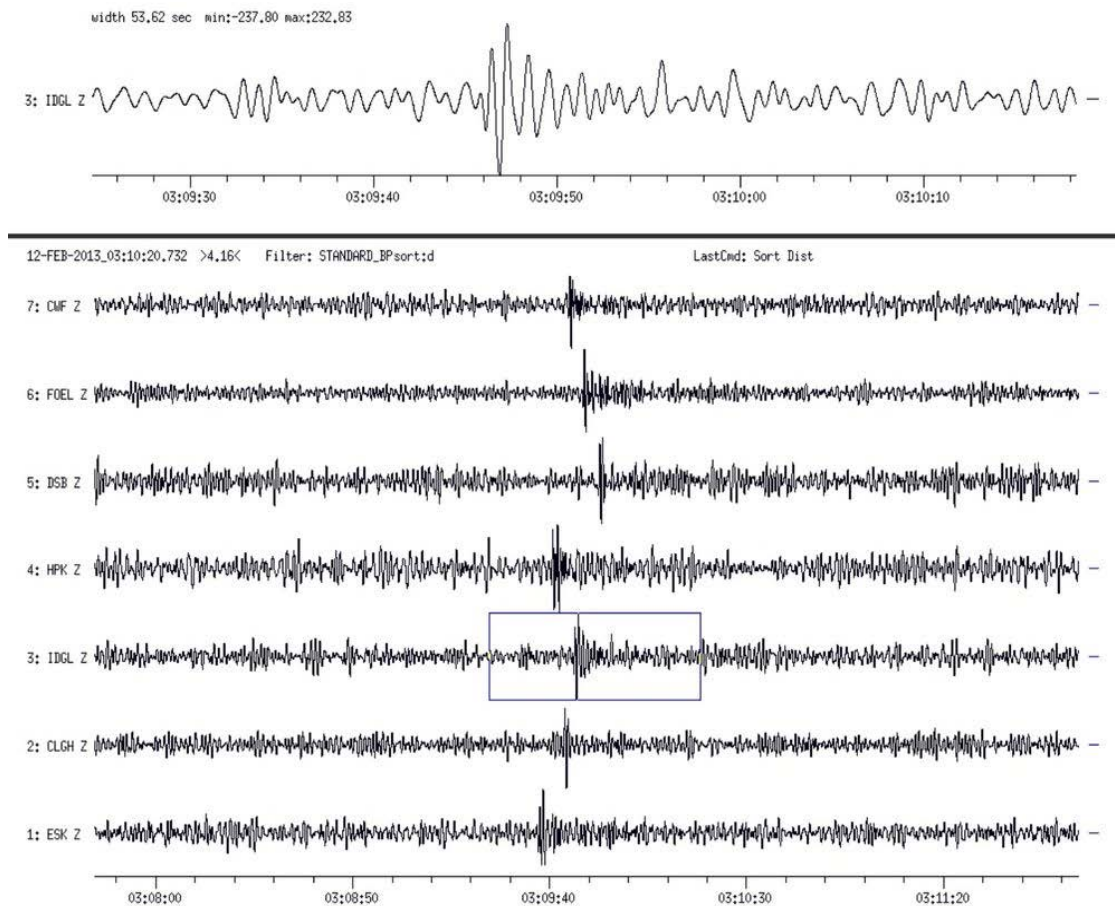


Figure 11.1.

11.1 CTBTO Operations in Ireland

Tom Blake

The National Data Centre (NDC) continued to grow and expand with the arrival on a six month sabbatical of Dr Yochai Ben Horin from the NDC Tel Aviv, Israel. During his period he collaborated with Blake, Grange, Horan and Collins on seismic data analysis and interpretation (**Figure 11.1.1**),



Figure 11.1.1. L to R: C. Horan, P. Grange, Y. Horin, L. Collins, T. Blake

and software fine tuning and development of the main system Seiscomp3 with Grange and Bucas in **Figure 11.1.2.**, which included:

- setup and configured workstations for data analysis,
- configured and fine-tuned event detection for local events in the Ireland region,
- determined the event workflow,
- implemented procedure to follow after manual confirmation of a local event,
- fully implemented the automatic notification system for local events.

Currently there is an automatically generated website for the display of local events.

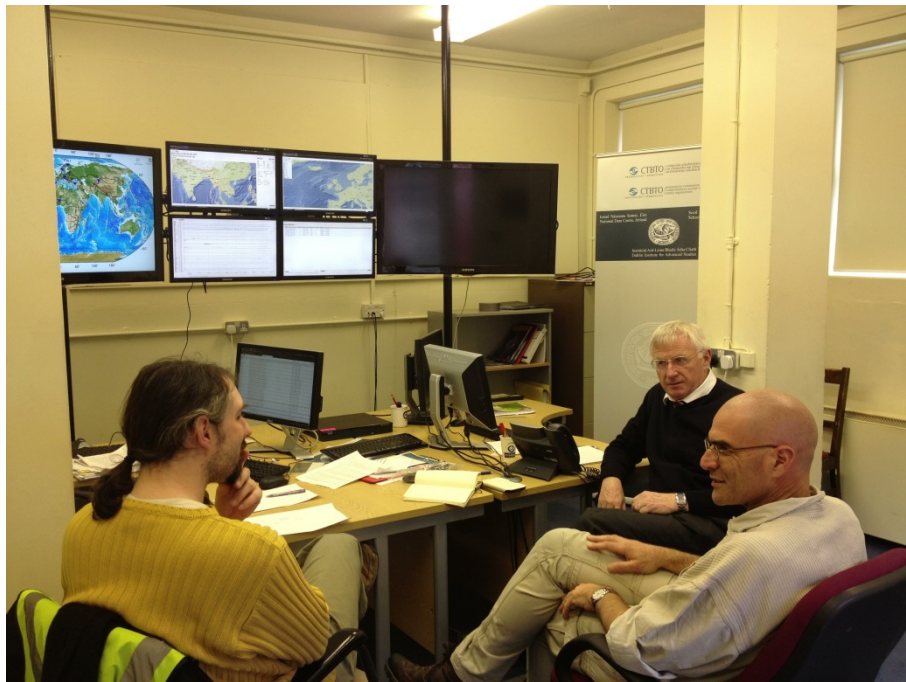


Figure 11.1.2. L to R, J.F. Bucas, Y. Ben Horin, T. Blake

The NDC took delivery of VPN routers etc for the establishment of secure links for the data transfer. The secure virtual private network between the NDC in Merrion and the CTBTO in Vienna has been implemented and successfully tested.

This will insure that data collected and exchanged between the sites are not tampered with.

11.2 Involvement in CTBTO Internationally

Tom Blake

CTBTO Technical Working Group B

Blake attended the August Meeting of Technical Working Group B at CTBTO in Vienna which discussed the OSI Build-UP Training exercises in Hungary earlier this year and the preparedness of the organisation to launch the logistical preparation for the International Field Exercise IFE14 in Jordan next year.

On-Site Inspection operations.



Thomas Blake, explaining the Seismic Aftershock Monitoring System (SAMS). This system is used during the first days of an on-site inspection to detect the seismic events with distinct seismic signatures that follow a nuclear explosion.

Figure 11.2.1.

Blake has been invited by the Irish Government to represent Ireland at the forthcoming CTBTO On-Site Inspection (OSI) Workshop 21 in Yangzhou, China, in November and in his capacity also as sub-team leader for Seismic Aftershock Monitoring Systems (SAMS) for the International Field Exercise IFE14 in Jordan in 2014.

11.3 CTBTO studentship

Blake, Lebedev, Emily Neenan

Ms Emily Neenan was successful in her application for CTBTO funding and was awarded a Young Scientist Award Grant for one year of M.Sc. research. She is now registered as M.Sc. student at Trinity College Dublin and is carrying out her research on surface-wave array imaging of Asia at the National Data Centre for CTBTO in DIAS, under the supervision of Dr Sergei Lebedev and Tom Blake.

12 Collaboration with wider research community

12.1 Collaborations

Dr Jiatie Pan of the China Earthquake Administration, Beijing, has been awarded Chinese government funding to come to DIAS to work with S. Lebedev for 4 months. Their collaborative project is on seismic imaging of central Mongolia, where an array of wide-band seismic stations has been operated by the CEA for about 2 years. The goal of the project is to determine the isotropic and anisotropic structure of the crust and upper mantle and gain new insight into the enigmatic Phanerozoic assembly of Mongolia. Dr. Pan arrived and started at DIAS on December 16, 2013.

12.2 Visitors

- **Dr Yochai Ben Horin** from the National Data Centre, CTBTO, Tel Aviv, Israel.
- **Professor Matt Yedlin** from the Department of Electrical and Computer Engineering, University of British Columbia, Vancouver, B.C. Canada.
- **Dr. Wolfram Geissler** (Alfred Wegener Institute for Polar and Marine Research, Germany), 14 November 2013
- **Dr. Sébastien Chevrot** (Observatoire Midi Pyrénées, Toulouse, France), 21-24 November 2013
- **Dr Jiatie Pan** (China Earthquake Administration, Beijing, China), 16 December 2013 – 15 April 2014

13 Public outreach

13.1 Seismology in Schools (Seismeolaíocht sa Scoil) Project

T. Blake

The Seismology in School (SIS) programme continues to attract potential schools throughout the country. Aspiring schools to the programme will have to be 100% financing of equipment and DIAS consulting costs which includes education and training for teachers and students. Current membership stands at 60 schools, 2 IT colleges in Dublin and Sligo, and 3 Geoparks. The SIS programme is still hampered by inadequate funding and no permanent staff to maintain and develop the programme. The programme currently has 58 participating schools, Institutes of Technology, university colleges and geoparks.

The Copper Coast Geopark, Bunmahon, Waterford is playing a very important role in the raising levels of awareness of the SIS and regularly have information meetings about the seismometer in their centre. The most recent secondary school to join the programme is Good Counsel College, New Ross Co Wexford. There is currently a waiting list of 4 schools wishing to join the SIS programme.

A visitor to the SIS programme in DIAS for one week was Professor Matt Yedlin from the Department of Electrical and Computer Engineering, University of British Columbia, Vancouver, B.C. Canada. This visit was a very specific attempt to upskill in relation to the seismometer used in SIS programme which he wants to introduce in to B.C. Canada.

Below is the current map of the distribution of centres around Ireland that are in the SIS programme:

SIS Seismic Network 2013

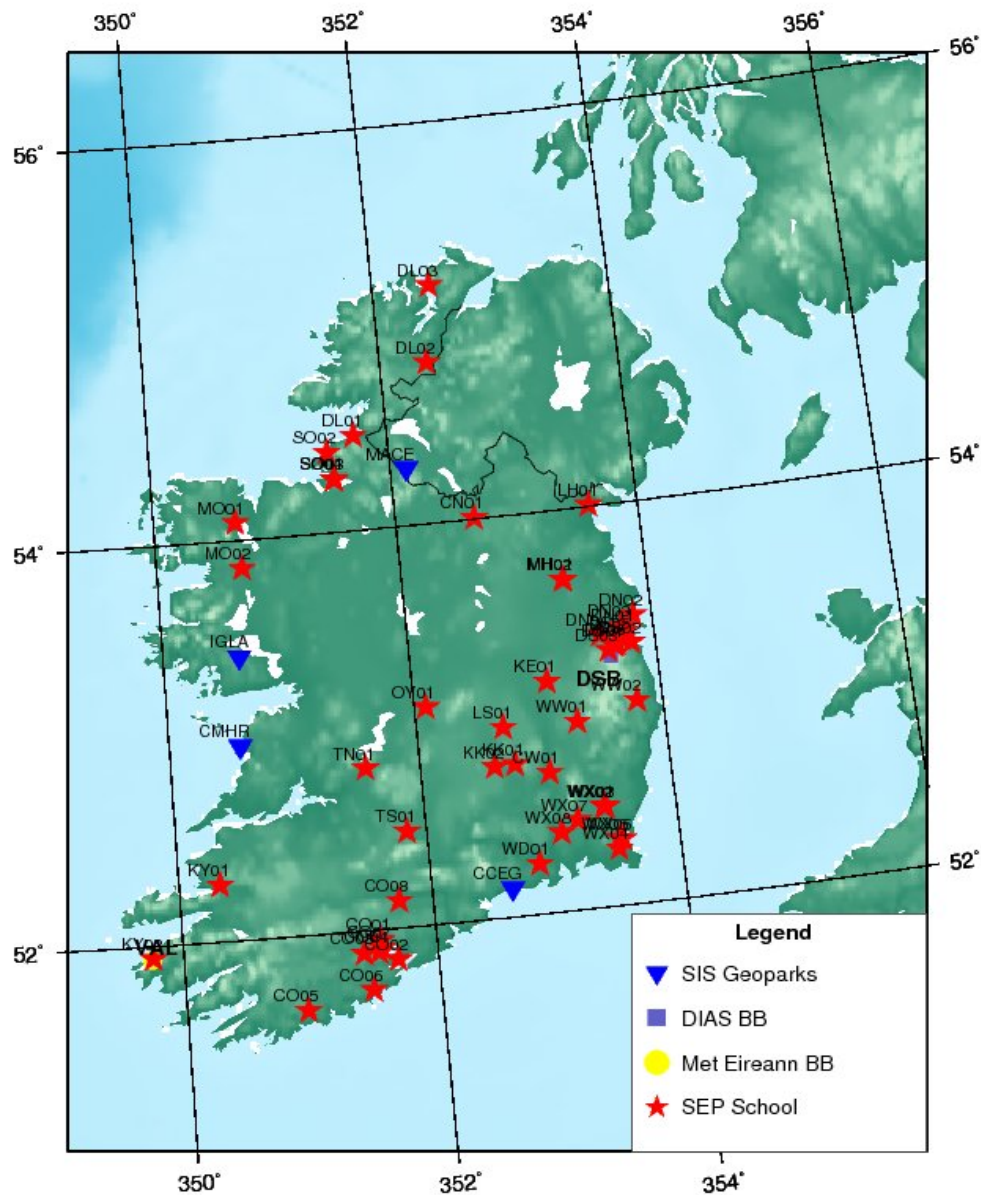


Figure 13.1.1.

The SIS programme will feature again when we team up with the Geological Survey Ireland to participate in the 50th BT Young Scientist Exhibition to take place in the Royal Dublin Society (RDS) Ballsbridge in January 2014.

Presentation:

Neenan, E., T. Blake, and S. Lebedev (2013), Seismology in Schools: Five-year report on a practical outreach program aimed at Irish primary and secondary schools. Irish Geological Research Meeting, Derry, 2 March.

13.2 BT Young Scientist Exhibition Jan 2013

We were invited by GSI to participate in the Geosciences stand in the Ecozone at the BTYSE. The DIAS display included SIS material, earthquake monitoring equipment with hands-on experiments, animated interactive seismological software and material about CTBTO operations and the NDC in DIAS. The stand was very well received by student and the public alike.

13.3 Other Media

Blake participated in several media events throughout the year on TV, radio and in the print media regarding local earthquakes in the Irish Sea and Celtic Sea, and the nuclear blast in Korea.

14 Training, Short Courses, Workshops and Seminars

14.1 Training

14.1.1 Summer of Applied Geophysical Experience

Thomas Farrell and Robert Delhaye travelled to the US in mid-June to attend the Summer of Applied Geophysical Experience (SAGE) program in Santa Fe, New Mexico. This three-week long intensive summer school exposes the students to a wide range of geophysics techniques, forming and maintaining productive international ties with both geophysicists and institutions. Both Farrell and Delhaye will continue to represent DIAS through the SAGE program by contributing to poster presentations that will be presented at the American Geophysical Union (AGU) fall meeting in December.

14.1.2 International German Summer School on Hydrology

Sarah Blake attended an International German Summer School on Hydrology in Germany. Jan Vozar attended an ECSITE'13: EarthCube Summer Institute for Technology Exploration 2013 in San Diego.

14.2 Short Courses

14.3 Seminars

8 March 2013	Prof. Kerry Gallagher – Transdimensional (Inverse) Modelling in Earth Sciences.
21 March 2013	Prof. Nick Bagdassarov - Lithosphere heterogeneity from petrology and electrical conductivity of xenoliths.
4 April 2013	Prof. Gideon Rosenbaum - Subduction segmentation during slab rollback and the origin of oroclines.
19 April 2013	Dr. Juan Carlos Afonso - Multi-observable probabilistic inversion for the thermochemical structure of the Earth: current state of affairs.
22 April 2013	Prof. Ian Bastow - Precambrian plate tectonics: seismic evidence from northern Hudson Bay.

2 May 2013	Dr. Yochai Ben Horin - Scientific issues related to Comprehensive Nuclear-Test Ban Treaty (CTBT).
24 June 2013	Dr. Marion D. Jegen (SEG European 2013 Honorary Lecturer) - Joint inversion: The way forward to a comprehensive Earth model.
10 September 2013	Prof. Matthew J. Yedlin - Tutorial on Ray Theory.
11 September 2013	Dr. Aurora Burd - A tale of three plumes: Electrical conductivity beneath the Pampean Shallow Subduction region and Payún Matrú Volcanic Field, Argentina.
12 September 2013	Prof. Matthew J. Yedlin - A Uniform Asymptotic Expansion for Maxwell's Equations.
19 September 2013	Dr. Yochai Ben Horin - Is there seismicity in Ireland?
4 October, 2013	Matteo Ravenna - A Reversible jump Markov chain Monte-Carlo inversion method for layering and amplitude of seismic velocity variations: An application to 1D structure of the lower mantle.
14 November 2013	Dr. Alan D. Chave - Magnetotelluric Data, Stable Distributions and Impropriety: An Existential Combination.
14 November 2013	Dr. Wolfram Geissler - Geophysical studies in the Fram Strait and along the Svalbard continental margins
27 November 2013	Dr. Volker Rath - Past climate change from borehole temperatures: perspectives on the last glacial cycle.

15 Invitations and Conference Sessions organized

Everyone to edit/complete

15.1 Invitations

- Jones, A.G., 2013. Calibrating laboratory observations using field data. Invited paper at: EGU, Vienna, Austria, 8-12 April.
- Jones, A.G., 2013. Insights into the Continental Lithosphere from Electromagnetic Studies Combined with Other Geoscientific Data: a Plea for Embracing Holistic Modelling that Satisfies all Available Data. Invited presentation at: Workshop on “Structure and Dynamics of the Lithosphere/Asthenosphere System”, Paris, 19-20 November.
- Jones, A.G., 2013. Cratonic lithosphere: an electrifying view. Invited paper at: AGU, San Francisco, 9-13 December.
- Jones, A.G., 2013. Modeling the physical properties and composition of the mantle lithosphere using magnetotellurics combined with other information. Invited paper at: AGU, San Francisco, 9-13 December.
- Lebedev, S. and A.J. Schaeffer, 2013. Seismic tomography with millions of waveforms and global upper-mantle heterogeneity, with a zoom-in on the Arctic. Invited seminar, Univ. Oslo, 24 October.

Lebedev, S., 2013. Invited Chair, “The Lithosphere-Asthenosphere Boundary in Different Oceanic Settings” session, “Structure and Dynamics of the Lithosphere/Asthenosphere System” Workshop, Collège de France, Paris, 19-20 November.

Lebedev, S., 2013. Global tomography and mantle dynamics, Invited seminar, University of Southern California, Los Angeles, 6 December.

Lebedev, S. and A.J. Schaeffer, 2013. Seismic Tomography of the Arctic: Continental Cratons, Ancient Orogens, Oceanic Lithosphere and Convecting Mantle Beneath. Invited paper, AGU Fall Meet., San Francisco, 9-13 December.

15.2 Sessions organized

Lebedev, S. (co-convenor). Anisotropy and small-scale heterogeneity in the solid Earth: Observations, models and implications. EGU General Assembly 2013, April 7-12, Vienna, Austria.

Jones (lead convenor). Non-seismic imaging of the continents. EGU, Vienna, Austria, 8-12 April.

Jones (co-convenor). Constraints and Uncertainties on the Composition and Structure of the Earth's Lithosphere, Upper Mantle, and Transition Zone from Multidisciplinary Studies. AGU, San Francisco, 9-13 December.

16 Miscellanea

A.G. Jones

- Member, *Royal Irish Academy*
- Member, *Committee of Heads of Irish Geoscience Institutions*
- National Correspondent for Ireland, *International Association of Geomagnetism and Aeronomy*
- Member, *Royal Irish Academy's Geosciences Committee*
- Member, *Geological Survey of Ireland's Consultative Committee*
- Member, *Geo-Electromagnetism Committee, Chinese Geophysical Society*
- Science Officer, *Seismology Division, European Geosciences Union*
- International Editor, *Earth, Planets and Space*
- Topical Editor, *Geochemistry, Geophysics, Geosystems (G-cubed)* special theme on *Lithosphere-Asthenosphere Boundary*

S. Lebedev

- Associate Editor, *Geochemistry, Geophysics, Geosystems (G-cubed)*
- Institutional representative, *Incorporated Research Institutions for Seismology (IRIS)*
- Working group member, *European Plate Observing System (EPOS)*
- Working group member, *AlpArray*
- Titular Member (member for Ireland), *European Seismological Commission (ESC)*
- An interview: "How solid is the Earth's crust where tectonic plates collide?" Broadcast on 10th Feb. 2011 on 103.2 Dublin City FM, on 'The Show with an Irish Spin on Science' with Seán Duke.
- Lebedev's global tomography figure is being used in the 10th edition of the Laboratory Manual in Physical Geology for the American Geosciences Institute (AGI) and National Association of Geoscience Teachers (NAGT) (published by Pearson).

Z. Martinec

- Editor, *International Journal of Geophysics*.

17 Productivity

Bold underlined: Currently in DIAS

Bold italicised underlined: Previously in DIAS

17.1 Publications in International Literature

1. Adetunji, A.Q., I.J. Ferguson, and **A.G. Jones** (2014), Crustal and lithospheric scale structures of the Precambrian Superior-Grenville margin. *Tectonophysics*, accepted, 18 December, 2013.
2. Afonso, J.C., **J. Fullea**, W.L. Griffin, S.Y. O'Reilly, Y. Yang, **A.G. Jones**, and J.A.D. Connolly (2013), Three-dimensional multi-observable probabilistic inversion for the compositional and thermal structure of the lithosphere and upper mantle. I: *a priori* petrological information and geophysical observables, *J. Geophys. Res.*, **118**, 1-32, doi: 10.1002/jgrb.50124.
3. Afonso, J.C., **J. Fullea**, Y. Yang, J.A.D. Connolly, and **A.G. Jones** (2013), Three-dimensional multi-observable probabilistic inversion for the compositional and thermal structure of the lithosphere and upper mantle. II: General methodology, *J. Geophys. Res.*, **118**, 1650-1676, doi: 10.1002/jgrb.50123.
4. **Agius, M.R.**, and **S. Lebedev** (2013), Tibetan and Indian lithospheres in the upper mantle beneath Tibet: Evidence from broadband surface-wave dispersion. *Geochem. Geophys. Geosyst.*, **14**, 4260-4281, doi: 10.1002/ggge.20274.
5. Fry, B., F. Davey, D. Eberhart-Phillips, and **S. Lebedev** (2013), Depth variable crustal anisotropy, patterns of crustal weakness, and destructive earthquakes in Canterbury, New Zealand, *Earth Planet. Sci. Lett.*, in press.
6. **Fullea, J.**, **M.R. Muller**, **A.G. Jones**, and J.C. Afonso (2013), The lithosphere-aesthenosphere system beneath Ireland from integrated geophysical-petrological modeling - II: 3D thermal and compositional structure. *Lithos*, **189**, 49-64, doi:10.1016/j.lithos.2013.09.014.
7. Hobbs, B.A., G.M. Fonseca, **A.G. Jones**, N. de Silva, N. Subasinghe, G. Dawes, N. Johnson, T. Cooray, D. Wijesundara, N. Suriyaarachchi, T. Nimalisiri, K. Prematilake, **D. Kiyan**, and **D. Khoza** (2014), In search of Geothermal Energy Potential in Sri Lanka: A preliminary magnetotelluric survey of the thermal springs. *Journal of the Geological Society of Sri Lanka*, **15**, 69-83.
8. **Jones, A.G.** (2013), Imaging and observing the Electrical Moho. *Invited Review, Tectonophysics, "Moho" special issue*, **609**, 423-436, doi:10.1016/j.tecto.2013.02.025.

9. **Jones, A.G.** (2014), Reconciling different equations for proton conduction using the Meyer-Neldel compensation rule. *Geophysics, Geochemistry, Geosystems*, **15**, in press, doi:10.1002/2013GC004911.
10. **Jones, A.G.**, J.C. Afonso, **J. Fulla**, and F. Salajegheh (2014), The lithosphere-asthenosphere system beneath Ireland from integrated geophysical-petrological modeling - I: Observations, 1D and 2D hypothesis testing and modelling. *Lithos*, **189**, 28–48, doi:10.1016/j.lithos.2013.10.033.
11. **Jones, A.G.**, S. Fishwick, R.L. Evans, **M.R. Muller**, and **J. Fulla** (2013), Velocity-conductivity relations for cratonic lithosphere and their application: Example of Southern Africa, *Geophysics, Geochemistry, Geosystems*, **14**, No. 4, 806-827, doi: 10.1002/ggge.20075, ISSN: 1525-2027.
12. **Jones, A.G.**, J. Ledo, I.J. Ferguson, J.A. Craven, M.J. Unsworth, M. Chouteau, and J.E. Spratt (2013), The electrical resistivity of Canada's lithosphere and correlation with other parameters: Contributions from LITHOPROBE and other programmes. *Canadian Journal of Earth Sciences*, accepted 08 January 2014.
13. Kelbert, A., A. Kuvshinov, J. Velimsky, T. Koyama, J. Ribaud, J. Sun, **Z. Martinec** and C.J. Weiss (2014), Global 3-D electromagnetic forward modelling: A benchmark study. *Geophysical Journal International*, accepted January 21, 2014.
14. **Khoza, D.**, **A.G. Jones**, **M.R. Muller**, R.L. Evans, S.J. Webb, **M. Miensopust**, and the SAMTEX team (2013), Tectonic model of the Limpopo belt: Constraints from magnetotelluric data. *Precambrian Research*, **226**, 143-156, doi: 10.1016/j.precamres.2012.11.016.
15. **Khoza, D.**, **A.G. Jones**, **M.R. Muller**, R.L. Evans, **M.P. Miensopust**, and S.J. Webb (2013), Lithospheric structure of an Archean craton and adjacent mobile belt revealed from 2D and 3D inversion of magnetotelluric data: example from southern Congo craton in northern Namibia. *Journal of Geophysical Research*, **118**, Issue 8, 4378–4397, doi: 10.1002/jgrb.50258
16. **Kiyan, D.**, **A.G. Jones**, and **J. Vozar** (2013), The inability of magnetotelluric off-diagonal impedance tensor elements to sense oblique conductors in 3-D inversion. *Geophysical Journal International*, **196**, 1351–1364, doi:10.1093/gji/ggt470.
17. Konrad, H., M. Thoma, I. Sasgen, V. Klemann, K. Grosfeld, D. Barbi, and **Z. Martinec** (2013), The deformational response of a viscoelastic solid Earth model coupled to a thermomechanical ice sheet model. *Surveys in Geophysics*, accepted, October 13, 2013.
18. **Lebedev, S.**, **J. M.-C. Adam**, and T. Meier (2013), Mapping the Moho with seismic surface waves: A review, resolution analysis, and recommended inversion strategies. Invited Review, *Tectonophysics, Moho* special issue, **609**, 377–394.
19. **Mandolesi, E.**, and **A.G. Jones** (2013), Magnetotelluric inversion based on Mutual Information, *Geophysics Journal International*, Submitted December 2013, Accepted subject to revision February 2014.

20. **Martinec, Z.** (2013), Mass-density Green's functions for the gravitational gradient tensor at different heights. *Geophysical Journal International*, in press, online access since January 3, 2014, doi:10.1093/gji/ggt495.
21. Matsuno, T., A.D. Chave, **A.G. Jones**, **M.R. Muller**, and R.L. Evans (2013), Robust magnetotelluric inversion. *Geophysical Journal International*, **196**, 1365–1374, doi:10.1093/gji/ggt484.
22. **Miensopust, M.P.**, P. Queralt, **A.G. Jones**, and the 3D modellers (2013), Magnetotelluric 3D inversion - a recapitulation of two successful workshops on forward and inversion code testing and comparison. *Geophysical Journal International*, **193**, 1216-1238, doi: 10.1093/gji/ggt066.
23. Ogaya, X., P. Queralt, J. Ledo, A. Marcuello, and **A.G. Jones**, 2014. Geoelectrical baseline model of the subsurface of the Hontomín site (Spain) for CO2 geological storage in a deep saline aquifer: a 3D magnetotelluric characterization. *International Journal of Greenhouse Gas Control*, accepted, 14 March 2014
24. Sasgen, I., H. Konrad, E.R. Ivins, M.R. van den Broeke, J. Bamber, **Z. Martinec**, and V. Klemann (2013), Antarctic ice-mass balance 2003 to 2012: regional reanalysis of GRACE satellite gravimetry measurements with improved estimate of glacial-isostatic adjustment based on GPS uplift rates. *The Cryosphere*, **7**, 1499-1512.
25. **Schaeffer, A.J.**, and **S. Lebedev** (2013), Global shear-speed structure of the upper mantle and transition zone. *Geophys. J. Int.*, **194**, 417-449. [Winner, GJI Student Author Award for best paper, 2013 (A.J. Schaeffer).]
26. **Schaeffer, A.J.**, and **S. Lebedev** (2013), Global heterogeneity of the lithosphere and underlying mantle: A seismological appraisal based on multimode surface-wave dispersion analysis, shear-velocity tomography, and tectonic regionalization. *Invited Review* in: "The Earth's Heterogeneous Mantle," Springer, accepted September 9, 2013.
27. **Schmoldt, J.-P.**, and **A.G. Jones** (2013), A novel anisotropic inversion approach for magnetotelluric data from subsurfaces with orthogonal geoelectric strike directions. *Geophysical Journal International*, **195**, 1576-1593, doi:10.1093/gji/ggt355.
28. Sodoudi, F., X. Yuan, R. Kind, **S. Lebedev**, **J. Adam**, E. Kästle, F. Tilmann (2013), Seismic evidence for stratification in composition and anisotropic fabric within the thick lithosphere of Kalahari Craton. *Geochemistry, Geophysics, Geosystems*, **14**, 5393-5412, DOI: 10.1002/2013GC004955, 2013.
29. Spada, M., I. Bianchi, E. Kissling, **N. Piana Agostinetti**, and S. Wiemer (2013), Combining controlled-source seismology and receiver function information to derive 3-D Moho topography for Italy. *Geophys. J. Int.*, **194**, 2, 1050-1068.
30. Spratt, J., T. Skulski, J.A. Craven, **A.G. Jones**, D. Snyder, and **D. Kivan**, (2014), Magnetotelluric investigations of the lithosphere beneath the central Rae Craton, mainland Nunavut, Canada. *Journal of Geophysical Research*, accepted 20 January 2014.
31. Sun, D., M.S. Miller, **N. Piana Agostinetti**, P.D. Asimow, and D. Li (2013), Modelling

high frequency waves in the slab beneath Italy, *Earth Pla. Sci. Lett.*, in press.

32. **Tirel, C.**, J.-P. Brun, E. Burov, M.J.R. Wortel, and **S. Lebedev** (2013), A plate tectonics oddity: Caterpillar-walk exhumation of subducted continental crust. *Geology*, **41**, 555-558.
33. Vanicek, P., R. Kingdon, M. Kuhn, A. Ellmann, W.E. Featherstone, M.C. Santos, **Z. Martinec**, C. Hirt, and D. Avalos (2013), Testing Stokes-Helmert geoid model computation on a synthetic gravity field: experiences and shortcomings. *Studia Geophys. Geod.*, **57**, 369-400.

17.2 Theses

Agius, M.R., “The structure and dynamics of the lithosphere beneath Tibet from seismic surface-wave analysis” (supervisor: S. Lebedev). Trinity College Dublin, degree awarded April, 2013.

Adam, J. M.-C., “Seismic structure and anisotropy in southern Africa’s lithosphere: Constraints from broad-band surface-wave dispersion” (supervisor: S. Lebedev). Trinity College Dublin, degree awarded April, 2013.

Dostal, J., Modelling of the Magnetic Field Induced by Ocean Circulation. Ph.D. thesis, Institute for Meteorology, Free University in Berlin, submitted for the defence in January 30, 2014 (supervisors Z. Martinec and M. Thoma).

17.3 Invited presentations

Lebedev, S. and **A.J. Schaeffer**. Seismic tomography with millions of waveforms and global upper-mantle heterogeneity, with a zoom-in on the Arctic. Invited seminar, Univ. Oslo, 24 October 2013.

Jones, A.G., 2013. Calibrating laboratory observations using field data. Invited paper at: EGU, Vienna, Austria, 8-12 April.

Jones, A.G., J. Ledo, I.J. Ferguson, J.A. Craven, M.J. Unsworth, M. Chouteau and J.E. Spratt, 2013. The electrical resistivity of Canada's Lithosphere: Ian Gough's lasting legacy to Canadian Geoscience. Invited paper at: IAGA, Merida, Mexico, 26-31 August.

Jones, A.G., 2013. Geophysical petrological modelling of the thermal and compositional structure of the lithosphere – integrating elevation, potential fields, seismology magnetotelluric and surface heat flow data. Invited keynote paper at: SAGA, Kruger Park, South Africa, 6-9 October.

Jones, A.G., J.S. Daly, A. Allen, R. Goodman, N.H. Hunter Williams, M. Lee, D. Reay, M. Feely, P. Hanly, R. Pasquali, N. Piana Agostinetti, S. Lebedev, M. Long, J. Fulla, J. Vozar, J. Campanya, S. Blake, M. de Block, R. Delhaye, T. Farrell, T. Fritschle, N. Willmont Noller, T. Waters, (Muller, M., Yeomans C.) (2013), IRETherm: Research and Exploration Challenges in Assessing Ireland's Deep Low-Enthalpy Geothermal Energy Potential: Overview, Status Quo and Quo Vadimus. GAI Conference, Kilkenny, 13 November, invited oral presentation.

- Jones, A.G.**, 2013. Insights into the Continental Lithosphere from Electromagnetic Studies combined with other geoscientific data: a Plea for embracing holistic modelling that satisfies all available Data. Invited keynote paper at: Workshop on "Structure and Dynamics of the Lithosphere/Asthenosphere System", College de France, Paris, 19-20 November.
- Jones, A.G.**, 2013. Cratonic lithosphere: an electrifying view. Invited keynote paper at: AGU, San Francisco, USA, 9-13 December.
- Jones, A.G.**, 2013. Modeling the physical properties and composition of the mantle lithosphere using magnetotellurics combined with other information. Invited keynote paper at: AGU, San Francisco, USA, 9-13 December.
- Lebedev, S.**, Global tomography and mantle dynamics, Invited seminar, University of Southern California, Los Angeles, 6 December 2013.
- Lebedev, S. and A.J. Schaeffer.** Seismic Tomography of the Arctic: Continental Cratons, Ancient Orogens, Oceanic Lithosphere and Convecting Mantle Beneath. (Invited paper talk, 9 December), AGU Fall Meet., San Francisco, 9-13 December 2013.
- Sachl, L., and D. Einspigel. Simple benchmarks for ocean models, a comparison study. Presentation at: Seminar on Geodynamics, Charles University in Prague, 20 November 2013.
- Sachl, L. LSG Ocean Model - Introduction and Preliminary Results. Presentation at: Week of Doctoral Students 2013, Charles University in Prague, 6 June 2013.
- Schaeffer, A.J.**, Heterogeneity and anisotropy of the Earth's upper mantle: from global to regional scales. Invited Seminar. School of Geological Sciences, University College Dublin, January 2013.
- Schaeffer, A.J.**, and **S. Lebedev.** Heterogeneity and anisotropy of the North American upper mantle, imaged using multimode waveform tomography. Invited talk. GSC GEM Diamonds Project, University of British Columbia, Robson Square, Canada, February 2013.